CORE
Metadata, citation and similar papers at core.ac.uk
Provided by Louisiana State University

Louisiana State University
LSU Digital Commons

LSU Doctoral Dissertations | Graduate School

2012

Metabolic downregulation during diapause in embryos of Artemia franciscana

Yuvraj Nanasaheb Patil
Louisiana State University and Agricultural and Mechanical College, yuvrajnpatil@gmail.com

Follow this and additional works at: https://digitalcommons.lsu.edu/gradschool_dissertations

Recommended Citation
Patil, Yuvraj Nanasaheb, "Metabolic downregulation during diapause in embryos of Artemia franciscana" (2012). *LSU Doctoral Dissertations*. 323.
https://digitalcommons.lsu.edu/gradschool_dissertations/323

This Dissertation is brought to you for free and open access by the Graduate School at LSU Digital Commons. It has been accepted for inclusion in LSU Doctoral Dissertations by an authorized graduate school editor of LSU Digital Commons. For more information, please contactgradetd@lsu.edu.

METABOLIC DOWNREGULATION DURING DIAPAUSE IN EMBRYOS OF *ARTEMIA FRANCISCANA*

A Dissertation

Submitted to the Graduate Faculty of the
Louisiana State University and
Agricultural and Mechanical College
in partial fulfillment of the
requirements for the degree of
Doctor of Philosophy

in

The Department of Biological Sciences

by
Yuvraj N. Patil
M.S. Pharm, National Institute of Pharmaceutical Education and Research, India, 2003
B. Pharm, Pune University, India, 2001
December 2012

For my family, for their patience and unshakable support.

ACKNOWLEDGMENTS

Many individuals have a role, direct or otherwise in helping me in my research. Much of my appreciation goes to my mentor, Dr. Steven Hand who guided me, provided constructive criticism and helped me hone my research skills. I would like to thank Dr. Michael Menze for help with early experiments on Artemia embryos and helpful insights on the topic. I thank Dr. William Stickle for assistance with necessary equipment for field work. I would like to thank Dr. Terry Bricker for his helpful discussion on antibody work and the generous donation of RUBISCO antibody. I thank Brad Marden of Great Salt Lake *Artemia* LLC, Utah for his valuable help with collecting diapause embryos of Artemia franciscana and providing logistic help with field experiments carried out at Great Salt Lake. Finally, I would like to thank my committee members as well as current and past members of the Hand lab for helpful discussions and assistance with field experiments. This study was supported by the National Institutes of Health (grant 2RO1DK046270-14A1) and the National Science Foundation (grant IOS-0920254).

TABLE OF CONTENTS

LIST OF TABLES

LIST OF FIGURES

ABSTRACT

Encysted embryos of *Artemia franciscana* undergo a dramatic respiratory depression upon release from the adult female as they enter a state of hypometabolism termed diapause. The mechanisms by which such a respiratory depression is achieved remain unexplained. Evidence presented here shows that strategic enzymes involved in trehalose catabolism are inhibited during diapause, namely trehalase, hexokinase, pyruvate kinase and pyruvate dehydrogenase. Trehalose is the sole source of fuel in the embryos of *A. franciscana*, and hence downregulation of trehalose catabolism results in severe limitation of metabolic fuel available to the embryo during diapause. Western blot data demonstrates that pyruvate dehydrogenase becomes phosphorylated during entrance into diapause, and as a consequence, one would predict PDH to be strongly inhibited in this state. Restriction of glycolytic flux will lead to metabolic 'starvation' of the mitochondrion, and in turn will reduce mitochondrial oxidative phosphorylation during diapause. Measurements of ATP, ADP and AMP show that substantial decreases occur in ATP:ADP ratio and in adenylate energy charge during diapause.

Respiration studies conducted with embryo lysates document a depression of oxidative phosphorylation during diapause in the case where substrates for respiratory complex I (pyruvate+malate) are used as the fuel source. Reduced respiration through complex I is corroborated by the increased phosphorylation of pyruvate dehydrogenase. When substrates for complexes I and II (pyruvate+malate+succinate) are added simultaneously, the increased electron flow through the electron transport system allows the detection of respiratory inhibition by the phosphorylation system (i.e., the $F_1.F_o$-ATP synthase, adenine nucleotide transporter, and phosphate transporter). This inhibition of the phosphorylation system is diminished as diapause lysates are diluted, which suggests the presence of an unidentified inhibitor.

Finally, measurements of catalytic activity for respiratory complexes extracted from isolated mitochondria in the presence of phosphatase inhibitors reveal a minor decrease in complex I activity during diapause and a drop in activity of complex IV, the latter effect being minimized by COX excess capacity. Taken together, restriction of glycolytic carbon to the mitochondrion appears to the primary mechanism for the *in vivo* metabolic arrest in *A. franciscana* embryos during diapause, which is accentuated by inhibitions within the mitochondrion itself.

CHAPTER 1

INTRODUCTION

Diapause is a specific type of dormancy that is genetically programmed and triggered by endogenous physiological factors in response to environmental cues (Denlinger 2002, Denlinger 2012, Koštál 2006). Typically diapause is entered prior to the onset of adverse environmental conditions. The diapause program is an alternative developmental pathway that delays direct morphogenesis and is characterized by ontogenetic arrest for a period spanning weeks to months (Koštál 2006). Developmental arrest may be accompanied by metabolic arrest depending on the developmental stage and the species (Denlinger 2002, Hahn and Denlinger 2011, Hand et al. 2011, Reynolds and Hand 2009, Denlinger et al. 2012). The survival time of an organism during exposure to environmental stresses that limit energy availability is largely related to the degree of metabolic depression achieved. In order to withstand such environmental challenges, it is crucial to depress both energy consuming and energy producing pathways. Otherwise it is possible that cellular energy reserves would be depleted and the organism will reach an energetic state from which recovery is not possible (Hardewig and Hand 1996). The diapause program can thus serve as a protective mechanism for the organism.

Preparation for diapause involves differential gene expression that can control a number of features of the diapause phenotype (Hahn and Denlinger 2011, MacRae 2010). Diapause can occur at one or more specific stages for a given species. Species demonstrating an obligate diapause will arrest development at the same point(s) in the life cycle every generation regardless of the environmental conditions, whereas in species such as the brine shrimp *Artemia franciscana* Kellogg, which display facultative diapause, environmental conditions or maternal influence determines whether the adult female will produce diapausing embryos (Hahn and

Denlinger 2007, Denlinger 2002, Denlinger et al. 2012). Diapause differs from quiescence, the latter serving as an acute response to inimical conditions such as hypoxia or dehydration. Quiescence is characterized by developmental and metabolic depression which begins promptly after the environmental conditions become unfavorable and generally resumes after the conditions return to normal (Drinkwater and Crowe 1987, Hahn and Denlinger 2007). Diapausing animals resume normal development only after diapause is terminated due to exposure to termination cues such as dehydration and low temperature, which then must be followed by environmental conditions favorable for development (Drinkwater and Crowe 1987, Koštál 2006).

It can be argued that the deepest metabolic arrest associated with diapause occurs in gastrula-stage embryos of the *Artemia franciscana* (Clegg et al. 1996, Reynolds and Hand 2004). In addition to exhibiting a high degree of metabolic depression, the abundance of field-collected embryos and dehydrated post-diapause embryos makes *A. franciscana* a suitable candidate for studying embryonic diapause. Considering a large number of studies on insect diapause have been published (Denlinger 2002, Hahn and Denlinger 2011 and references therein), the amount of work published on *A. franciscana* diapause is relatively limited, and the mechanism of diapause regulation in *A. franciscana* embryos remains largely unexplored. The primary objective of research presented in this dissertation is to advance the knowledge of the various regulatory steps involved in the metabolic depression observed during diapause in *A. franciscana*.

1.1 Diapause and Metabolic Downregulation in *Artemia franciscana* Embryos

A. franciscana inhabit hypersaline environments such as the Great Salt Lake (UT) and salt water cisterns of the San Francisco Bay (CA). In early fall, in response to environmental cues like photoperiod, population density and changes in salinity, *A. franciscana* females switch

from ovoviviparous reproduction to oviparous reproduction and produce diapause-destined embryos (Clegg and Conte 1980). Oviparous embryos cease development at gastrulation after which they are released into the environment (Clegg and Conte 1980, Qiu and MacRae 2010). These late gastrula embryos are made up of roughly 4000 cells and have a selectively permeable cyst wall which allows only water and gases to diffuse across (Clegg and Conte 1980). When released from the adult female, the diapause-destined embryos have respiration values that are close to those of actively metabolizing embryos (Clegg et al. 1996). However, over the period of about 5 days post-release, respiration decreases to barely detectable levels. This decrease in metabolic activity is slow compared to the much faster metabolic depression seen as embryos enter quiescence when exposed to anoxia, a transition which occurs in minutes to hours (Carpenter and Hand 1986a, Hand and Gnaiger 1988).

The diapause program affords *A. franciscana* embryos some important benefits. Diapause plays a vital role in maintaining the viability of *A. franciscana* embryos for an extended period after their release from the female. One of the main advantages of metabolic depression achieved in diapause is conservation of the embryo's metabolic fuel, trehalose. Based on respiratory quotients and biochemical measurements of stored fuel, the substrate for respiration in *A. franciscana* embryos is purely carbohydrate, and it is the disaccharide trehalose that forms the bulk of this store prior to hatching (Dutrieu 1960, Muramatsu 1960, Emerson 1963, Clegg 1964, Carpenter and Hand 1986a). Trehalose is catabolized during preemergence embryonic development, fueling the glycolytic pathway and also enabling the production of glycerol, which is required for hatching of the embryos (Clegg 1964, Clegg and Conte 1980, Drinkwater and Crowe 1991, Dutrieu 1960). Conserving trehalose via metabolic depression allows the embryos to develop and hatch unhindered when diapause is ultimately terminated.

Trehalose has been shown to accumulate in desiccation tolerant tissues of plant and animal species (Clegg 2001). Trehalose is able to stabilize proteins and membranes during freezing and drying (Crowe et al. 2005). Numerous *in vitro* studies have demonstrated the ability of molecules like trehalose to protect the structure and function of plasma membranes and proteins (Crowe et al. 1987, Crowe et al. 2005, Timasheff 2002). The ability of trehalose to stabilize macromolecules during water stress is due to two physical properties, namely the ability to form sugar glasses (vitrification) and to hydrogen bond to macromolecules in the place of water (water replacement theory) (Crowe et al. 1998, Webb 1965). In addition, because it is a non-reducing sugar, trehalose does not undergo browning reactions with the amine groups of proteins (Crowe and Clegg, 1973). The protective capacity of trehalose extends to other forms of water stress, such as freezing and freeze-drying (Buchanan et al. 2005, Crowe et al. 2005, Yancey 2005). Thus trehalose appears to have a dual role in *A. franciscana* embryos as a metabolic substrate and a protectant during desiccation.

Diapause embryos of *A. franciscana* embryos are either washed ashore or stay afloat on the surface of the lake while overwintering. The remarkably robust diapause in *A. franciscana* may be instrumental in the ability of shoreline-deposited embryos to experience bouts of partial dehydration and rehydration without hatching prematurely, for example in the middle of winter. In comparison, if embryos were no longer in diapause, they would hatch after brief cycles of dehydration and rehydration and ultimately perish in the harsh environmental conditions. Another potential advantage of diapause in *Artemia* embryos could be protection against damage from oxygen free radicals due to downregulation of mitochondrial activity during diapause (Clegg et al. 1996, Reynolds and Hand 2004). As discussed by Stuart and Brown (2006), reactive oxygen species (ROS) such as superoxide are produced routinely during respiration. Accumulation of ROS could lead to oxidative damage to DNA and other essential

macromolecules. Diapause embryos in normoxic bodies of water such as the Great Salt Lake (UT) or during direct exposure to air would be expected to have a lower risk of accruing ROS-mediated damage.

In response to unfavorable environmental conditions, post-diapause *A. franciscana* embryos can undergo quiescence during preemergence development with a degree of metabolic depression comparable to that seen in diapause embryos. Substantial research on quiescence induced by anoxia in post-diapause embryos has been published on this state and the regulatory role of intracellular acidification (Busa and Crowe 1983, Busa and Nuccitelli 1984, Carpenter and Hand 1986a, van Breukelen et al. 2000, Hochachka and Guppy 1987, Hand and Hardewig 1996, Hand et al. 2011), the concomitant decrease in protein turnover (Kwast and Hand 1993, 1996; Hofmann and Hand 1994, Anchordoguy and Hand 1994, van Breukelen et al. 2000), decrease in mRNA turnover (Eads and Hand 2003a,b; Hardewig et al. 1996, van Breukelen et al. 2000) and the mechanisms underlying the acidification (Covi and Hand 2005, Covi et al. 2005). Because quiescence is an *acute* response to adverse environmental conditions, it is conceivable that the mechanisms responsible for metabolic depression during diapause are different. The published information on diapause in *A. franciscana* is far more limited than on anoxia-induced quiescence. Consequently, the metabolic changes occurring during diapause, as well as underlying mechanisms, are not well documented.

A number of gene transcripts are upregulated during diapause in *A. franciscana*. Included among these are a transcriptional regulator p8, the glycolytic enzyme glucose-6-phosphate isomerase (GPI), mitochondrial uncoupling protein and several heat shock proteins (Qiu et al. 2007). A majority of the upregulated mRNA transcripts has been associated with protective and cellular downregulation (MacRae 2010). These results are of limited utility,

however, because virtually nothing is currently know about the downstream functions of the respective proteins in diapause.

Previous work has documented the utility of H_2O_2 incubation as a procedure to promote diapause termination for *A. franciscana* embryos (Van Stappen et al. 1998). However, the mechanism by which this empirical approach with H_2O_2 actually induces the effect is completely unknown. Robbins et al. (2010) compared the ability of H_2O_2 and NO to trigger development in both quiescent and diapause embryos of *A. franciscana*. The failure of NO to break the diapause state was attributed by these authors to its hypothesized role in solely enhancing post-diapause embryo development by driving changes in cell structure and gene expression. The inferences drawn in this work are speculative, because they rely solely on hatching tests and do not contribute to our mechanistic understanding of diapause. However, the capacity of H_2O_2 to terminate diapause does provide food for thought about the myriad of signaling pathways that may be interlinked in regulating diapause. It is well documented that exposure to specific environmental stimuli such as light, desiccation and cold promotes breakage of diapause and the resumption of cyst development and metabolism (Drinkwater and Crowe 1987, Van Der Linden et al. 1988, Drinkwater and Clegg 1991, Nambu et al. 2008). Yet the interconnection among these diverse stimuli and H_2O_2 remains a mystery.

Drinkwater and Crowe (1987) showed that intracellular acidification is not required for maintaining diapause and that alkalinization of diapause embryos of *A. franciscana* does not enable these cysts to hatch. Therefore although there is insufficient data to completely rule out pH_i transitions as an underlying mechanism in diapause (Clegg 2011), it seems unlikely. Later work by Drinkwater and Crowe (1991) tracked the gradual changes in trehalose, glycogen and glycerol during diapause under conditions of varying salinity but no attempt was made to contrast the difference in metabolic flux between diapause and post-diapause embryos. Based on

inhibition of trehalose catabolism observed in quiescent *A. franciscana* embryos (Carpenter and Hand 1986a) and other evidence of glycolytic inhibition in dormant states such as estivation of snails (Rees and Hand 1991), we test the hypothesis that substrate limitation to the mitochondrion is required for metabolic depression. Chapter 2 pursues this rationale to establish the role of substrate limitation as a vital factor causing metabolic arrest in diapause.

Reynolds and Hand (2004) presented a bioenergetic analysis of isolated mitochondria from diapause and post-diapause embryos, which documented very little difference in mitochondrial structure or function between these states. While this study effectively eliminated a number of possibilities by which diapause mitochondria might be downregulated, other possibilities still remain as open questions. For example, with isolated mitochondria, one cannot rule out the possibility that changes could have occurred in phosphorylation/dephosphorylation of mitochondrial components during the isolation process, or that a diffusible inhibitor might have been removed. With this in mind, Chapter 3 is devoted to functional analyses of mitochondria in tissue homogenates, in order to evaluate whether some of the inhibition observed for intact embryos might be detected with this approach.

Based on the results of embryo lysate study detailed in chapter 3, an inhibition of complex I was observed during diapause, which was supported by inhibition of pyruvate dehydrogenase previously documented (Patil et al. 2012). An inhibition of the oxidative phosphorylation system was also observed in embryo lysates during diapause, and this inhibition diminished as the lysates were diluted. In chapter 4, the possibility that changes in the activities of mitochondrial complexes may contribute to metabolic downregulation during diapause is explored. Phosphatase inhibitors were employed at every step of mitochondrial isolation, solubilization of complexes and analysis to preserve any phosphorylation-based modifications that may exist. The chapter also explores the role of pyruvate dehydrogenase complex in

metabolic downregulation during diapause by studying the activity of the partially-purified enzyme complex in the presence of phosphatase inhibitors.

1.2 Research Aims of This Dissertation

The overall objective of this dissertation is to improve our understanding of the physiological and biochemical mechanisms regulating metabolism during diapause in embryos of the brine shrimp *A. franciscana*. Chapter 2 primarily focuses on the role of substrate limitation to the mitochondrion in promoting metabolic depression during diapause. To test the hypothesis that substrate limitation is achieved by strategic enzyme inhibition in the metabolic pathway for trehalose catabolism (trehalose hydrolysis to glucose, glycolysis, and entry of glycolytic carbon into the tricarboxylic acid cycle), I employed biochemical assays to measure concentrations of pathway metabolites. Based on the metabolic crossover point theorem, I used ratios of products to substrates to pinpointed sites of enzymatic inhibition that served to limit carbon flux to the mitochondria. I also used respirometry to demonstrate the decrease in respiration of embryos during entry into diapause and to compare respiration between diapause and post-diapause embryos. I performed Western blot analysis to measure the extent of inhibition of pyruvate dehydrogenase during diapause.

Chapter 3 focuses on the evaluation of mitochondrial function in *A. franciscana* by utilizing high resolution respirometry to quantify respiratory inhibition in concentrated homogenates prepared from diapause and post-diapause embryos. I tested the hypothesis that a diffusible inhibitor may exist in diapause embryos that could depress respiration. Specifically I measured oxygen consumption in homogenates of diapause and post-diapause embryos at various dilutions in the presence of different substrates and respiratory modulators. If inhibition were detected in concentrated extracts, then one would predict it would be diminished by sequential dilutions.

In chapter 4, I focus on another aspect of reversible inhibition of mitochondrial activity, i.e., the inhibition of mitochondrial complexes in diapause embryos as a result of phosphorylation. I tested the hypothesis that one or more mitochondrial complexes in diapause embryos are inhibited as a result of enzyme phosphorylation. Specifically, I evaluated the activity of individual respiratory complexes prepared from disrupted mitochondria from diapause and post-diapause embryos in the presence of phosphatase inhibitors. I also carried out a comparison of the kinetic properties of pyruvate dehydrogenase complex isolated from diapause and post-diapause embryos. The assay and partial purification of the complex was performed in the presence of phosphatase inhibitors.

CHAPTER 2

METABOLIC DOWNREGULATION AND INHIBITION OF CARBOHYDRATE CATABOLISM DURING DIAPAUSE IN EMBRYOS OF *ARTEMIA FRANCISCANA*

2.1 Introduction

Diapause is a programmed arrest of development that is controlled by endogenous physiological factors, and depending on the developmental stage and species in question, may or may not involve a substantial depression of metabolism (Denlinger 2002, Clegg 2011, Hahn and Denlinger 2011, Hand et al. 2011, MacRae 2010, Reynolds and Hand 2009). Entry into diapause begins even while conditions are adequate to support normal development. Preparation for diapause involves differential gene expression that can control a number of features of the diapause phenotype (Hahn and Denlinger 2011, MacRae 2010). It is arguable that one of the deepest metabolic arrests associated with diapause occurs in embryos of the brine shrimp *Artemia franciscana* (Clegg et al. 1996, Reynolds and Hand 2004). Mechanisms controlling this downregulation in energy metabolism are currently unclear as are the sites of inhibition. In this paper we build upon the benchmark study by Clegg et al. (1996) in order to characterize this metabolic depression, identify sites of inhibition, and explore the ramifications of this severe arrest of energy flow.

A. franciscana embryos enter diapause in the gastrula stage of embryogenesis (Clegg and Conte 1980). Development is suspended and metabolism is downregulated during diapause, and for habitats like the Great Salt Lake, these events serve to prevent hatching and preserve nutrient stores while the embryo floats on the lake or after it has washed ashore. Shoreline deposited embryos may be subjected to cycles of dehydration and rehydration. Overwintering embryos, whether on the lake or shore, eventually break diapause as a result of cold exposure and/or

dehydration (Drinkwater and Crowe 1987, Drinkwater and Clegg 1991). Shoreline deposited embryos are washed back into the lake in the spring and resume active metabolism and development.

For various arrested states like diapause, when energy availability is limited, survival time of organisms is directly proportional to the degree of metabolic depression achieved (Hochachka and Guppy 1987, Hand and Hardewig 1996, Hand 1998, Lutz and Milton 2004, Storey and Storey 2007). The most quantitative assessment currently available (Clegg et al. 1996) indicates that the metabolic depression during entry into diapause is profound in *A. franciscana* embryos. Embryos used by Clegg et al. (1996) were synchronized to within 24 h of the time of release from ovigerous females. Across the intervening 20 days after release, the respiration rate dropped to approximately 2% of the initial rate. Thus while the developmental cessation is complete by the time embryos are released from the female, the metabolic depression requires many days. Based on respiratory quotients and biochemical measurements of stored fuels, the substrate for respiration in *A. franciscana* embryos is purely carbohydrate (Dutrieu 1960, Muramatsu 1960, Emerson 1963, Clegg 1964, Carpenter and Hand 1986a), and it is the disaccharide trehalose that forms the bulk of this fuel prior to hatching (Clegg 1964, Dutrieu 1960, Carpenter and Hand 1986a). Thus, resolving the mechanisms by which trehalose catabolism is arrested during diapause is central to an understanding of the overall energetic arrest.

In thus study we quantify the depression of metabolism in *A. franciscana* embryos (temporally-synchronized to within 4 h) during the entrance into diapause and identify proximal sites in carbohydrate catabolism that mediate this arrest. Inhibition of one or more enzymes in the pathway of trehalose catabolism could restrict carbon availability in the form of pyruvate to the mitochondrion, and explain in part the depression of respiration observed. While the

physiological factors initiating the overall diapause phenotype remain unexplained (Drinkwater and Crowe 1987, Drinkwater and Clegg 1991, Qiu and MacRae 2010, Clegg 2011, Hand et al. 2011) results of this study indicate that restriction of oxidative substrate involves an orchestrated interplay at multiple enzymatic sites.

2.2 Methods

Collection and Preparation of Synchronized Diapause Embryos

Adult animals were collected in September-October from the Great Salt Lake, Utah by subsurface tows with a 50 cm diameter, 165 micron mesh, conical plankton net. Females in these collections carried large numbers of encysted embryos in their ovisacs that were destined for release in the state of diapause. Adults were immediately rinsed free of any previously-released/adherent embryos, gently transferred to two aerated holding tanks (each approximately 485 liters in volume) filled with lake water filtered with a 125 micron sieve, and then maintain onboard the research vessel. The adults were incubated in the two holding tanks for 4 h at an average density of 205 shrimp per liter (119 males/liter; 86 females/liter), after which the diapause cysts released during this period were separated from adults by filtration with brass sieves. Diapause embryos were further separated from adult fecal pellets based on density. A total of 1-2 g of embryos were collected from each holding tank, and these were stored as independent samples. The 4-h synchronized diapause embryos were maintained at ambient temperature in 1.25 M NaCl, containing 200 units/ml nystatin, 50 μg/ml kanamycin, and penicillin-streptomycin (50 μg/ml), protected from light, and used for respiration and Western blot studies described below.

Bulk Diapause and Post-Diapause Embryos

Bulk (non-synchronized) diapause cysts were collected from the lake surface by towing a plankton net through windrows (‘streaks’) of *A. franciscana* cysts. Encysted embryos were then

separated from adults and stored temporarily in lake water. After further cleaning back on shore, the bulk diapause cysts (1-2 kg) were kept at room temperature protected from light in 1.25 M NaCl, containing 200 units/ml nystatin, 50 μg/ml kanamycin, and 50 μg/ml penicillin-streptomycin. Prior to use for biochemical experiments or mitochondrial isolations, bulk diapause embryos were rinsed and incubated in 35 ppt artificial seawater (Instant Ocean, East Lake, OH) for 4 days at room temperature to allow any embryos that had broken diapause to hatch as free-swimming larvae. These larvae were removed and the remaining diapause cysts used for experimentation.

Dried, post-diapause embryos of *A. franciscana* from the Great Salt Lake, Utah were obtained from Great Salt Lake *Artemia*, LLC, Ogden, UT (grade: laboratory reference standard) and stored at -20°C. These post-diapause cysts were first hydrated in 0.25 M sodium chloride on ice for a minimum of 4 h after which they were incubated in 0.25 M sodium chloride at room temperature for 8 h. Hatching percentage was above 90%.

Oxygen Consumption of Synchronized Diapause Embryos

At selected time intervals, 30-80 mg of diapause embryos were filtered from storage medium with DryWipe filters (Chicopee Mills, Inc., New Brunswick, N.J., USA), rinsed with deionized water, and blotted to remove external water. Embryos were added to the 2.0 ml chambers of an Oxygraph-2K (OROBOROS Instruments, Innsbruck) and respiration rate measured at 25°C in an air-saturated medium of 35 ppt artificial seawater with kanamycin added at a final concentration of 50 μg/ml. Special 10 mm stir bars coated with PEEK plastic and fitted with Viton sleeves were set at a stirring rate of 300 rpm. These stir bars served to minimize mechanical damage to the embryos. After closing the chamber, a 10 min period was allowed for stabilization and then oxygen consumption recorded for an additional 10 min. Background measurements without embryos were made before and after each run. Data were digitally

recorded using DatLab4 software and oxygen flux was calculated as the negative time derivative of the oxygen concentration. Oxygen sensors were calibrated routinely at air saturation and in oxygen depleted media.

Preparation of Perchloric Acid Extracts and Analyses of Glycolytic Intermediates

To prepare perchloric acid extracts, triplicate 1 g samples of diapause and post-diapause embryos were collected on DryWipe filters and transferred to precooled mortars containing liquid nitrogen. The frozen cysts were ground into a fine powder and then extracted in 5 ml of 6% perchloric acid (PCA) using a ground glass homogenizer. The cyst extracts were kept at 0-4°C at all times. The crude extracts were centrifuged at 10,000 g for 10 min. The PCA-insoluble pellet was resuspended in 10 ml of 0.5 M NaOH prior to measuring protein by the method of Peterson (1977). The PCA-soluble supernatant was titrated to neutrality with 0.5 M K_2CO_3 and centrifuged at 10,000 g for 5 min to remove perchlorate salts. The extract was frozen in liquid nitrogen and stored at -80°C until analyses of metabolites were performed.

Neutralized PCA extracts were thawed and filtered with nylon syringe filters (Nalgene; 0.22 μm pore size), and assayed spectrophotometrically or fluorometrically for glycolytic intermediates using NADH- and NADPH-linked enzymatic assays (Lowry and Passonneau 1972; Carpenter and Hand 1986a). The final volume of all reaction mixtures was 1.0 ml and the reactions were conducted at 25°C. Glucose was estimated by adding crude extract to a reaction mixture containing 5.6 units of hexokinase (HK), 1 mM $MgCl_2$, 0.2 mM dithiothreitol (DTT), 0.05 mM $NADP^+$, 0.3 mM ATP, 50 mM Tris/HCl buffer (pH 8.1) and measuring the increase in absorbance of NADPH at 340 nm. Glucose-6-phosphate was similarly assayed by addition of crude extract to a reaction mixture containing 1.2 units of G6P dehydrogenase, 0.5 mM DTT, 0.05 mM $NADP^+$, and 50 mM Tris/Cl^- buffer (pH 8.1). Fructose-6-phosphate was measured by addition of PCA extract to a reaction mixture containing 7.5 units of phosphoglucoisomerase, 0.5

mM DTT, 0.05 mM $NADP^+$, 50 mM Tris/Cl^- (pH 8.1) and measuring change in absorbance at 340 nm. Glyceraldehyde-3-phosphate, dihydroxyacetone phosphate, and fructose-1,6-bisphosphate were assayed by the sequential additions of 4.0 units of glyceraldehyde-3-phosphate dehydrogenase, 12.2 units of triosephosphate isomerase, and 0.42 units of aldolase to a reaction mixture containing the crude extract, 3 mM DTT, 7.5 μM NADH, and 50 mM imidazole/Cl^- buffer, pH 7.5. Phosphoenol pyruvate and pyruvate were measured by adding the crude extract to a reaction mixture containing 50 mM phosphate buffer (pH 7), 2 mM $MgCl_2$, 200 μM ADP, 0.15 mM NADH, 0.15 U/ml pyruvate kinase and 0.2 U/ml lactic dehydrogenase (Lowry and Passonneau 1972). Owing to the nature of the pyruvate carrier (pyr/H^+ symport; Denton and Halestrap 1979), pyruvate concentrations in the cytosol and mitochondrial matrix are assumed to be equilibrated during diapause when mitochondrial ΔpH is probably zero. Any increase in matrix pyruvate for energized post-diapause embryos (due to a ΔpH of 0.5; Kwast and Hand 1996) would make little difference to cytosolic pyruvate concentration since its accumulation into the mitochondria at equilibrium would be small [3-fold into ~5% of the cell volume in *A. franciscana* embryos, since the cell volume occupied by mitochondria is about 5% (Rees et al. 1989) and matrix volume is roughly 50% of total mitochondrial volume in the semi-condensed/condensed states (Scalettar et al. 1991)]. In any case, matrix accumulation of pyruvate would be partially offset by its consumption by PDH (Denton and Halestrap 1979).

Measurement of Acetyl CoA

Acetyl-CoA was extracted from diapause and post-diapause embryos with organic solvent and enriched with ion exchange chromatography following the methods described by Minkler et al. (2008). Cysts were ground to powder in a pre-cooled mortar containing liquid nitrogen as above. Ground tissue powder (1 g) was then extracted with 5 ml of a 3:1 mixture of acetonitrile/isopropanol (V+V) in a ground glass homogenizer on ice. Next 1.7 ml of 0.1 M

KH_2PO_4 buffer (pH 6.7) was added and the extract re-homogenized. The homogenate was then centrifuged at 20,000 x *g*, 4°C for 5 min. Acetyl CoA in the supernatant was enriched by chromatography on an anion exchange column composed of 2-(-2-pyridyl)ethyl-functionalized silica gel (Cat. # 54127-U, Sigma-Aldrich Chemical Co., St. Louis, MO, USA). Immediately prior to loading onto the column, the extract was acidified by addition of glacial acetic acid (0.25 ml per ml extract). The column was pre-conditioned with a solution of acetonitrile/isopropanol/water/acetic acid in the proportion 9:3:4:4 (V+V+V+V). After application of the sample and subsequent flow through, the column was washed with 1 ml of the acetonitrile/isopropanol/water/acetic acid solution to remove unbound material. The acetyl CoA was then eluted with about 1ml of methanol/0.25 M ammonium formate (pH 7.0) in the ratio 4:1 (V+V). In order to concentrate acetyl CoA, the eluant was vacuum-dried and then stored at -80°C. Prior to HPLC analysis (see below), each sample was reconstituted in 0.1 ml deionized water.

HPLC Measurements of Adenylates, Acetyl CoA and Trehalose

Both adenylates and acetyl CoA were analyzed using the same HPLC protocol, which was modified from Menze et al. (2005). PCA extracts containing adenylates and the reconstituted acetyl CoA samples were first filtered (0.22 μm pore size). HPLC analyses were performed with a Dionex HPLC system (Dionex, Sunnyvale, CA), which included a PDA-100 photodiode array detector, GP-50 gradient pump, and AS50 autosampler. Samples were maintained at 4°C prior to injection and then applied to a 4.6 mm x 250 mm reversed phase Synergy 4μ Hydro-RP column. The analytes were eluted isocratically for 10 min with a starting buffer of 50 mM K_2HPO_4/KH_2PO_4 containing 10 mM tetrabutylammonium bisulfate at a flow rate of 1 ml/min at 25°C. A linear gradient from 0% to 40% acetonitrile was then applied over 40 min. The absorbance of the eluent was monitored with a photodiode array detector at

wavelengths ranging from 190 to 390 nm. Peaks corresponding to acetyl CoA or adenylates were identified by comparison to retention times obtained with bona fide standards. Concentration of analyte in the sample was determined from measurement of peak area at 260 nm wavelength. Calibration curves were linear over the range assayed.

For trehalose analysis, aliquots of PCA extracts were filtered as before and carbohydrate peaks separated with a Dionex MA-1 column (250x4 mm I.D.) operating at 25°C. The mobile phase was 600 mM NaOH at a flow rate of 0.3 ml/min. Peaks corresponding to trehalose were identified by comparison of retention times to the trehalose standard (Ferro Pfanstiehl Laboratories, Inc., Waukegan, IL, USA). The eluted peaks were quantified using pulsed amperometric detection employing waveform-A on a Dionex ED40 module. Calibration curves were linear over the range assayed.

It is appropriate to note that we assumed that the measured concentrations of adenylates for embryo tissue were equal to those in the cytosolic compartment. Since ATP is concentrated in the mitochondria, and ADP even more so, this assumption will lead to an underestimate of the cytosolic ATP/ADP ratio. In rodent hepatocytes in the energized state this underestimate is ~33-60% (Seiss et al 1977, Akerboom et al 1978). However, the underestimate is apt to be considerably smaller in *A. franciscana* embryos due to the reduced cell volume occupied by mitochondria (5%) compared to a value of 23% for rodent hepatocytes (Beauvoit et al 1994). How this underestimate alters between diapause and post-diapause in *A. franciscana* embryos is unknown. Consequently, our mass action ratios for cytoplasmic enzymes using tissue ATP and ADP values are only approximate.

Western Blot Analysis

Whole embryos (50 mg samples) were homogenized at room temperature directly in 2 ml of Laemmli sample buffer composed of 62.5 mM Tris-HCl (pH 6.8), 2% SDS, 25% glycerol, and

5% β-mercaptoethanol. The homogenate was boiled for 5 min and the sample separated on a SDS PAGE gel (10 % acrylamide) along with biotinylated standard protein markers. Separated proteins were transferred to a nitrocellulose membrane using a standard Western blot protocol. The membrane was probed with primary antibody against phospho-PDH site 1 [polyclonal PhosphoDetect Anti-PDH-E1α (pSer293), rabbit host; Merck KGaA, Darmstadt, Germany] at 4°C overnight. After washing, the membrane was then incubated with secondary antibody against rabbit IgG conjugated to horseradish peroxidase. The anti-rabbit IgG secondary antibody is conjugated to horse radish peroxidase (HRP) and visualized with Lumiglo chemiluminescent reagent (Cell Signaling Technology). An antibody against α-tubulin [rabbit host; Cell Signaling Technology, Danvers, MA] was used as a loading control in all blots. Quantification of bands was performed with Quantity One Basic 4.6.9 (Bio-Rad, Hercules, CA).

Statistical Analyses

Analyses were performed with GraphPad Prism statistical software (ver. 5.04, GraphPad Software, La Jolla, CA, USA.), and significance was evaluated by *t-test*. A p-value of ≤ 0.05 was considered significant.

2.3 Results

Metabolic Depression for Synchronized Diapause Embryos

Diapause embryos of *A. franciscana* from the Great Salt Lake, UT, which were synchronized to within 4 h of release from ovigerous females, display a rapid decrease in respiration rate during the first 3 days after release, followed by a slower decline through day 26 (open symbols, **Fig. 2.1**). For these data collected in 2009, the earliest time point obtained was for day 1 post-release, and results collected for other time points are expressed relative to this value. This format allows comparison to the data reported for diapause embryos from San

Francisco Bay, CA (solid symbols, **Fig. 2.1**; Clegg et al. 1996). The absolute respiration rates for the 2009 diapause embryos from the Great Salt Lake (average for the two independent holding tanks), were 3.46 pmol O_2 s^{-1} mg $embryo^{-1}$ at day 1 and 0.07 pmol O_2 s^{-1} mg $embryo^{-1}$ at day 26, which indicate a metabolic depression across this interval alone of over 98%. Taking into account the overall profile for both data for San Francisco Bay and the Great Salt Lake, the percent depression would be well beyond 99%.

Collection and 4-h synchronization of diapause embryos was repeated in 2011 with additional time points collected immediately after release (inset, **Fig. 2.1**). In 2011 the temperature of the lake water was much warmer, and the embryos were not as uniformly released in the diapause state compared to 2009. Some of the released embryos hatched during the holding period, and the resulting larvae were eliminated from the pool. Higher and more variable respiration rates are clearly evident, and the profile underscores the variation that exists from year-to-year. Nevertheless, by day 26, respiration rate eventually declined to 1.4% of the day 0 value.

Comparison of Adenylates in Diapause and Post-Diapause Embryos

The concentration of ATP in diapause embryos is about 5 fold lower as compared to post-diapause embryos, and ADP is not statistically different between the two states (**Table 2.1**). AMP was 20-fold higher in diapause embryos compared to post-diapause. While the elevated AMP and significantly lower concentration of ATP in diapause are consistent with an energy-limited state, the drop in ATP is not as strong as that measured under anoxia in post-diapause embryos (Stocco et al. 1972, Carpenter and Hand 1986a, Rees et al. 1989, Anchordoguy and

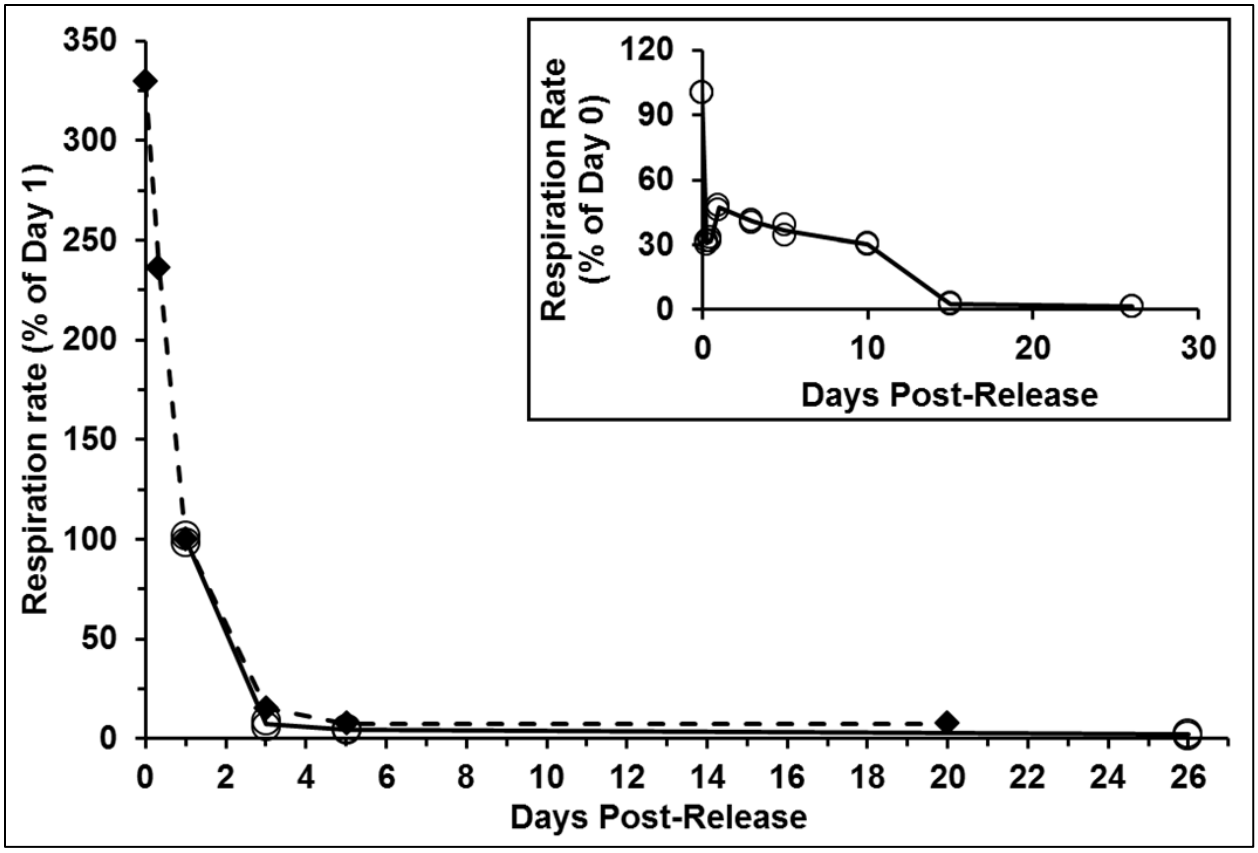

Figure 2.1. Depression of respiration rate for diapause embryos of *A. franciscana* from the Great Salt Lake (solid line) as a function days post-release. Embryos were synchronized to within 4 h of their release from ovigerous females. Independent replicates for each batch collected in 2009 are displayed by superimposed open circles. Data are also provided for San Francisco Bay embryos (dashed line, solid diamonds; Clegg et al. 1996) expressed relative to the day 1 values to allow comparison. Inset: Respiration data collected in 2011 for synchronized embryos from the Great Salt Lake illustrate the variation evident from year-to-year. Data are expressed as a percentage of the day 0 value.

Hand 1994). The adenylate energy charge [AEC; calculated as ([ATP]+1/2[ADP])/ ([ATP]+[ADP]+[AMP])] in the diapause state was calculated to be 0.25 versus 0.91 in post-diapause embryos (**Table 2.1**). In contrast the AEC after 24 h of anoxia in post-diapause embryos is approximately 0.09 (Anchordoguy and Hand 1994).

Inhibition of Carbohydrate Catabolism during Diapause

As discussed earlier, the primary metabolic fuel for embryos prior to hatch is the carbohydrate trehalose (Dutrieu 1960, Muramatsu 1960, Emerson 1963, Clegg 1964,

Clegg and Conte 1980, Carpenter and Hand 1986a), and thus insights into the mechanism of inhibition of carbohydrate catabolism are key to explaining arrest of respiration rate seen above during diapause entry. Product/substrate ratios for primary carbon compounds involved in pathway flux (i.e., pathway intermediates) are used here to identify potential inhibition sites (crossover points) in the pathway (Chance et al. 1958, Rolleston 1972, Lehninger 1975). The crossover theorem predicts that when deceleration of a reaction occurs because of an inhibitory influence one would expect a decrease in the ratio of product to substrate.

Table 2.1. Adenylate levels in diapause and post diapause embryos. Concentrations are expressed as mean ± SE, N = 10 (diapause), N = 8 (post-diapause). Asterisks indicate statistical differences, $p \leq 0.0001$ (diapause versus post-diapause for AMP, ATP, ATP/ADP, and AEC). ADP concentration is not statistically different between diapause and post-diapause embryos.

Adenylates	**Diapause (µmoles/g embryo)**	**Post-diapause (µmoles/g embryo)**
AMP	0.622 ± 0.036*	0.031 ± 0.005
ADP	0.126 ± 0.010	0.112 ± 0.006
ATP	0.168 ± 0.008*	0.812 ± 0.010
ATP/ADP	1.306 ± 0.036*	7.300 ± 0.276
AEC	0.253 ± 0.009*	0.908 ± 0.002

The product to substrate ratio for the enzyme trehalase calculated for diapause and post-diapause embryos (**Fig. 2.2**) was significantly lower in diapause as compared to post-diapause embryos, indicating an inhibition at the trehalase reaction during diapause. Inhibition of trehalase would reduce the flow of metabolic fuel into the glycolytic pathway. The level of glucose-6-phosphate in diapause embryos was about 14-fold lower as compared to post-diapause embryos (**Table 2.2**), and the product to substrate ratio for hexokinase in diapause is strikingly lower than the ratio in post-diapause embryos (**Fig. 2.3A**). The strong negative crossover point at hexokinase in diapause suggests a potent inhibition of its activity.

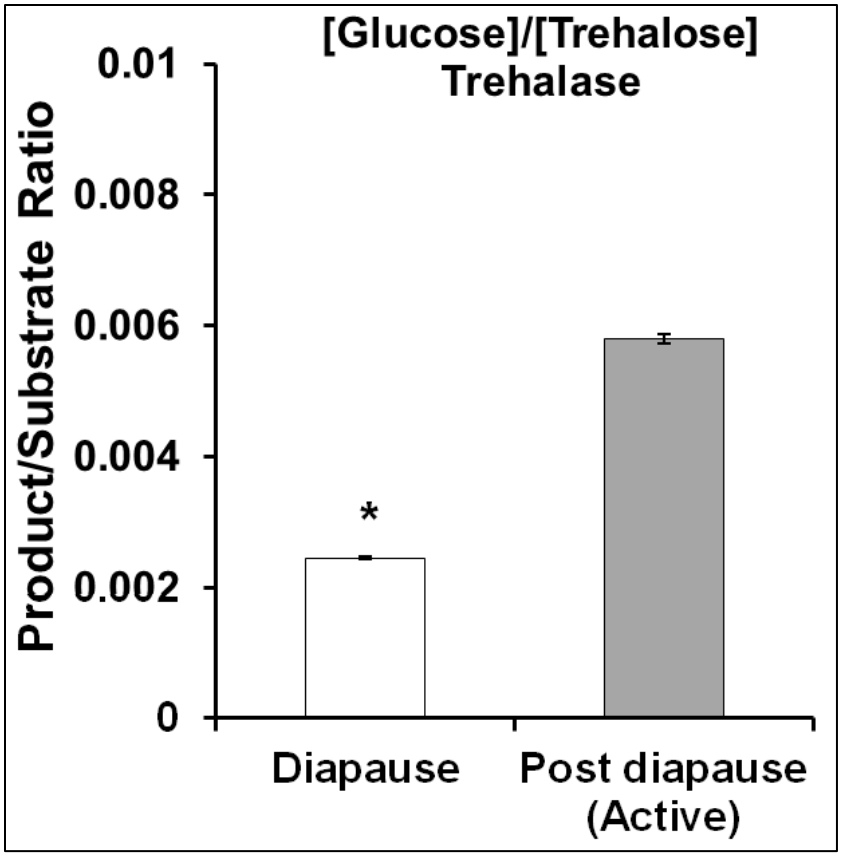

Figure 2.2. Product to substrate ratios for the trehalase reaction in diapause embryos (open bar) compared to that for post-diapause embryos (grey bar). Values are mean ± SEM for N = 4. Asterisk denotes statistical significance with $p \leq 0.0001$.

The concentration of fructose-6-phosphate was also determined to be substantially lower in diapause embryos as compared to post-diapause embryos (**Table 2.2**). The product to substrate ratio for phosphoglucoisomerase, which catalyzes the interconversion between glucose-6-phosphate and fructose-6-phosphate, is higher in diapause embryos as compared to the post-diapause embryos (**Table 2.3**), which does not indicate any inhibition of this enzyme in diapause. The depletion of glucose-6-phosphate due to the upstream inhibition of hexokinase likely causes the increased ratio. The product to substrate ratio (fructose-1,6-bisphosphate/fructose-6-phosphate) for phosphofructokinase is higher in diapause embryos as compared to the post-diapause (**Table 2.3**), again indicating a lack of inhibition at this step. The

tissue concentrations of fructose-6-phosphate and fructose-1,6-bisphosphate were both lower in diapause embryos (**Table 2.2**), as were levels of dihydroxyacetone phosphate.

Glyceraldehyde-3-phosphate was undetectable in extracts of diapause embryos and consequently product to substrate ratios could not be determined for aldolase and triose phosphate isomerase in diapause embryos. The next three glycolytic intermediates downstream of aldolase were also too low for detection. The enzymes involved in this segment of the glycolytic pathway namely glyceraldehyde-3-phosphate dehydrogenase, phosphoglycerate

Table 2.2. Selected glycolytic intermediates measured in diapause and post-diapause embryos. Data are expressed as mean ± SEM, N=5. Glyceraldehyde-3-phosphate concentration is the below detection limits (not detected, *n.d.*) in diapause embryos.

Selected Glycolytic Intermediates	**Diapause nmol/g cysts**	**Post-diapause nmol/g cysts**
Glucose	405.88 ± 7.13	326.33 ± 2.36
Glucose-6-phosphate	17.95 ± 0.63	251.14 ± 2.16
Fructose-6-phosphate	6.51 ± 0.40	50.92 ± 0.53
Fructose-1,6-bisphosphate	2.75 ± 0.02	7.61 ± 0.54
Dihydroxyacetone phosphate	10.77 ± 0.05	43.19 ± 1.88
Glyceraldehyde-3-phosphate	*n.d.*	4.16 ± 0.21
Phosphoenol pyruvate	38.11 ± 0.465	22.6 ± 0.45
Pyruvate	5.73 ± 0.285	14.07 ± 0.945
Acetyl CoA	0.232 ± 0.041	1.328 ± 0.068

kinase, phosphoglycerate mutase and enolase, catalyze near-equilibrium reactions and typically do not exhibit a high degree of regulation within the pathway (e.g., Heinrich and Rapoport 1974, Crabtree and Newsholme 1985).

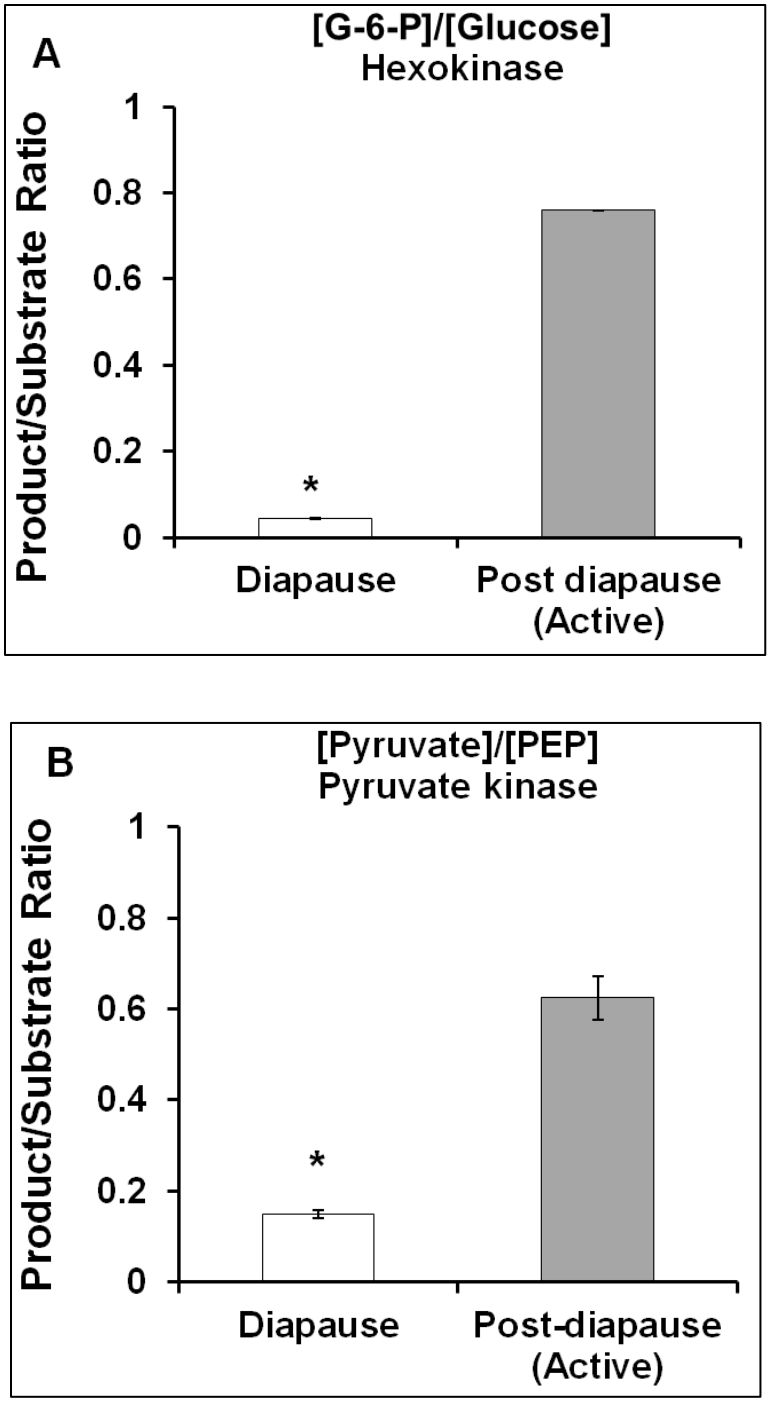

Figure 2.3. Product to substrate ratios for the hexokinase reaction (A) and the pyruvate kinase reaction (B) in diapause embryos (open bar) compared to that for post-diapause embryos (grey bar). Values are mean ± SEM for N = 4. Asterisk denotes statistical significance with $p \leq 0.0001$.

Phosphoenolpyruvate measured in diapause was substantially higher compared to post-diapause embryos, and pyruvate concentration was significantly lower (**Table 2.2**). The product to substrate ratio for pyruvate kinase (pyruvate/phosphoenol pyruvate) was 0.15 ± 0.009 (mean ± SE) in diapause embryos, while the ratio in post-diapause embryos was significantly higher (0.62 ± 0.048), which indicates a significant inhibition for this enzyme during diapause (**Fig. 2.3B**).

Table 2.3. Product to substrate ratios for phosphoglucoisomerase and phosphofructokinase do not indicate inhibition of these enzymes. Values are expressed as mean ± SEM, N = 5; $p \leq 0.0001$. Asterisks indicate statistical difference.

Product/Substrate	**Enzyme**	**Diapause**	**Post-diapause**
[fructose-6-phosphate]/ [glucose-6-phosphate]	***Phosphoglucose isomerase***	0.362 ± 0.012*	0.201 ± 0.0009
[fructose-1,6-bisphosphate]/ [fructose-6-phosphate]	***Phosphofructo-kinase***	0.403 ± 0.007*	0.144 ± 0.005

Restriction of Carbon Flux into the Mitochondrion

The mitochondrial pyruvate dehydrogenase complex (PDC) is a key gateway step for entry of the carbon flux from the glycolytic pathway to the mitochondrion. PDC is responsible for catalyzing the conversion of pyruvate and acyl CoA to form acetyl CoA. The product to substrate ratios for PDC suggests an inhibition of the enzyme complex in diapause (**Fig. 2.4**). PDC inhibition would restrict carbon entry into the TCA cycle and thus reduce the capacity of the mitochondrion for oxidative phosphorylation.

PDC can be inhibited by phosphorylating pyruvate dehydrogenase (PDH) subunit E1α at three phosphorylation sites (Kolobova et al. 2001, Patel and Korotchkina 2001). Phosphorylation at site 1 (serine 293) causes the PDC to be inhibited by almost 90%. Western blot analysis shows the phosphorylated form of PDH (pPDH) in bulk (non-synchronized)

diapause embryos is approximately two-fold greater than for post-diapause embryos (**Fig. 2.5A**). Next, pPDH was evaluated in diapause embryos that had been synchronized to within 4 h of release from ovigerous females.

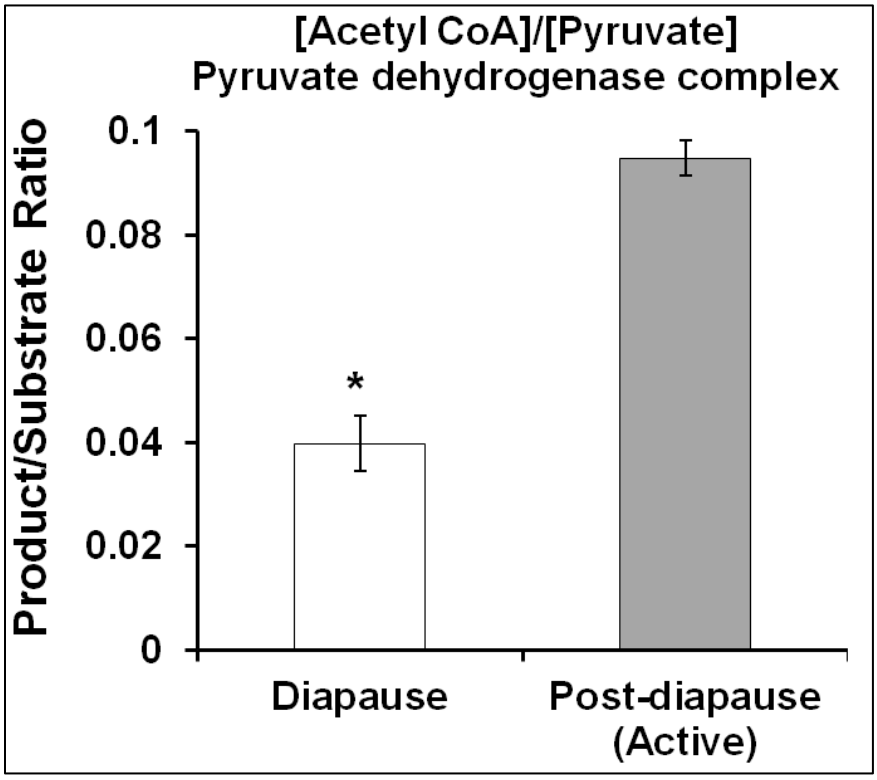

Figure 2.4. Product to substrate ratios for the pyruvate dehydrogenase complex reaction in diapause embryos (open bar) compared to that for post-diapause embryos (grey bar). Values are mean ± SEM for N = 3 (diapause) and N = 6 (post-diapause). Asterisk denotes statistical significance with $p \leq 0.0001$.

As a function of days after release, pPDH (normalized to α-tubulin) progressively increases by 400% (**Fig. 2.5B**). The greater amount of pPDH in the diapause state is consistent with the inhibition of PDC as predicted by metabolite analyses.

Calculation of MAR/*K*'eq Values for Catabolic Reactions

Based on our metabolite measurements, we have calculated values for the mass action ratio divided by the equilibrium constant (MAR/*K*'eq) for the trehalase reaction and steps in the

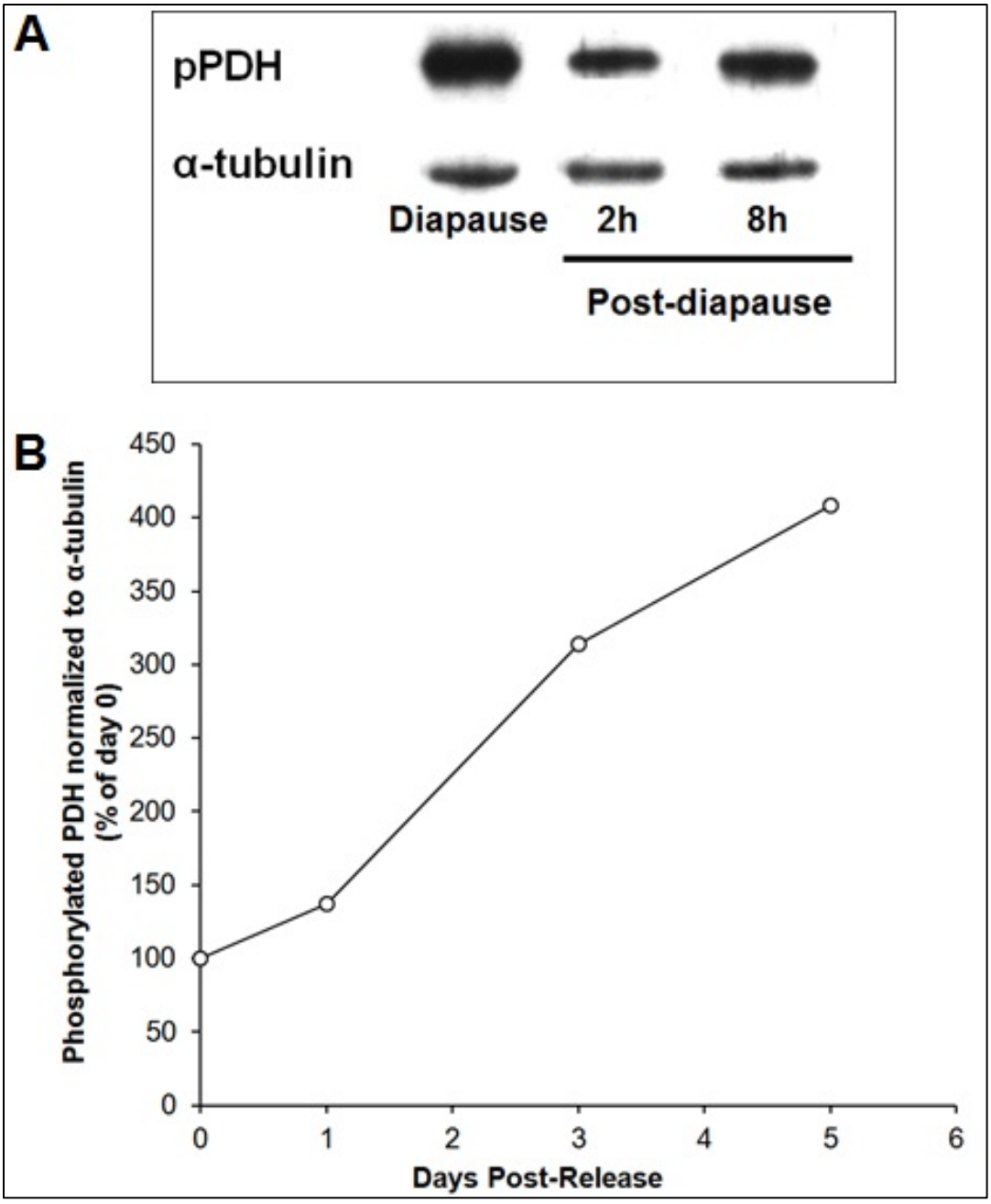

Figure 2.5. Western blot analysis of the phosphorylation status of pyruvate dehydrogenase (pPDH) in diapause and post-diapause embryos. (A) pPDH in bulk (non-synchronized) diapause embryos compared to post-diapause embryos incubated for 2 and 8 h at room temperature. α-tubulin is shown as the loading control. Relative intensity of pPDH is greater in diapause embryos than during post-diapause. (B) pPDH normalized to α-tubulin is shown for 4-hour synchronized diapause embryos as a function of days post-release from ovigerous females. Intensity was quantified by densitometry and increases 4-fold across the time interval shown. Antibody against phosphorylated PDH site 1 (serine 293, subunit E1α) was employed.

glycolytic pathway for post-diapause (active) embryos (**Fig. 2.6**). Insufficient metabolite data are available for the PDH reaction. For a given reaction, the MAR/*K*'eq indicates the extent of displacement from equilibrium. Values for log MAR/*K*'eq < -1.3 (MAR/*K*'eq less than 0.05)

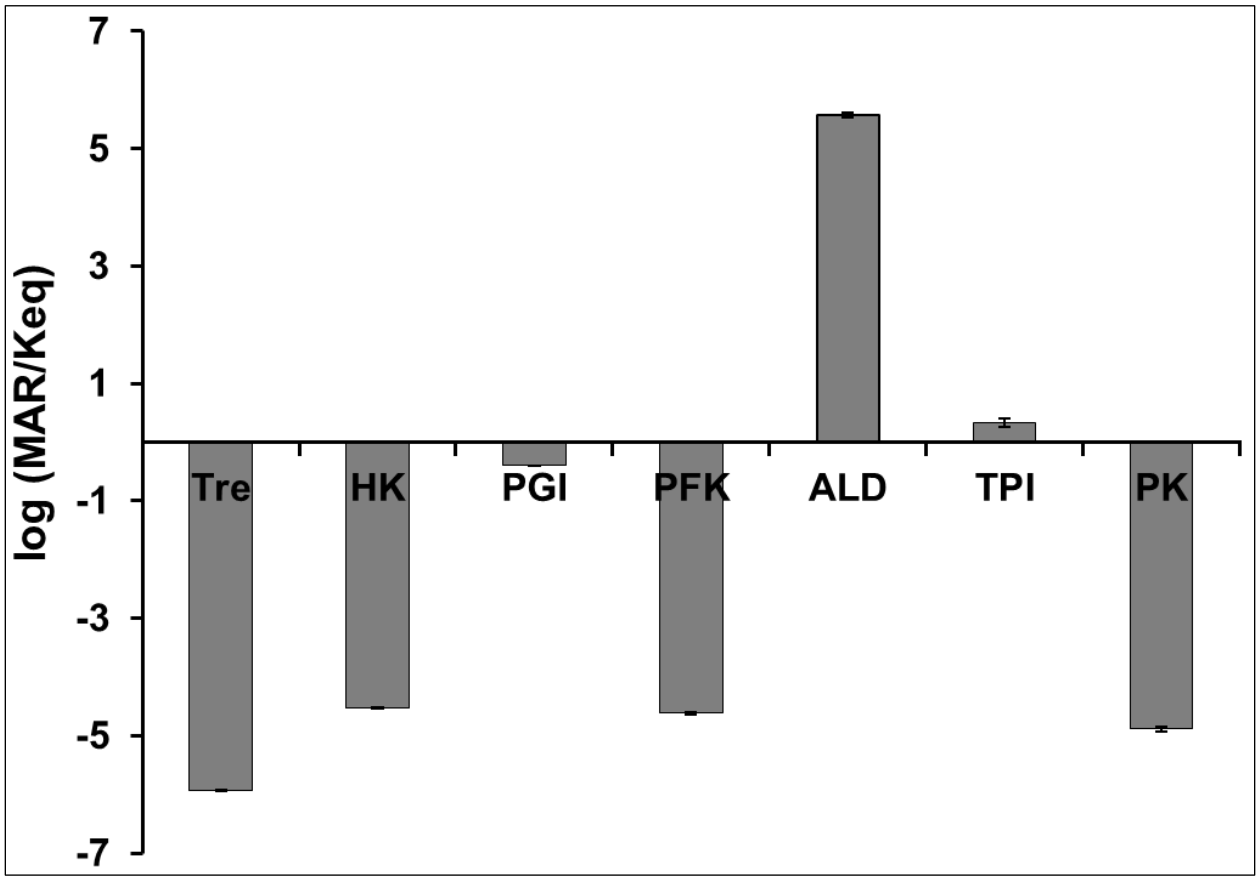

Figure 2.6. Comparison of MARs with their respective equilibrium constants (*K*'eq) for trehalase and several glycolytic reactions. The MAR values (means±SEM) were calculated from post-diapause metabolite values. Values of the ratio MAR/*K*'eq of less than 0.05 (log MAR/*K*'eq < -1.3) indicate reactions that are far from thermodynamic equilibrium (Rolleston 1972). *K*'eq values for trehalase (Tre = 1682), hexokinase (HK = 3900) and phosphofructokinase (PFK = 910) are as given in Carpenter and Hand (1986a); *K*'eq values for phosphoglucoisomerase (PGI = 0.509), aldolase (ALD = 6.31 X 10-5), triose phosphate isomerase (TPI = 0.0455) and pyruvate kinase (PK = 3.15 X 105) were calculated from ΔGo' values as given in Lehninger (1982) using $\Delta G^{o\prime} = -2.303\ RT \log K'eq$.

were taken to indicate non-equilibrium reactions (Rolleston 1972). It is generally agreed that enzymes catalyzing reactions displaced far from equilibrium typically have an enhanced

potential for regulation of flux through a pathway (Rolleston 1972, Heinrich and Rapoport 1974, Crabtree and Newsholme 1985, Rees and Hand 1991). The resulting MAR/*K*'eq analysis shows trehalase, hexokinase, phosphofructokinase and pyruvate kinase as ideal candidates for points of metabolic regulation.

2.4 Discussion

The results of the present study suggest that the metabolic activity during diapause is arrested as a consequence of the orchestrated interplay of multiple enzyme inhibitions (**Fig. 2.7**). The outcomes of this metabolic arrest manifest as a restriction of the glycolytic pathway and a concomitant limitation of glycolytic input to the mitochondrion aided additionally by depression at the pyruvate dehydrogenase complex. This substrate deprivation to mitochondria, which likely occurs progressively soon after release of the diapause embryo from the female, may be largely responsible for the time-dependent drop in embryonic respiration observed over the ensuing days (**Fig. 2.1**). The rate of oxygen consumption decreases by over 99% during diapause entry, and it should be emphasized that some or all of this low residual rate could be unrelated to mitochondrial oxidative phosphorylation. This point underscores the magnitude of the respiratory inhibition during diapause. Due to the limited availability of synchronized embryos, time-course data for changes in the status of cellular adenylates are unavailable, but a drop in ATP is clearly evident in non-synchronized embryos collected in bulk from the lake surface. Decreased glycolytic intermediates (**Table 2.2**) suggest that in a system with very high concentrations of stored fuel (trehalose), the global arrest of cellular metabolism is a means to conserve the fuel. Based on comparisons of product to substrate ratios in diapause versus post-diapause embryos, four sites of inhibition are identified: reactions catalyzed by trehalase, hexokinase, pyruvate kinase, and pyruvate dehydrogenase (**Fig. 2.7**). The values for MAR/*K*'eq

for all four enzyme steps (**Fig. 2.6**) indicate displacement far from equilibrium and consequently possess regulatory potential. Trehalase is the entry point for carbon into the glycolytic pathway; hence an inhibition of trehalase could be viewed as a key step in downregulating metabolism during diapause.

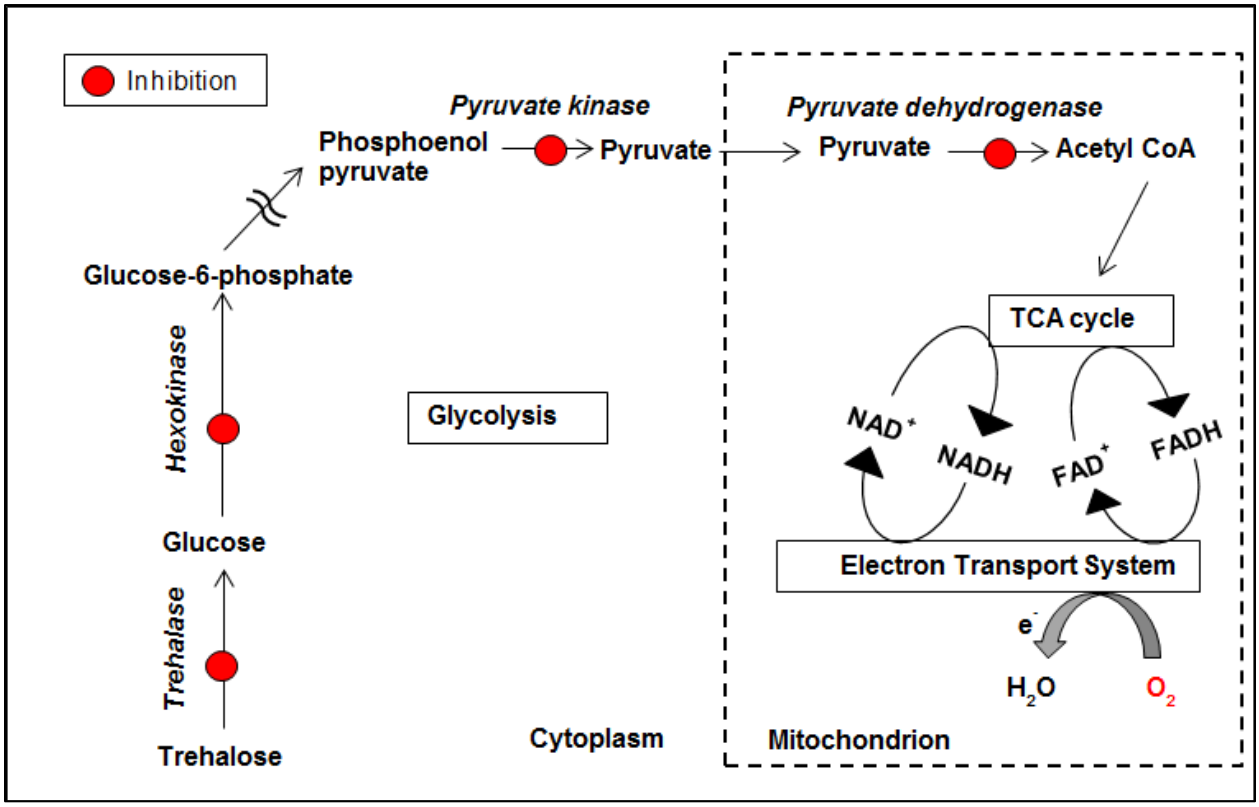

Figure 2.7. Schematic representation of metabolic arrest in *A. franciscana* during diapause. Carbon flux is depressed at trehalase, two control sites in the glycolytic pathway (HK, PK), and at least one site in the mitochondrion (PDC). The restricted glycolytic pathway could lead to substrate limitation in the mitochondrion and promote downregulation of oxygen consumption.

The first enzyme step inhibited within the glycolytic pathway is that catalyzed by hexokinase, and the negative crossover point at the step is strong in diapause. It is pertinent to note that during anaerobic quiescence in *A. franciscana* embryos, three enzymes of carbohydrate catabolism (trehalase, hexokinase, and phosphofructokinase, PFK) are inhibited (Carpenter and Hand 1986a). Evidence indicates that this metabolic arrest under anoxia is strongly dependent on

acidic pH_i, and further, that these same three steps are blocked by artificial acidification of embryos under fully normoxic conditions (aerobic acidosis). The point here is inhibition of PFK is conspicuously absent during diapause based on the present study. If acidification of pH_i is in some way involved in the metabolic depression during diapause (see discussion below), it is surprising that PFK is apparently not impacted. The kinetic sensitivities of these three enzymes from *A. franciscana* embryos have been characterized (Hand and Carpenter 1986, Rees et al. 1989, Carpenter and Hand 1986b).

Pyruvate delivery to the mitochondrion as a substrate for the TCA cycle to support oxidative phosphorylation is essential if respiration is to be uninterrupted during this stage of development in *A. franciscana* embryos. During diapause, product to substrate ratios indicate that reactions catalyzed by pyruvate kinase (PK) and pyruvate dehydrogenase complex (PDC) are depressed (**Figs. 2.3B, 2.4**). PK can be inhibited by phosphorylation, which reduces its affinity for its substrate phosphoenol pyruvate (Siebenaller 1979) and for its key activator fructose-1,6-bisphosphate. The enzyme is also important in regulating the glycolytic versus oxidative phosphorylation poise of cell metabolism (Christofk et al. 2008, Vander Heiden et al. 2009). We were unsuccessful in identifying an antibody that could recognize PK from *A. franciscana* embryos and distinguish its phosphorylation states. Pyruvate formed by PK in the glycolytic pathway is transported into the mitochondrion to be processed by PDC. The amount of the phosphorylated PDC (site 1 on subunit E1α) is higher in non-synchronized diapause embryos than in post-diapause embryos (**Fig. 2.5**), which is supported by the increase in pPDH seen for synchronized embryos as a function days post-release from females. Both observations are consistent with inhibition of the enzyme during diapause. We were unable to calculate the proportion of phosphorylated PDC due to the absence of an antibody that could detect total PDC in *A. franciscana* embryos.

Our measurements of adenylates in bulk diapause embryos collected from the surface of the Great Salt Lake show lower amounts of ATP and higher amounts of AMP than present in post-diapause embryos (**Table 2.1**). As mentioned earlier, this drop in ATP is less severe than during anoxia in post-diapause embryos. The poise of diapause adenylates could be in part a reflection of the embryo pH_i that is not depressed at least in early diapause, as reported by (Drinkwater and Crowe 1987); in contrast, acidification of pH_i under anoxia in post-diapause embryos is very dramatic (from $\geq$ 7.9 under normoxia, to 6.7-6.8 after an hour of anoxia, to as low as pH 6.3 overnight under anoxia; e.g., Busa et al. 1982, Kwast et al. 1995, Clegg et al. 1995, Covi et al. 2005). Clegg (2011) suggests there could be a role for pH_i in the metabolic depression during diapause, and that time-course measurements of pH_i are needed during the entire metabolic depression phase after embryos are release from the female. If pH_i is involved in diapause, it also would be of interest to know from where the protons arise. At least for anoxia, one concept proposes that in addition to acidification from NTP hydrolysis, proton may be released from acidic intracellular compartments (Covi et al. 2005, Hand 2011). Unpublished observations mentioned by Drinkwater and Crowe (1987) and Drinkwater and Clegg (1991) indicate that exposure of embryos to anoxia during early diapause can depress pH_i.

It is appropriate to note that mitochondria isolated from diapause and post-diapause embryos display quite similar capacities for oxidative phosphorylation (Reynolds and Hand 2004). Thus, mitochondrial inhibition during diapause must be a consequence of substrate limitation *in vivo* and/or an inhibition not preserved in the isolated mitochondria. A diffusible metabolite/inhibitor only present in intact embryos or a covalent modification not retained during the isolation procedure would be among some of the possibilities. The elevated PDH phosphorylation during diapause discussed above was captured by rapidly quenching and extracting whole embryos with a denaturing reagent that prevented phosphatase activity from

reversing the effect. The possibility of a diffusible inhibitor accumulated during diapause is currently being explored.

Many mysteries remain regarding the severe metabolic depression occurring during diapause. It is not yet known if there is some molecular signaling agent within the embryo that might facilitate the process. For example, it has been documented that nitric oxide is *not* involved with breakage of (release from) the diapause state (Robbins et al. 2010). While it is clear that diapause embryos, freshly released from ovigerous females, possess an alkaline pH_i (Drinkwater and Crowe 1987), it is unclear whether or not there is any change in pH_i under normoxia as the metabolic depression phase progresses. Certainly the pattern is strikingly different from the time-course of anoxic shutdown in these embryos, which can occur in the order of minutes (e.g., Hand and Gnaiger 1988). Perhaps differential gene expression contributes in some manner to the metabolic downregulation during diapause (Hahn and Denlinger 2011, MacRae 2010, Hand et al. 2011). Nevertheless, the results of the present study allow a more complete picture to be painted of the physiological and biochemical events occurring during one of the most profound metabolic arrests documented for animals under normoxia.

CHAPTER 3

RESPIRATION IN EMBRYO LYSATES REVEALS DIMINISHED COMPLEX I ACTIVITY AND INHIBITION OF THE PHOSPHORYLATION SYSTEM DURING DIAPAUSE IN *ARTEMIA FRANCISCANA*

3.1 Introduction

The diapause program is an alternative developmental pathway that delays direct morphogenesis and is characterized by ontogenetic arrest for a period spanning weeks to months (Koštál 2006). Diapause is genetically programmed and triggered by endogenous physiological factors in response to environmental cues; typically entry into this state precedes the onset of adverse environmental conditions and thus can serve to prepare the organism for ensuing stresses (Denlinger 2002, Denlinger 2012, Koštál 2006). Initiation of diapause involves differential gene expression that can control a number of features of the diapause phenotype (Hahn and Denlinger 2011; Qiu and MacRae 2010). A growing body of work on insect diapause has shed some light on possible mechanisms of hormonal control of the endogenous triggers such as diapause hormone and ecdysteroid (for reviews see Denlinger 2012, Hahn and Denlinger 2011). Developmental arrest may be accompanied by metabolic arrest depending on the developmental stage and the species in which diapause occurs (Denlinger 2002, Hahn and Denlinger 2011, Hand et al. 2011, Reynolds and Hand 2009, Denlinger et al. 2012). In some species, metabolic depression is not constantly maintained, and bouts of metabolic activity occur presumably to replenish fuel (Hahn and Denlinger 2011, Denlinger 2012). In contrast, it is arguable that one of the deepest metabolic arrests associated with diapause occurs in embryos of the brine shrimp *A. franciscana* (Clegg et al. 1996, Reynolds and Hand 2004, Patil et al. 2012). Respiration is depressed by over 99%, and at least part of the arrest is attributable to restriction of metabolic fuel to the mitochondrion (Patil et al. 2012). In this study we report evidence that there is also

diminished complex I activity and inhibition of the phosphorylation system as measured in concentrated lysates of *A. franciscana* embryos.

Adult *A. franciscana* females switch from ovoviviparous to oviparous reproduction in response to environmental cues (Dutrieu 1960, Berthelemy-Okazaki and Hedgecock 1987, Drinkwater and Clegg 1991,). The embryos thus formed are encysted and released into the water column where over a period of days they exhibit respiratory depression (Clegg et al. 1996, Patil et al. 2012). It should be noted that the metabolic depression is not synchronized with developmental arrest. Development is halted at the gastrula stage before the encysted embryos are released (Clegg and Conte 1980, Berthelemy-Okazaki and Hedgecock 1987). When released from the adult female, the diapause destined embryos have respiration values that are close to those of actively metabolizing embryos, however over the period of about 5 days post-release, the respiration decreases dramatically to barely detectable levels (Clegg et al. 1996; Patil et al 2012). This decrease in metabolic activity is relatively slow compared to the much faster metabolic depression seen as embryos enter quiescence when exposed to anoxia, a transition which occurs in minutes to hours (Carpenter and Hand 1986a, Hand and Gnaiger 1988). In principle, the more protracted depression during diapause would allow time for differential gene expression to contribute to the process. Drinkwater and Crowe (1987) showed that intracellular acidification apparently is not required for maintaining diapause in *A. franciscana*, and that alkalinization of diapause embryos does not enable these cysts to hatch, which supports the notion that mechanisms regulating diapause and quiescence are different. Indeed inhibition sites within the glycolytic pathway differ between diapause and quiescence (Carpenter and Hand 1986a, Patil et al. 2012). Whether or not there is a role of acidification of pH_i in the metabolic arrest during diapause is still debated (Clegg 2011).

Reynolds and Hand (2004) investigated mitochondrial bioenergetics of diapause embryos of *A. franciscana* and found that, at least in isolated mitochondrial preparations, there were no major differences in mitochondrial function between diapause and post-diapause embryos. However, the results with isolated mitochondria do not rule out the possibility that there could have been removal of an endogenous inhibitor during the purification process or a change in covalent modification of mitochondrial enzymes during the time required for isolation. For example, by homogenizing embryos in a SDS denaturing buffer, Patil et al. (2012) were able to demonstrate that phosphorylation of pyruvate dehydrogenase (which is associated with inhibition of the enzyme) occurred during entry into diapause. In this chapter, I report evidence that supports an inhibition of oxidative phosphorylation during diapause. ADP-stimulated (state 3) respiration rates were measured along with uncoupled respiration to evaluate oxidative phosphorylation capacity of the mitochondria when electrons were donated through either complex I or through complex I and II combined. Evidence present shows that pyruvate-based respiration through Complex I is substantially diminished in lysates from diapause embryos at all dilutions tested. Further, uncoupled control ratios indicate that the phosphorylation system is inhibited in diapause and that this inhibition is eliminated as the extract is diluted, a result consistent with the presence of an inhibition in diapause embryos.

3.2 Methods

Reagents

Sucrose was obtained from J.T. Baker (Paris, KY). All other reagents used were of the highest quality available and were purchased from either Fisher Scientific (Pittsburgh, PA) or Sigma-Aldrich (St. Louis, MO).

Processing of *A. franciscana* Embryos

All embryos originated from the Great Salt Lake, UT. Encysted diapause embryos were collected during the fall of 2009, 2010, and 2011. The embryos were washed and stored in 1.25 M NaCl with kanamycin (50 μg/ml), penicillin-streptomycin (50 μg/ml) and nystatin (200 units/ml) at room temperature. Prior to each assay, diapause embryos were incubated in 35 ppt artificial seawater (Instant Ocean™; Aquarium Systems, Mentor OH, USA) with orbital shaking (110 rpm) at room temperature for 4 days to allow non-diapause embryos to hatch; larvae and empty shells were removed using a separatory funnel. The viability of diapause embryos was confirmed periodically with the method described by Reynolds and Hand (2004). Briefly, unhatched cysts were dried at ambient temperature and humidity for up to two weeks. The dried cysts were treated with 3 % hydrogen peroxide prepared in 0.4 M NaCl for approximately 30 min. After rinsing with 0.25 M NaCl, the cysts were incubated as described above (35ppt artificial seawater, 4 d). After 4 days, the percentage hatching was determined. The number of nauplii divided by the total number counted (i.e. unhatched cysts + nauplii) was used to calculate percent viability. Cyst batches with a hatching percentage above 70% were considered to be suitable for study. It should be noted that some cysts are exceptionally refractory to diapause breakage with the above technique depending on the depth of diapause.

Dehydrated post-diapause embryos (Grade: laboratory reference standard) from the Great Salt Lake were obtained from Sander's Brine Shrimp Company (Ogden, UT) in 2008, 2010 and 2012. The dried embryos were stored at -20° C. In preparation for use in an experiment, these embryos were hydrated in 0.25 M NaCl at 0° C overnight. The embryos were then allowed to develop under normoxic conditions in 0.25 M NaCl at room temperature for 8 h. The hatching percentage for post-diapause embryos, as determined above in 35 ppt artificial seawater, was above 90%.

Preparation of Embryo Lysates for Respiration

Prior to homogenization, the hydrated cysts (10-20 g) were dechorionated by treatment with antiformin solution (1 % hypochlorite, 0.4 M sodium hydroxide, and 60 mM sodium carbonate) for 15-20 min at room temperature, followed by three rinses with ice-cold 0.25 M NaCl. Embryos were then incubated in ice-cold 1 % (w/v) sodium thiosulfate for 5 min and were rinsed two times with cold 0.25 M NaCl. Finally, embryos were incubated for 3-5 minutes in cold 40 mM hydrochloric acid prepared in 0.25 M sodium chloride, followed by three rinses with 0.25 M NaCl.

After dechorionation, the embryos were homogenized 1:1 (W/V) with a teflon-glass Potter-Elvehjem tissue homogenizer (Thomas Scientific, Swedesboro, NJ) in ice-cold medium composed of 0.5 M sucrose, 150 mM KCl, 2 mM $MgCl_2$, 10 mM KH_2PO_4, 1 mM EGTA, 0.5 % (w/v) bovine serum albumin (fatty acid free, fraction V), and 20 mM HEPES and titrated to pH 7.5 with 1.0 M KOH. The resulting homogenate was centrifuged at 1000 X *g* for 10 min at 4°C. The semi-transparent supernatant was collected with a 10 ml pipette, taking care to exclude the entire uppermost layer of lipoprotein and any material from the pellet fraction, and then stored on ice. Generally about 6.8 ml of this concentrated supernatant can be prepared from 10 g of hydrated embryos. Protein content was measured using Coomassie Plus (Bradford) assay kit (Thermo Fisher Scientific Inc., Rockford, IL). The protein content of the lysate was typically 30-34 mg/ml.

Oxygen Flux Measurements

Respiration measurements on embryo lysates were made at 25°C with an Oxygraph-2K (OROBOROS Instruments, Innsbruck) with polarographic oxygen sensors. Oxygen concentration and its time derivative, oxygen flux, were digitally recorded with OROBOROS Datlab 4 software. Oxygen sensors were calibrated routinely at air saturation and in oxygen

depleted media. The 2 ml respiration chamber was filled with undiluted lysate, or else lysate was added to homogenization medium in the chamber to yield final dilutions of 1/4, 1/10, and 1/100. Because of the high oxygen fluxes measured for the undiluted lysate and the 1/4 diluted lysate, oxygen concentration of the respiration chamber was elevated by raising the stopper partially, flushing the gas phase with ultrapure O_2, allowing equilibration with the liquid phase with stirring for the time necessary to reach 500-600 nmol O_2/ml, and then closing the chamber. The gain for the sensors was set at 2 instead of the default setting of 4 for these studies at high oxygen. Steady state oxygen flux was measured first without any additions, which corresponded to respiration with endogenous substrates and endogenous ADP (denoted as Ee). Next ADP (final concentration 2.5 mM) was then added to the chamber and respiration was recorded (E3). E3 denotes respiration with endogenous substrates and excess, exogenous ADP. ADP-stimulated respiration with saturating Complex I substrates (state 3) was initiated by adding 15 mM pyruvate plus 2 mM malate (E3PM). ADP-stimulated respiration with saturating Complex I plus Complex II substrates (state 3) was initiated by adding 15 mM pyruvate, 2 mM malate and 10 mM succinate (E3PMS). In some cases, E3PM and E3PMS measurements were carried out in separate trials. It is appropriate to note that all Complex II assays were performed without rotenone. Preliminary experiments verified that no differences were observed in succinate-stimulated respiration the presence or absence of rotenone. Next, the respiration mixture was titrated with FCCP (typically 0.5 µM increments) to determine the maximum electron transport system (ETS) capacity in the uncoupled state; for more concentrated extracts, an initial addition of 2-4 µM FCCP was made followed by 0.5 µM increments to reach the maximum uncoupled rate, in order to constrain the time and oxygen utilization from the chamber (E3PMu or E3PMSu). Finally, residual (non-mitochondrial) oxygen consumption was measured by addition of 2.5 µM antimycin A and used in data background correction. During respirometry

runs, the oxygen in the chamber was periodically replenished to the starting values with the procedure described earlier. Respirometric traces obtained with a typical protocol are shown in **Figure 3.1.**

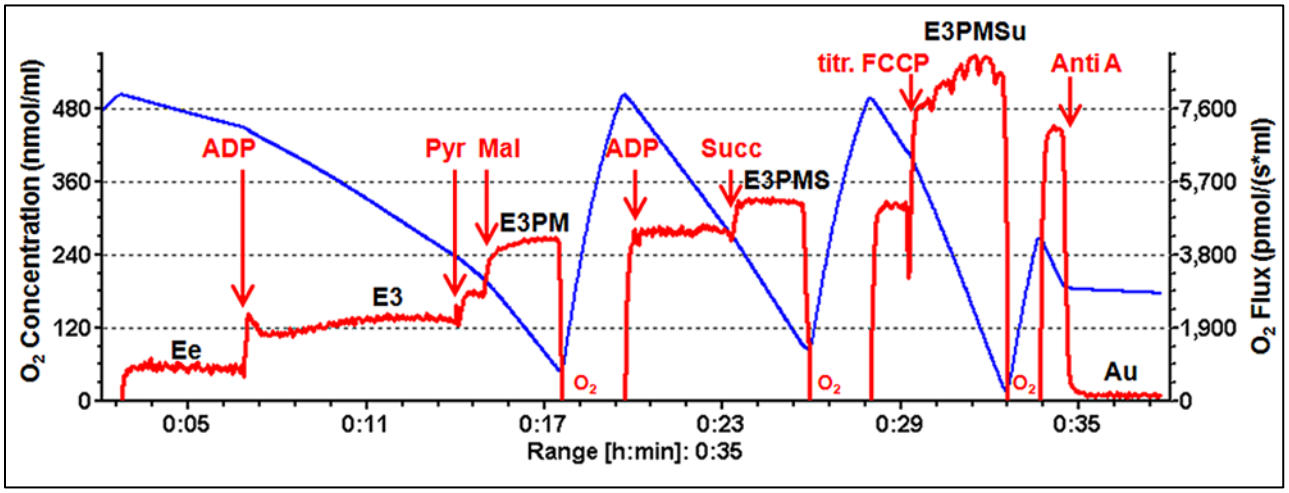

Figure 3.1. Representative tracing of a respiration experiment conducted with lysate from post-diapause embryos of *A. franciscana* at 1/4 dilution. The blue trace represents oxygen concentration while the red trace depicts oxygen flux. Combined substrates for Complex I and Complex II are used in this experiment. The sequence of additions are indicate by arrows (2.5 mM ADP, 15 mM pyruvate, 2 mM malate, 2.5 mM ADP, 10 mM succinate, FCCP titration (4 µM, 0.5 µM, 0.5 µM, 0.5 µM, 0.5 µM, 0.5 µM = 6.5 µM total), and 2.5 µM antimycin A. Steady-state respiratory conditions are labeled: Ee – respiration of mitochondria with only endogenous substrates and endogenous ADP; E3 – respiration with endogenous substrate and exogenous (saturating) ADP; E3PM – respiration with endogenous substrate plus exogenous pyruvate+malate and ADP; E3PMS – respiration with endogenous substrate plus exogenous pyruvate+malate+succinate and ADP; E3PMSu – uncoupled respiration after titration with FCCP; Au – residual (non-mitochondrial) oxygen consumption.

3.3 Results

The quantity of mitochondria in diapause embryos is statistically indistinguishable from post-diapause embryos, based on mitochondrial protein extractable from embryos (Reynolds and Hand 2004). Thus decreased respiration in diapause versus post-diapause lysates reported below is not due to a difference in mitochondrial densities.

Oxidative-Phosphorylation Capacity using Complex I Substrates

Oxygen consumption supported by endogenous fuel (Ee) in the post-diapause lysate decreases modestly with increasing dilution (**Fig. 3.2**; note that rates are expressed per mg of mitochondrial protein in the assay). The effect of dilution is more pronounced when exogenous ADP is added (E3). Both respiratory treatments emphasize the contribution of endogenous substrates to mitochondrial respiration. E3PM was measured by addition of pyruvate and malate in presence of ADP. Addition of pyruvate and malate to undiluted lysates does not result in increased oxygen consumption and indicates the presence of a saturating amount of endogenous fuel. Titration with FCCP was used to uncouple the mitochondria and provide maximum ETS capacity obtainable with complex I substrates (E3PMu).

Respiration in lysates from diapause embryos fueled by endogenous substrates (Ee) decreases markedly with dilution, which is consistent with lower substrate levels as compared to post-diapause embryos (**Fig. 3.3**).The Ee oxygen flux measured for the undiluted and $1/4^{th}$ diluted diapause lysates is similar to the flux measured in corresponding dilutions for post-diapause embryo lysates indicating saturating amounts of endogenous fuel at these dilutions in diapause embryos. Addition of ADP to the various dilutions of diapause lysate demonstrates a similar trend as that seen in post-diapause lysates. ADP fueled stimulation of oxygen flux (E3) decreases with increasing dilution.

Addition of pyruvate+malate to undiluted diapause lysates does not stimulate respiration indicating that, like post-diapause embryo lysates, the endogenous pyruvate levels are likely saturating in concentration. Despite apparent saturating levels of endogenous fuel, the oxygen flux values measured in undiluted lysates are lower in diapause embryos as compared to post-diapause lysates. Oxygen flux measured for each dilution after uncoupling with FCCP is

markedly lower in diapause lysates compared to post-diapause homogenates (E3PMu values for all dilutions in diapause lysates are significantly lower than E3PMu values for corresponding dilutions in post-diapause lysates, $P \leq 0.001$).

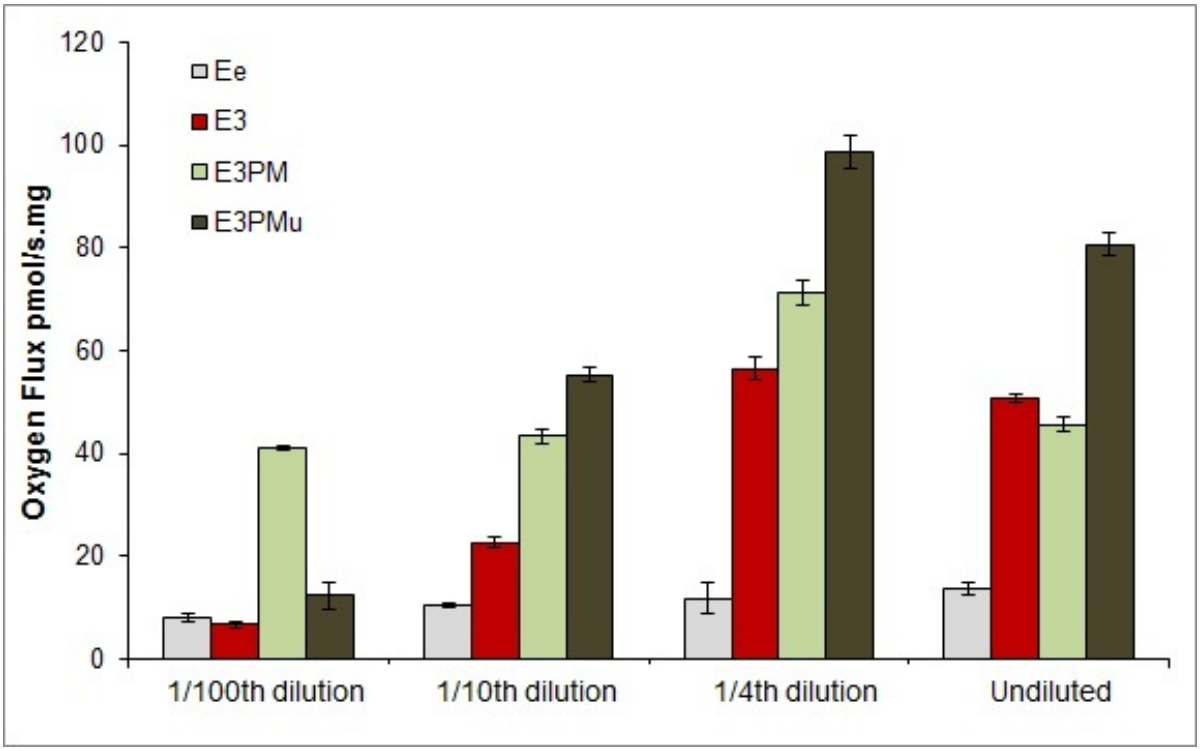

Figure 3.2. Oxygen consumption measured in lysates from *A. franciscana* post-diapause embryos at dilutions ranging from undiluted lysate to a 100-fold dilution with pyruvate and malate as respiratory substrates. Oxygen flux measured with only pyruvate and malate as substrates reflects the activity of mitochondrial complex 1. See legend to Figure 3.1for abbreviations. Values are reported as mean ± standard deviation, N = 4.

To allow more quantitative comparisons between post-diapause and diapause respiration, selected data have been re-plotted in **Figure 3.4**. E3 and E3PM measured in diapause embryo lysates were significantly lower when compared to corresponding oxygen fluxes in post-diapause embryo lysates at all dilutions ($p \leq 0.0001$). The overall downregulation of respiration observed with pyruvate+malate in diapause lysates is consistent with either compromised activity of

complex I and/or the inhibition of pyruvate dehydrogenase complex (PDC) (Patil et al. 2012). If PDH is inhibited during diapause, entry of pyruvate into the TCA cycle and subsequent generation of NADH for the ETS would be diminished.

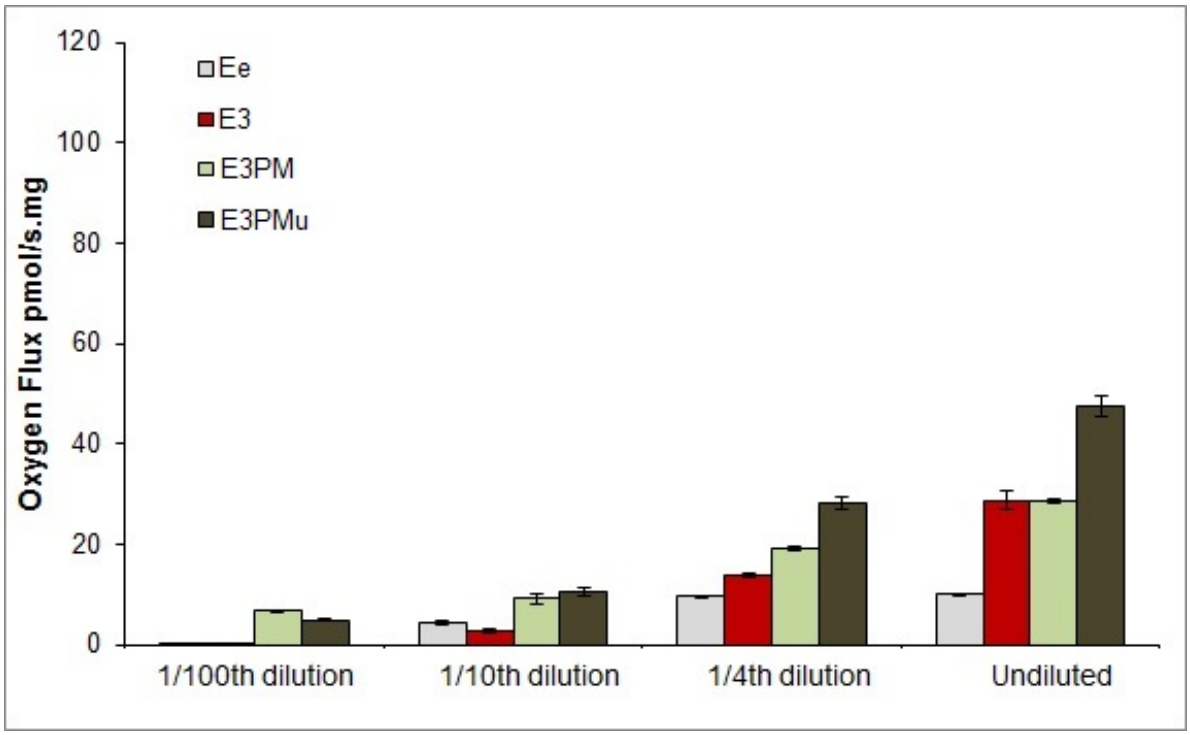

Figure 3.3. Oxygen consumption measured in lysates from *A. franciscana* diapause embryos at-dilutions ranging from undiluted lysate to a 100-fold dilution with pyruvate and malate as respiratory substrates. See legend to Figure 3.1 for abbreviations. Values are reported as mean ± standard deviation, N = 5.

Oxidative-Phosphorylation Capacity with Combined Complex I and Complex II Substrates

The combination of complex I and complex II substrates offers the potential to increase electron flow through the ETS. With an intact, fully-integrated TCA cycle as exists *in vivo* within a cell, complex I and II work simultaneously and introduce electrons into the ubiquinone pool (i.e., the Q-junction). Full operation of the citric acid cycle in isolated mitochondria, permeabilized cells or cell lysates requires addition of succinate to conventional substrates for complex I.

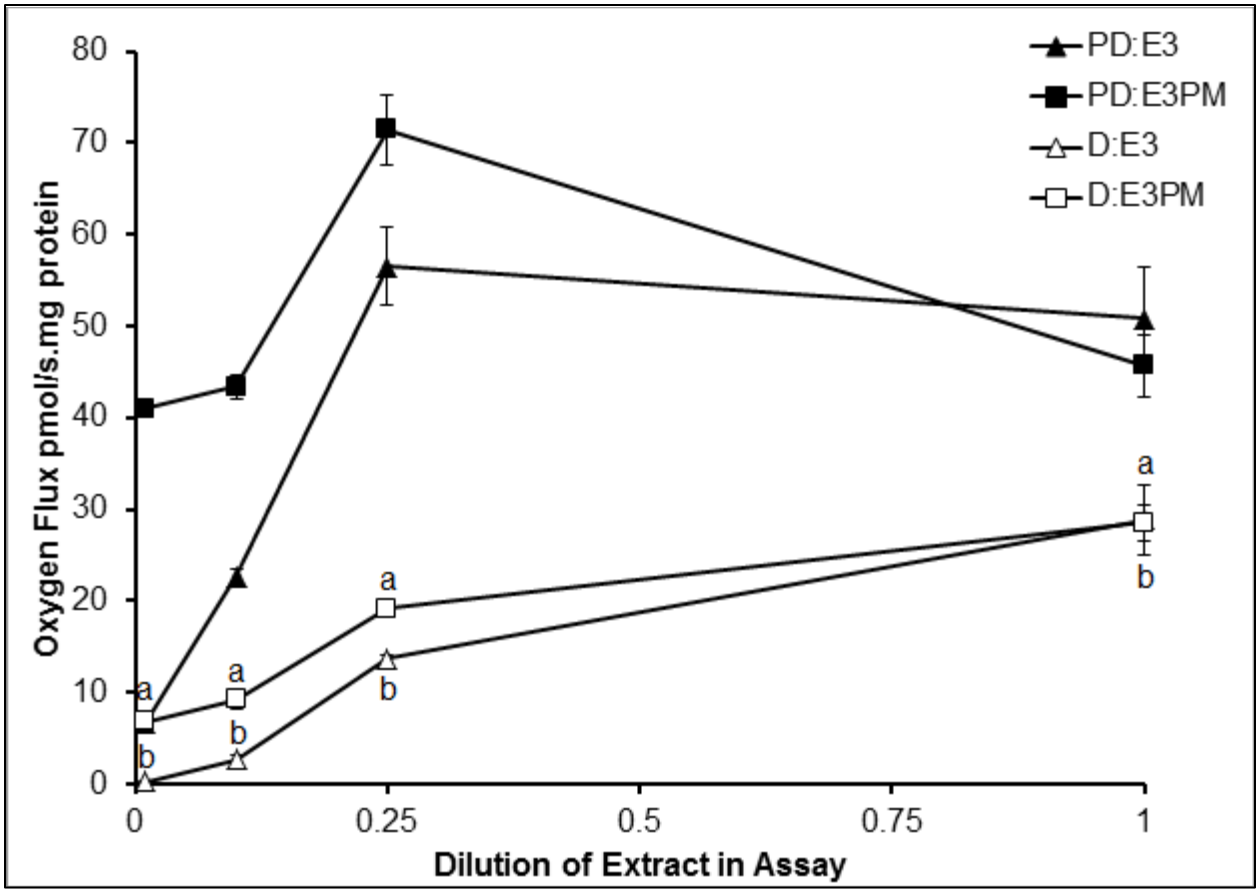

Figure 3.4. Oxygen flux stimulated by ADP (E3) and by ADP with exogenous pyruvate+malate (E3PM) as a function of dilution of lysates prepared from diapause and post-diapause embryos. Values are expressed as means ± standard deviation, N=4 (post-diapause), N=5 (diapause). E3PM and E3 values measured in diapause lysates were significantly lower (as indicated by 'a' and 'b' respectively) at all dilutions when compared to corresponding oxygen fluxes in post-diapause lysates at ($p \leq 0.0001$).

The TCA cycle is functionally not 'closed' when the substrate combination pyruvate+malate is used, because citrate and 2-oxoglutarate are exchanged rapidly for malate by the tricarboxylate and 2-oxoglutarate carriers and thus exit the mitochondrion. At higher electron flows achieved with combined substrates for complex I (electrons from NADH) and complex II (electrons from $FADH_2$) there is a greater likelihood to observe restrictions or inhibitions downstream of the Q-junction in the ETS and/or at other sites associated with oxidative phosphorylation (e.g., the phosphorylation system).

Addition of ADP stimulates respiration (E3) in post-diapause lysates in a dilution-dependent manner, which reflects the presence of endogenous respiratory substrates (**Fig. 3.5**). Addition of pyruvate+malate+succinate causes a pronounced stimulation of oxygen consumption (E3PMS) in post-diapause lysates that are diluted. Addition of this substrate combination increases oxygen consumption in undiluted lysate only modestly. In contrast to the results for complex I alone with only pyruvate+malate added, uncoupling of mitochondrial respiration

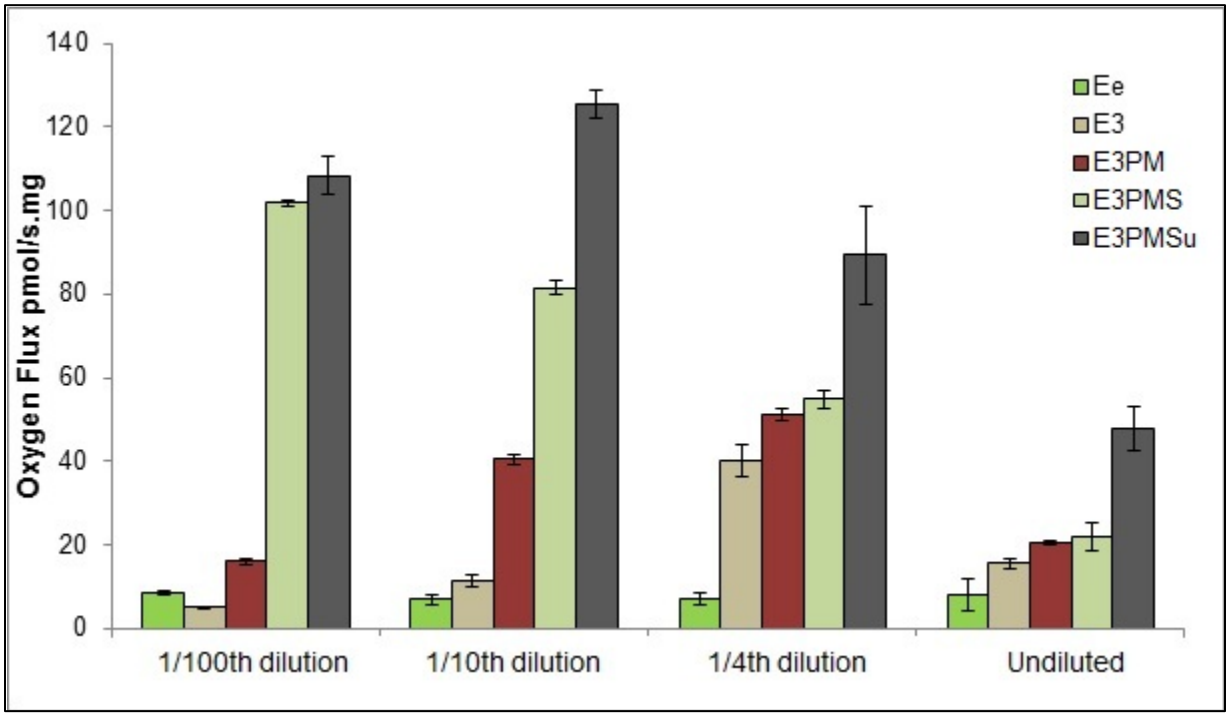

Figure 3.5. Oxygen consumption measured in *A. franciscana* post-diapause embryo lysate at various dilutions varying from undiluted lysate to a 100-fold dilution using pyruvate-malate and succinate as respiratory substrates. Oxygen flux measured using pyruvate-malate and succinate as substrates reflects the combined activity of mitochondrial complexes 1 and 2. The addition of different respiratory modulators enables the measurement of (a) Ee – respiration of mitochondria using only endogenous substrates and ADP, (b) E3 – state 3 respiration using endogenous substrate and exogenous (excess) ADP, (c) E3PM – state 3 respiration with exogenous pyruvate, malate and ADP, (d) E3PMS – state 3 respiration with exogenous pyruvate, malate, succinate and ADP and (e) E3PMSu – uncoupled respiration after titration with FCCP. Values are reported as mean ± standard deviation, N = 5.

by FCCP in the presence of pyruvate+malate+succinate exhibits an increase above E3PMS at all dilutions.

Addition of pyruvate+malate+succinate causes marked increase in oxygen flux in diluted diapause embryo lysates (**Fig.3.6**). Uncoupling by FCCP results in significantly increased oxygen consumption (E3PMSu) at all dilutions. To allow more quantitative comparisons for respiration generated with complex I plus complex II substrates, selected data have been re-plotted in **Figure 3.7**. In contrast to the pattern seen with pyruvate+ malate alone, there are no statistical differences observed between post-diapause and diapause for E3PMS, except at the lowest dilution (1/100). Importantly, the result emphasizes that when additional electron input

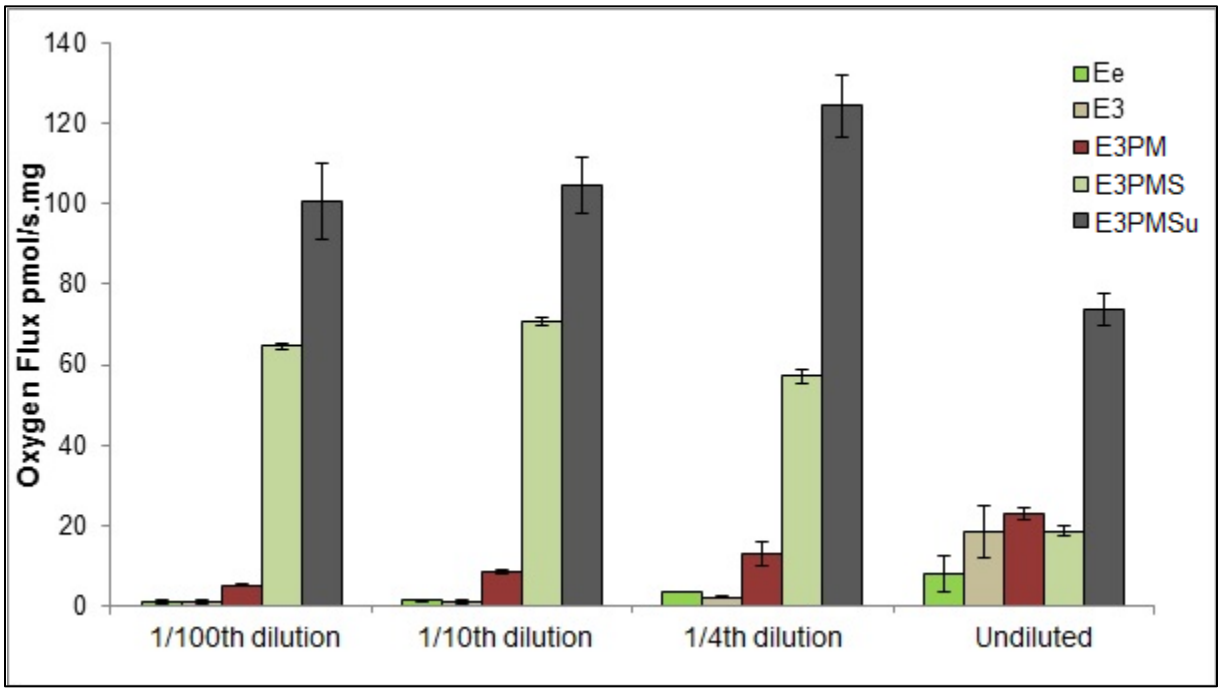

Figure 3.6. Oxygen consumption measured in *A. franciscana* diapause embryo lysate at various dilutions varying from undiluted homogenate to a 100-fold dilution using pyruvate, malate and succinate as respiratory substrates. The addition of different respiratory modulators enables the measurement of (a) Ee – respiration of mitochondria using only endogenous substrates and ADP, (b) E3 – state 3 respiration using endogenous substrate and exogenous (excess) ADP, (c) E3PM – state 3 respiration with exogenous pyruvate, malate and ADP, (d) E3PMS – state 3 respiration with exogenous pyruvate, malate, succinate and ADP and (e) E3PMSu – uncoupled respiration after titration with FCCP. Values are reported as mean ± standard deviation, N = 5.

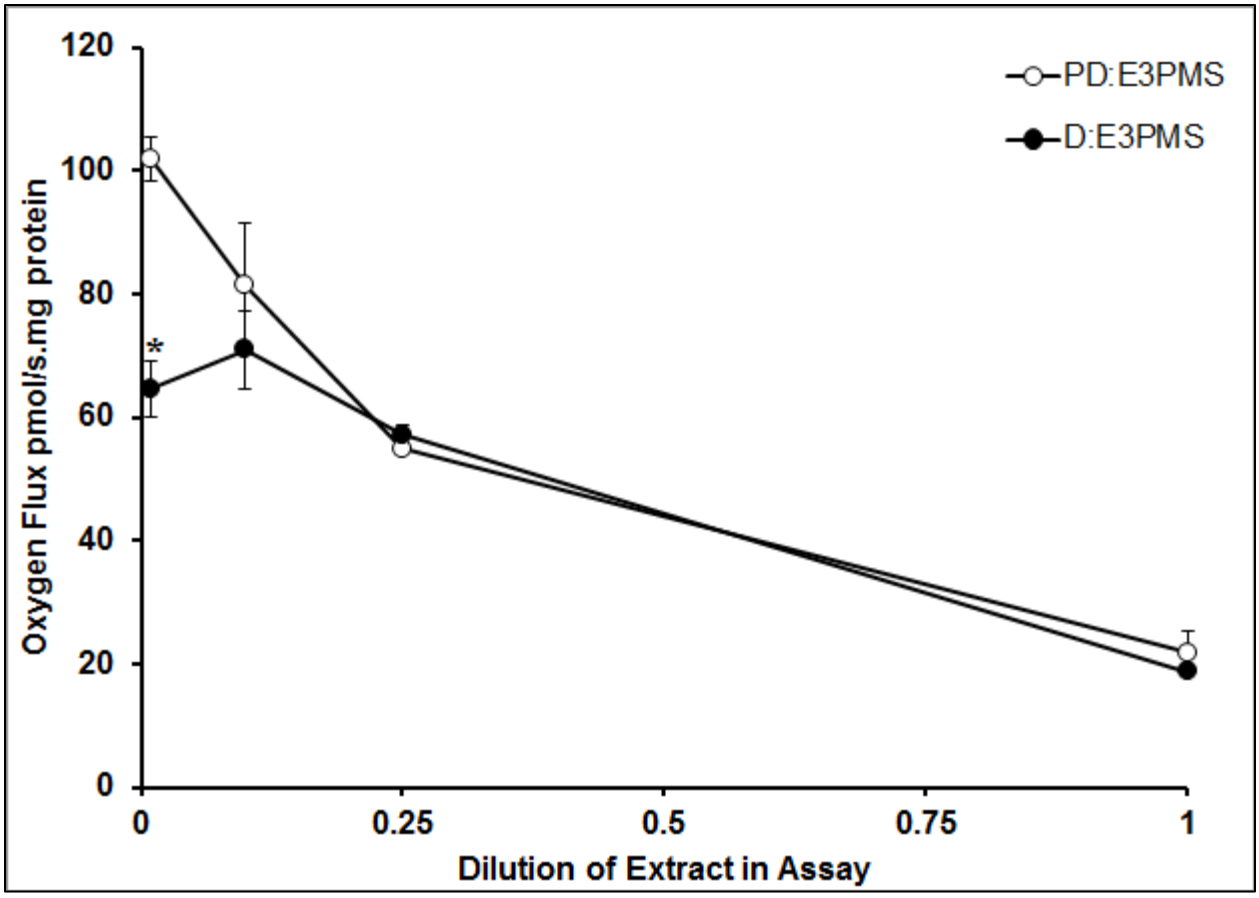

Figure 3.7. Oxygen flux stimulated by ADP with exogenous pyruvate+malate+succinate (E3PMS) as a function of dilution of lysates prepared from diapause and post-diapause embryos. Values are expressed as means ± standard deviation, N = 5. Statistical comparisons of E3PMS values for the undiluted ($p=0.168$), $1/4^{th}$ diluted ($p=0.063$) and $1/10^{th}$ diluted ($p=0.155$) lysates are statistically identical between diapause and post-diapause states. The E3PMS measured for $1/100^{th}$ diluted diapause lysate is statistically lower than that measured for the corresponding post-diapause lysate ($p \leq 0.0005$), as indicated by the asterisk.

from complex II is provided at the Q-junction, the restriction through complex I during diapause is no longer manifested in an inhibition of oxidative phosphorylation.

Uncoupled Control Ratios and Inhibition of the Phosphorylation System

The E3PMu/E3PM ratios for the $1/100^{th}$ dilution of diapause and post-diapause lysates are below unity (**Figs. 3.2, 3.3**), even at the lowest concentration typically used in the FCCP

titration series. Thus it appears that at 1/100 dilution of lysates, complex I-dependent respiration is very sensitive to FCCP addition. Consequently, I evaluated this issue further using a larger range of FCCP concentrations. As shown in **Figure 3.8A, B** reduction in oxygen flux is observed even at the lowest concentration of FCCP (0.001 µM).

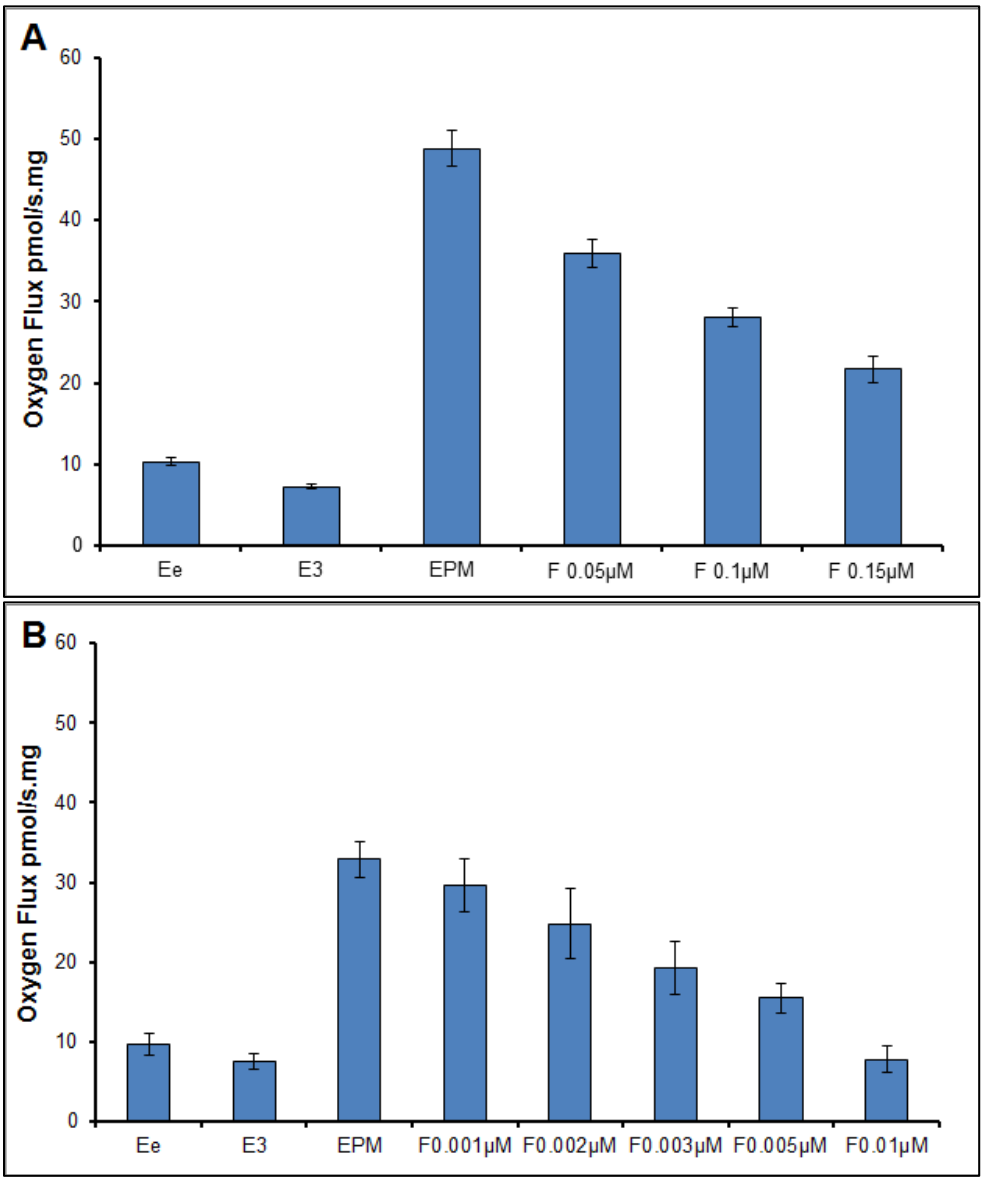

Figure 3.8. FCCP inhibition of respiration when driven by complex I substrates, as assayed with 1/100-diluted lysate from post-diapause embryos of *A. franciscana*. Ee denotes oxygen consumption with endogenous substrates. E3 represents respiration after addition of exogenous ADP. E3PM denotes stimulation due to pyruvate+malate in presence of exogenous ADP. **A.** This panel shows the inhibition observed with 0.05, 0.1 and 0.15 µM FCCP. **B**. Inhibition observed with 0.001, 0.002, 0.003 0.005 and 0.01 µM FCCP. Values are means ± standard deviation, N = 3.

Consequently, it is not possible to uncouple respiration with FCCP when 1/100-diluted lysates are driven by complex I substrates. Thus, results with 1/100-diluted lysates are eliminated from the evaluation of uncoupling control ratios presented below.

As shown in **Figure 3.9**, there are no statistical differences in uncoupled control ratios (E3PMu/E3PM) between diapause and post-diapause lysates with complex I substrates, and these ratios do not respond differently to dilution of the lysates. An uncoupled control ratio greater than unity indicates that maximum coupled respiration is limited by the phosphorylation system (i.e., the $F_1.F_o$-ATP synthase, adenine nucleotide transporter, and phosphate

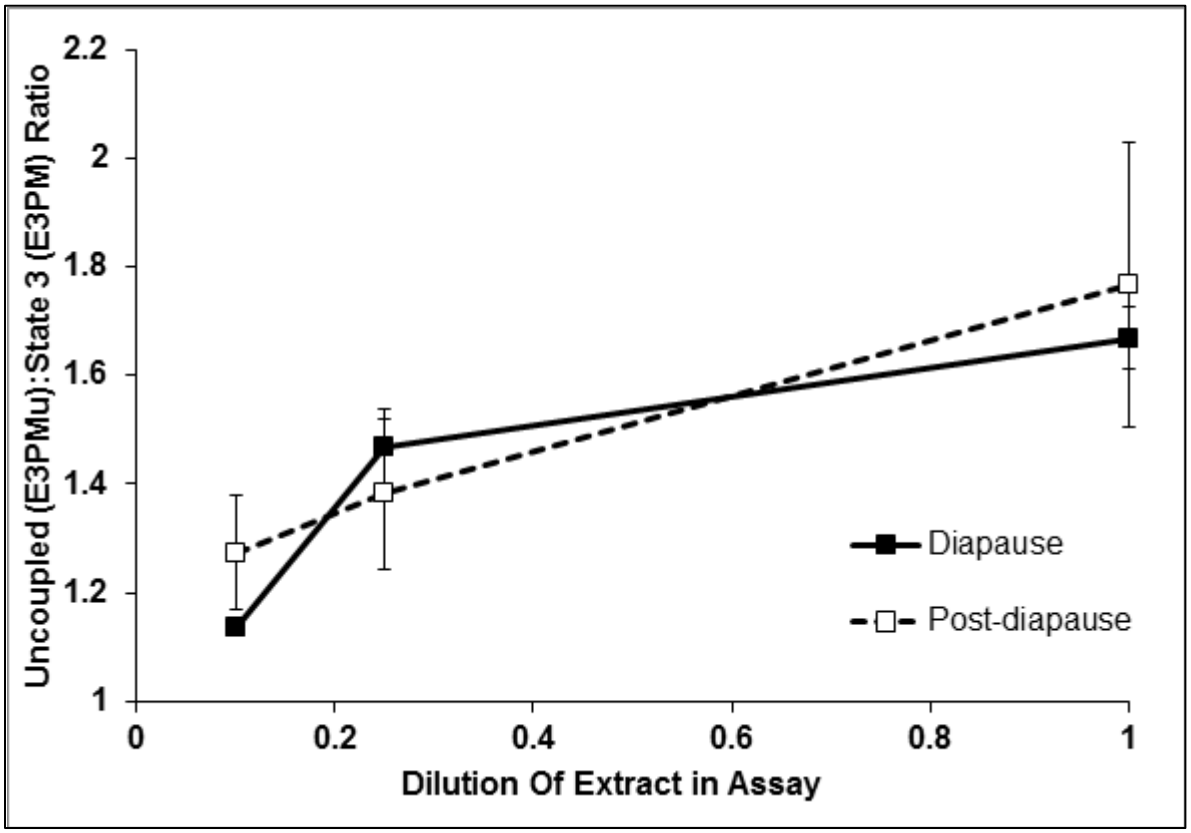

Figure 3.9. Ratio of uncoupled respiration to coupled state 3 respiration using exogenous pyruvate, malate and ADP as respiratory substrates at different dilutions of lysates prepared from diapause and post-diapause embryos of *A. franciscana*. Uncoupled respiration achieved by titration with FCCP represents the maximum respiratory capacity in mitochondria; the state 3 respiration with exogenous pyruvate and malate reflects the maximum electron transfer capacity of the mitochondrial complex 1. Ratios higher than unity indicate excess respiratory capacity at the given dilution. Values are reported as mean ± standard deviation, N =4

transporter), and thus there is apparent excess capacity of the ETS that is not utilized. Uncoupled control ratios obtained complex I plus complex II substrates (E3PMSu/E3PMS) for diapause and post-diapause embryo lysates are depicted in **Figure 3.10**. In this case, the patterns exhibited for post-diapause versus diapause are strikingly different. The uncoupled control ratio for undiluted diapause lysates is about 2-fold higher than for undiluted post-diapause lysates (significantly different, $p \leq 0.001$). The ratio for $1/4^{th}$ diluted diapause lysate is also about 2-fold higher

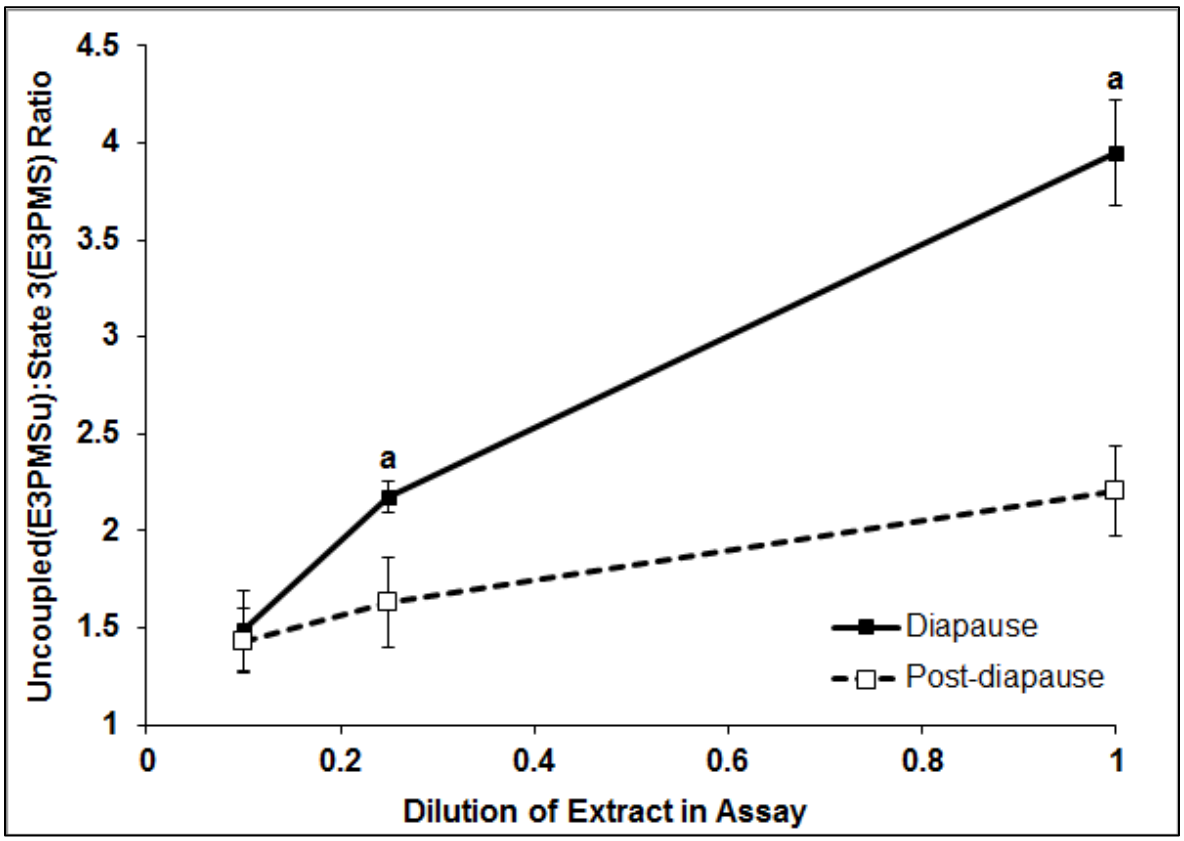

Figure 3.10. Ratio of uncoupled respiration to coupled state 3 respiration using exogenous pyruvate, malate, succinate and ADP as respiratory substrates at different dilutions of lysates prepared from diapause and post-diapause embryos of *A. franciscana*. Uncoupled respiration achieved by titration with FCCP represents the maximum respiratory capacity in mitochondria; the state 3 respiration with exogenous substrates reflects the maximum electron transfer capacity of the mitochondrial complexes 1 and 2. Ratios higher than unity indicate excess respiratory capacity at the given dilution. Ratios measured for diapause lysates at the undiluted and $1/4^{th}$ dilutions are significantly higher than the corresponding values for post-diapause embryo lysate, as indicated by 'a'. Values are reported as mean ± standard deviation, N = 5.

as compared to the corresponding dilution of post-diapause lysate (significantly different, $p \leq 0.01$). These data strongly suggest that during diapause, the phosphorylation system is limiting overall oxidative phosphorylation to a degree far greater than during post-diapause. Further, the inhibition of the phosphorylation system in diapause lysates is markedly diminished as a function of dilution, which provides strong evidence for the presence of a diffusible inhibitor during diapause. In other words, the inhibitory influence of a lysate component on the phosphorylation system in diapause embryos is eliminated as the lysate is diluted.

3.4 Discussion

This study provides evidence for a reduction in complex I-based respiration and inhibition of the phosphorylation system in *A. franciscana* embryos during diapause. The diminished activity through complex I may by explained in part or in full by inhibition of the pyruvate dehydrogenase complex as a result of phosphorylation, reported by Patil et al. (2012). Because the inhibition observed for the phosphorylation system is diminished as the lysate is diluted, this result is suggestive of a diffusible inhibitor molecule operating on the mitochondrion during diapause. Together with the restriction of fuel to the mitochondrion *in vivo* as documented in Chapter 2, the above features likely explain the vast majority of the metabolic arrest during diapause.

Levin et al. (2003) suggested that during diapause in insect larvae, a decrease in mitochondrial content could be responsible for decreased oxygen consumption. However, work by Reynolds and Hand (2004) shows that this is not the case with *A. franciscana*. The amount of mitochondrial proteins does not differ between mitochondria from diapause and post-diapause embryos suggesting that the observed decrease in embryonic respiration during diapause may be an active downregulation of mitochondrial function. Reynolds and Hand (2004) have reported

that the bioenergetic features of mitochondria isolated from diapause and post-diapause embryos are similar. It is however possible that the mitochondria may display different behavior *in vivo*. The current study used lysates prepared from *A. franciscana* embryos with very little dilution (1 part embryo:1 part medium) in an attempt to preserve some of the regulatory features that might have been lost during purification of isolated mitochondria. It further exploited the possibility of evaluating bioenergetic features of mitochondria in increasingly diluted embryo lysates.

Oxygen consumption in diapause lysates fueled by exogenously added substrates for complex I was substantially lower than that measured for post-diapause lysates at all dilutions. Because of the brief preparation time needed for preparation and assay of the lysates, it is probable that phosphorylation states of macromolecules existing *in vivo* were retained to some degree. This scenario is fully consistent with the requirement that whole embryos had to be instantaneously quenched in SDS-containing buffer to allow documentation of the increased degree of phosphorylation of pyruvate dehydrogenase during entry into diapause (Chapter 2). Indeed, because phosphorylation severely inhibits the enzyme, this covalent modification could preclude the delivery of electrons from NADH, produced via pyruvate oxidation, to the ETS.

Pyruvate import into the mitochondrion is mediated by a family of mitochondrial pyruvate carrier (MPC) proteins (Hildyard and Halestrap 2003, Herzig et al. 2012). While the MPC proteins are considered vital to the task of transporting pyruvate into the mitochondrial matrix (Herzig et al. 2012, Bricker et al. 2012), there are no published reports of this carrier being physiologically regulated, other than its dependence on mitochondrial ΔpH. Thus, it appears that there are no regulatory features that would suggest that it may play a role in reducing the pyruvate+malate dependent respiration observed in diapause lysates.

By increasing the input of electrons to the Q-junction by simultaneous addition of complex I and complex II substrates, a limitation of oxidative phosphorylation by the

phosphorylation system was detectable in diapause lysates. However, as the lysate was diluted, the high uncoupled control ratios in diapause lysates returned to the values measured for post-diapause lysates. As previously inferred, the result is consistent with the presence of an inhibitor specific to the diapause state. The nature of this compound is unknown, although there is precedence for metabolically-derived inhibitors that can specifically and potently impede the function of the adenine nucleotide transporter (see Discussion in Chapter 5). This transporter brings ADP into the mitochondrial matrix in exchange for ATP (Nicholls and Ferguson 2002); thus its arrest could severely restrict ATP synthesis.

In summary, this study underscores the importance of conducting bioenergetic analyses at multiple levels of biological complexity. Experiments with embryo lysates revealed new features contributing to the arrest of metabolism during diapause in *A. franciscana* that were not detectable with isolated mitochondria removed from the intracellular milieu.

CHAPTER 4

ACTIVITIES OF RESPIRATORY COMPLEXES AND PYRUVATE DEHYDROGENASE IN *ARTEMIA FRANCISCANA* EMBRYOS DURING POST-DIAPAUSE AND DIAPAUSE

4.1 Introduction

The metabolic depression exhibited by embryos of *Artemia franciscana* is arguably the most profound seen during diapause in nature (Clegg et al. 1996, Reynolds and Hand 2004, Patil et al. 2012). The 5 d period required by diapause embryo to achieve this remarkably low respiration rate (<1% of post-diapause) is indicative of an orchestrated downregulation of enzymatic activity (Patil et al. 2012) that serves to restrict carbohydrate catabolism and starve the mitochondrion of fuel. Limitation of oxygen consumption in the diapause embryo is aided further by direct inhibition of oxidative phosphorylation at the level of the mitochondrion, based on studies with embryos lysates (Chapter 3). Specifically, inhibition of complex I seen in these lysates supported the phosphorylation of pyruvate dehydrogenase during diapause that was previously documented (Patil et al. 2012). Inhibition of the phosphorylation system was also detected in diapause lysates, and this inhibition diminished as lysates were diluted (Patil et al. 2012). In this chapter, mitochondria were isolated from diapause and post-diapause embryos in the presence of phosphatase inhibitors, and then respiratory complexes were solubilized and their activities measured to test whether inhibition during diapause could be traced to the function of specific complexes.

Reynolds and Hand (2004) previously documented that the mitochondrial content of embryos does not change statistically between diapause and post-diapause. Hence the dramatic drop in respiration of diapause embryos could not be explained by a decrease in numbers of mitochondria. Further, the results of these authors clearly documented that bioenergetic features

of isolated mitochondria were very similar for the two states. The only major difference they observed was a decrease during diapause in both the activity and cytochrome *aa*3 content for cytochrome c oxidase (COX). However, the kinetic capacity of COX often exceeds the maximum rate for ADP-coupled respiration in many tissues (i.e., excess COX capacity), and embryos of *A. franciscana* show an apparently excess COX capacity of 31% (Reynolds and Hand, 2004). Any potential restriction in respiration attributable to a decrease in COX would be offset by its apparent excess capacity. Reduced COX activity was correlated with metabolic depression during estivation in some species of snails (Stuart et al. 1998, Bishop et al. 2002), but no estimate of excess COX capacity was reported. Thus, Reynolds and Hand (2004) concluded that the inhibition of metabolism *in vivo* during diapause was likely due to restriction of carbohydrate supply to the mitochondria (subsequently verified by Patil et al. 2012) and/or by an inhibition within mitochondria that was not maintained during the process used to isolate mitochondria (e.g., reversal of a covalent modification, or elimination of a diffusible inhibitor).

The sole source of metabolic fuel for the mitochondria in *Artemia* embryos is pyruvate arising from the glycolytic pathway fed by trehalose breakdown (Clegg 1964, Dutrieu 1960; Carpenter and Hand 1986a). Pyruvate is imported from the cytosol to the matrix and then converted by the pyruvate dehydrogenase complex (PDC) to acetyl coA, which then is oxidized by the TCA cycle. The NADH and $FADH_2$ produced serve as the electron donors for complex I and complex II, respectively (Nicholls and Ferguson 2002). The influx of glycolytic carbon is hence a crucial step in the operation of the electron transport system in embryos of *A. franciscana*. The PDC exists as a mitochondrial matrix complex with multiple subunits. Pyruvate dehydrogenase is a component of this large complex and is regulated by phosphorylation and dephosphorylation of subunit E1α at multiple sites (Kolobova et al., 2001; Patel and

Korotchkina, 2001). PDC thus possesses the potential to regulate mitochondrial function by limiting substrate supply to the TCA cycle.

In this study, I examined the hypothesis that changes in the activities of mitochondrial complexes may contribute to metabolic downregulation during diapause. In order to preserve any phosphorylation-based modifications that may exist, I employed phosphatase inhibitors in every step of mitochondrial isolation, solubilization of complexes, and analysis. I also examined the activity of PDC partially purified from diapause and post-diapause embryos in the presence of phosphatase inhibitors to determine its role in metabolic downregulation during diapause.

4.2 Methods

Reagents

Sucrose was obtained from J.T. Baker (Mfg. Mallinckrodt-Baker, Paris, KY). All other reagents used were of the highest quality available and were purchased from either Fisher Scientific (Pittsburgh, PA) or Sigma-Aldrich (St. Louis, MO).

Processing of *A. franciscana* Embryos

All embryos originated from the Great Salt Lake, UT. Encysted, diapause embryos were collected during the fall of 2009, 2010, and 2011. The embryos were washed and stored in 1.25 M NaCl with kanamycin (50μg/ml), penicillin-streptomycin (50μg/ml) and nystatin (200 units/ml). Prior to each assay, diapause embryos were incubated in 35 ppt artificial seawater (Instant Ocean™; Aquarium Systems, Mentor OH, USA) with shaking at room temperature for 4 days to allow non-diapause individuals to hatch; larvae and empty shells were removed using a separatory funnel. The viability of diapause embryos was confirmed periodically with the method described by Reynolds and Hand (2004). Briefly, unhatched cysts were dried at ambient

temperature and humidity for up to two weeks. The dried cysts were treated with 3 % hydrogen peroxide prepared in 0.4 M NaCl for approximately 30 min. After rinsing with 0.25 M NaCl, the cysts were incubated as described above (35ppt artificial seawater, 4 d). After 4 days the percentage hatching was determined. The number of nauplii divided by the total number counted (i.e. unhatched cysts + nauplii) was used to calculate percent viability. Cyst batches with a hatching percentage above 70% were considered to be suitable for study. It should be noted that some cysts are exceptionally refractory to diapause breakage with the above technique depending on the depth of diapause.

Dehydrated post-diapause embryos (Grade: laboratory reference standard) were obtained from Great Salt Lake *Artemia*, LLC (Ogden, UT, USA) in 2008, 2010 and 2012. The dried embryos were stored at -20° C. In preparation for experiments, these embryos were hydrated in 0.25 M NaCl at 0° C overnight. The embryos were then allowed to develop under normoxic conditions in 0.25 M NaCl at room temperature for 8 h. The hatching percentage for post-diapause embryos, as determined as above in 35 ppt artificial seawater, was above 90%.

Preparation of Isolated Mitochondria

Prior to homogenization, the cysts (10 – 20 g) were dechorionated by treatment with antiformin solution (1 % hypochlorite, 0.4 M sodium hydroxide, and 60 mM sodium carbonate) for 15-20 min at room temperature, followed by three rinses with ice-cold 0.25 M NaCl. Embryos were then incubated in ice-cold 1 % (w/v) sodium thiosulfate for 5 min and were rinsed two times with cold 0.25 M NaCl. Finally, embryos were incubated for 3-5 minutes in cold 40 mM hydrochloric acid prepared in 0.25 M sodium chloride, followed by three rinses with 0.25 M NaCl.

Dechorionated cysts were homogenized at 0° C in four volumes of homogenization medium using a Potter-Elvehjem tissue homogenizer (Thomas Scientific, Swedesboro, NJ). The

homogenization medium is composed of 0.5 M sucrose, 1 mM EGTA, 0.5 % (w/v) bovine serum albumin (fatty acid free, fraction V), 20 mM HEPES, 150 mM KCl, titrated to pH 7.5 with 1.0 M KOH and multiple phosphatase inhibitors (1 mM sodium fluoride, 1 mM sodium molybdate, 1mM sodium ortho-vanadate and 4mM sodium tartrate). The homogenate was centrifuged at 1000 X *g* for 10 min at 4°C min, and the resulting supernatant was centrifuged at 9000 x *g* for 15 min. This pellet was washed by resuspension in the starting volume of isolation buffer followed by centrifugation at 9000 x *g*. The pellet was resuspended in about 1 ml of isolation buffer and stored on ice for PDH purification or at -80°C for isolation of respiratory complexes. Protein content was measured using Coomassie Plus (Bradford) Assay Kit (Thermo Fisher Scientific Inc., Rockford, IL).

Preparation of Pyruvate Dehydrogenase Complex (PDC) from Isolated Mitochondria

PDC cannot be assayed directly in extracts of embryos because the activity is too low and the presence of cytosolic enzymes interferes with the measurement of NADH. To circumvent these problems, PDC was extracted from isolated mitochondrial preparations. Mitochondrial isolation was carried out as described above, and PDC was purified from mitochondria using a method as described by Pettit et al. (1982) with slight modifications. Isolated mitochondria were sedimented at 9000 X *g* for 15 min at 4°C, and the resulting pellet was resuspended in 50 mM N-(2-Acetamido)-2-aminoethanesulfonic acid (ACES) buffer, pH 6.4, containing the protease inhibitors phenylmethanesulfonylfluoride (PMSF), leupeptin, pepstatin A, and the same combination of phosphatase inhibitors as listed above in order to inhibit phosphatases that may be present in the mitochondrial preparation. Triton X-100 (0.5%) was then added to this suspension and rapidly mixed to solubilize PDC. The suspension was centrifuged at 30,000 X *g* for 30 min at 4°C, followed by addition of 10 mM MgCl2 and 0.02 mM thiamin pyrophosphate (TPP). The supernatant was acidified to pH 6.1 using 10% acetic acid and mixed for another 5

min. The resulting precipitate (not containing PDC) was removed by centrifugation at 30,000 X *g* for 10 min at 4°C. To the supernatant, 0.06 volume of 50% PEG-6000 was added, and the mixture was stirred for 10 min. The preparation was centrifuged at 30,000 X *g* for 10 min at 4°C, and the pellet containing PDC was resuspended in 50 mM MOPS (pH7.0). The suspension was centrifuged at 40,000 X *g* for 10 min to remove non-dissolved material. EGTA (2 mM) was added to the supernatant and mixed for 20 min, after which the mixture was centrifuged for 3.5 h at 105,000 X *g* at 4°C. The resulting PDC pellet was resuspended in 50 mM MOPS (pH 7.0) and kept on ice for immediate assay of catalytic activity.

Assay for Pyruvate Dehydrogenase Complex (PDC)

PDC was assayed by adding the enzyme preparation to a reaction mixture containing 1 mM $MgCl_2$, 2.6 mM Cysteine HCl, 0.225 mM TPP, 2 mM NAD^+ and 50 mM MOPS (pH 8.1) in a final volume of 1 ml at 25°C. The reaction was initiated by addition of 2 mM pyruvate followed by 0.15 mM coenzyme A. Increase in absorbance at 340 nm was recorded and used to calculate the initial velocity of PDC (Brown and Perham 1976, Rahman et al. 1996, Stanley and Perham 1980). Pyruvate concentration in the reaction mixture was varied in order to estimate the apparent K_m, which was calculated using Sigmaplot 9.1 (Module EK1.3, a curve-fitting program for enzymatic analysis).

Disruption of Mitochondria for Assay of Respiratory Complexes

Mitochondria, previously stored overnight at -80°C in 200 µl aliquots with phosphatase inhibitors, were thawed on ice and subjected to ultrasonic disruption. The preparation was kept on ice and lysed using a Branson Sonifier Model 250 (Danbury, CT) with three sequential pulses of 0.5 sec duration at 30 % power. The preparation was used immediately for assay of respiratory complexes.

Activity of Mitochondrial Complexes

Complex I activity (NADH-ubiquinone oxidoreductase): Spectrophotometric assay of complex I utilizes the reduction of decylubiquinone (DB) at 272 nm. The reaction mixture consists of 250 mM sucrose, 1 mM EDTA, 50 mM Tris-HCl pH 7.4, 10 μM DB, 2 mM KCN and 45 μg mitochondrial protein in a final volume of 1 ml. The reaction is initiated by adding 50 μM NADH and quantified the linear decrease in absorbance of DB at 272 nm for 1 min at 25°C. Rotenone (5 μg/ml; specific inhibitor of Complex I) is then added, and any rotenone-insensitive activity is measured for 1 min; the background rate is subtracted from the original, uninhibited rate (Trounce et al. 1996).

Complex II activity (succinate-ubiquinone oxidoreductase): Complex II activity is monitored by recording the reduction in absorbance of 2,6-dichlorophenolindophenol (DCPIP) at 600 nm, which is coupled to the reduction of DB by complex II. The reaction mixture consists of 50 mM potassium phosphate, pH 7.4, 20 mM succinate, 2 μg/ml antimycin A , 2 μg/ml rotenone, 2 mM KCN, 50 μM DCPIP and 30 μg mitochondrial protein in a final volume of 1 ml. The reaction is initiated by adding 50 μM DB, and the change in absorbance is monitored for 3 min at 25°C (Trounce et al. 1996).

Complex III activity (ubiquinol-ferricytochrome-c oxidoreductase): The assay monitors the reduction of cyt *c* at 550 nm catalyzed by complex III in presence of reduced decylubiquinone. The reaction mixture consists of 250 mM sucrose, 1 mM EDTA, 50 mM Tris-HCl, pH 7.4, 50 μM cyt *c*, 2 mM KCN and 30 μg mitochondrial protein in a final volume of 1ml. The reaction is initiated by adding 50 μM reduced decylubiquinone and monitoring the increase in absorbance at 550 nm for 1 min at 25°C. The experiment is repeated in the presence of 5 μg/ml antimycin A (a specific complex III inhibitor) and any background rate is subtracted from the original, uninhibited rate (Trounce et al. 1996).

Complex IV activity (cytochrome c oxidase, COX): Complex IV activity was readily measured by following the oxidation of reduced cyt *c* at 550 nm minus 540 nm (extinction coefficient 19.0 $mM^{-1}cm^{-1}$). The reaction mixture consisted of 10 mM potassium phosphate, pH 7.4, 20 µM ferrocytochrome c (reduced). The 1 ml reaction was initiated by addition of about 30 µg of mitochondrial preparation. The change in absorbance was recorded for up to 30 sec at 25°C. Cyt *c* (100 mg, Sigma Aldrich Chemical Co., from equine heart) was dissolved in 1 ml of 10 mM potassium phosphate, pH 7.4, and then 1.0 ml of 0.1 M L-ascorbate was added to reduce the cyt *c*. The mixture was loaded onto a 20-ml Sephadex G-25 column that was washed and pre-equilibrated with degassed 10 mM potassium phosphate, pH 7.4. The central portion of elution peak for cyt *c* was collected. The absorbance at 550 nm was used to calculate the stock concentration of fully reduced cyt *c* (extinction coefficient of 27.7 $mM^{-1}cm^{-1}$), which was stored in 0.1 ml aliquots at -80 °C (Trounce et al. 1996).

Complex V activity ($F_1.F_o$-ATP synthase): ATP hydrolysis is more easily studied than the ATP synthesis reaction (Nicholls and Ferguson, 2002). In this assay, ATP hydrolysis (ATPase activity) is measured indirectly as the rate of formation of NAD in a coupled reaction system that contains pyruvate kinase and lactate dehydrogenase. This design also serves to regenerate ATP and prevent ADP from inhibiting complex V. The assay mixture contains 25 µM Tris acetate (pH 7.5), 25 µM potassium acetate, 0.3 mM sucrose, 2 µM MgCl2, 0.4 µM NADH, 1 µM phosphoenolpyruvate, 2 µM ATP (pH 7), 2.8 units of lactate dehydrogenase and 3.0 units of pyruvate kinase in a final volume of 1 ml. The reaction is initiated by addition of about 20 µg of mitochondrial protein at 25^{o} C (Trounce et al., 1996). The change in the absorbance of NADH is monitored at 340 nm (Stiggall et al., 1979).

Statistical Analysis

Analyses were performed with GraphPad Prism statistical software (ver. 5.04, GraphPad Software, La Jolla, CA, USA.), and significance was evaluated by *t-test*. A p-value of ≤ 0.05 was considered significant.

4.3 Results

Activity of Pyruvate Dehydrogenase Complex

Figure 4.1 demonstrates there is only about a 10% decrease in the maximal velocities between PDC partially purified from diapause versus post-diapause mitochondria, respectively, in the presence of phosphatase inhibitors. **Table 4.1** depicts the maximum velocity of the enzyme preparations and their corresponding K_m values. These small differences in V_{max} for PDC likely reflect the ineffectiveness of the phosphatase inhibitors to fully protect the *in vivo* phosphorylation state of PDC during the long isolation procedure. Western blots showing the phosphorylation status of the partially purified PDC from diapause and post-diapause embryos are currently unavailable; however the samples are now available and work is underway to confirm the phosphorylation status for the two preparations. As a perspective, the difference in phosphorylation state between diapause and post-diapause embryos is observable only when whole embryos are immediately quenched by homogenization directly into SDS-containing buffer (Patil et al. 2012). An important corollary underscored by these results is that when covalent modification is involved in the control of a physiological process, the preservation of the modification is critical in order to document functional changes *in vitro*.

Complex I Activity

Complex I activity measured in disrupted mitochondria isolated in the presence of phosphatase inhibitors revealed a modest inhibition in diapause compared to post-diapause

embryos (**Fig. 4.2**). There is a loss of about 18% rotenone-sensitive activity in complex I during diapause. By comparison, state 3 respiration (with pyruvate plus malate) measured for

Table 4.1: Kinetic features of PDC isolated from mitochondria of diapause and post-diapause embryos in the presence of phosphatase inhibitors. Values are expressed as mean ± SEM, N = 3 nested replicate measurements. Significant differences exist between diapause and post-diapause for both K_m and V_{max} data sets ($p \leq 0.0005$).

Embryo State	K_m **(mM Pyruvate)**	V_{max} **(µM/min.mg)**
Post-Diapause	0.071 ± 0.0019	5.948 ± 0.048
Diapause	0.038 ± 0.0042	5.305 ± 0.080

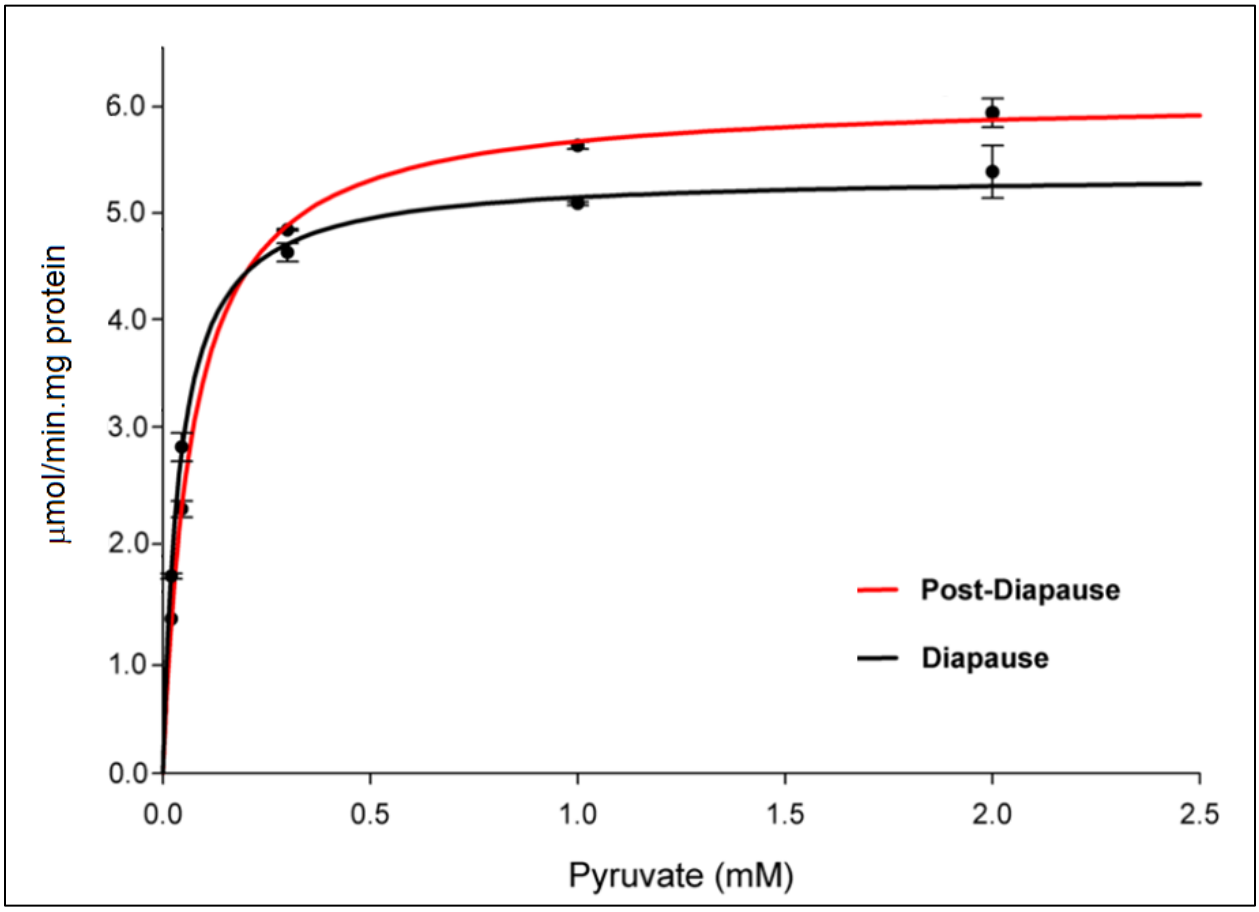

Figure 4.1. Comparison of PDC activity isolated from mitochondria of diapause (black trace) and post-diapause (red trace) embryos in the presence of phosphatase inhibitors. Values are expressed as mean ± SEM, N = 3 nested replicate measurements.

mitochondria isolated from post-diapause and diapause embryos, in the absence of phosphatase inhibitors, did not reveal a difference in rates (Reynolds and Hand 2004). The small difference between these studies could be due to the presence/absence of phosphatase inhibitors, but it may also reflect differences in mitochondrial bioenergetics previously documented from year-to-year among batches of diapause embryos (Reynolds and Hand 2004).

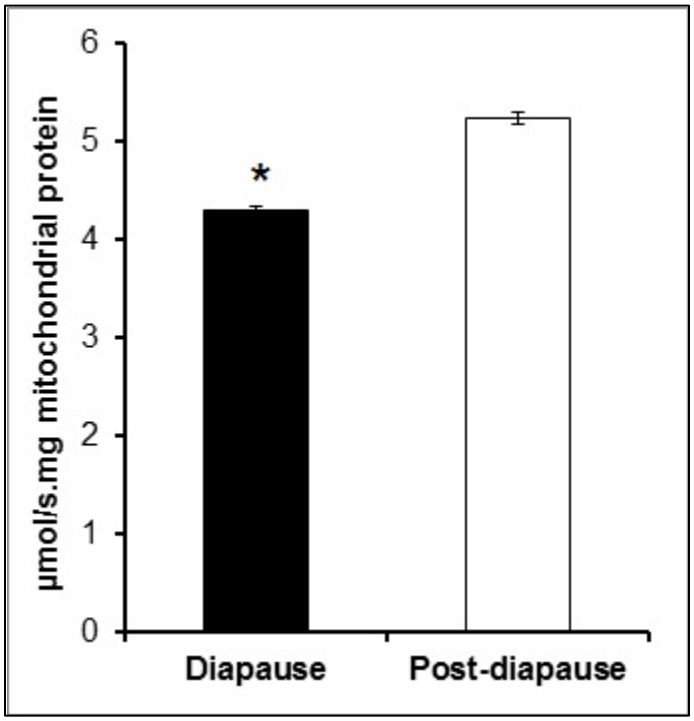

Figure 4.2. Comparison of complex I activities assayed with disrupted mitochondria isolated from diapause and post-diapause embryos in the presence of phosphatase inhibitors. Values are expressed as means ± SEM, N = 5. Asterisk denotes statistical significance ($p \leq 0.0001$).

Thus the substantial decrease in respiration rates observed for diapause lysates with exogenous complex I substrates (Patil et al. 2012) likely reflects the increased phosphorylation of PDH preserved in lysates and perhaps a small decrease in complex I capacity. It is appropriate to emphasize, however, that the predominant contributor to the overall arrest of embryo respiration

in vivo during diapause is the severe restriction in carbon supply to mitochondria as a consequence of the blockage of trehalose mobilization and glycolysis (Patil et al. 2012).

Comparison of Complex II Activity

Complex II activity measured in disrupted mitochondria of both diapause and post-diapause embryos revealed no difference in activities (**Fig. 4.3**). Again by comparison, state 3 respiration values (with succinate plus rotenone) measured for mitochondria isolated from post-diapause and diapause embryos, in the absence of phosphatase inhibitors, revealed either small differences or no differences depending on the collection year (Reynolds and Hand 2004).

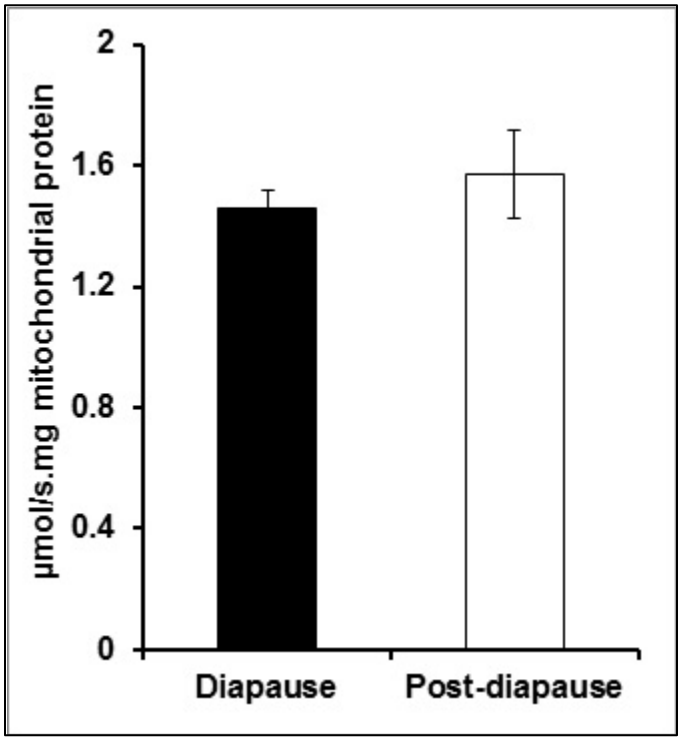

Figure 4.3. Comparison of complex II activity assayed with disrupted mitochondria isolated from diapause and post-diapause embryos in the presence of phosphatase inhibitors. Values are expressed as means ± SEM, N = 6. Complex II activity is not statistically different between diapause and post-diapause embryo mitochondria (p = 0.83).

Comparison of Complex III Activity

Antimycin-sensitive complex III activity was unchanged between disrupted mitochondria isolated from diapause and post-diapause isolated mitochondria in the presence of phosphatase inhibitors (**Fig. 4.4**). This result is consistent with the generally unchanged electron transport system (ETS) capacity in isolated mitochondria (Reynolds and Hand 2004).

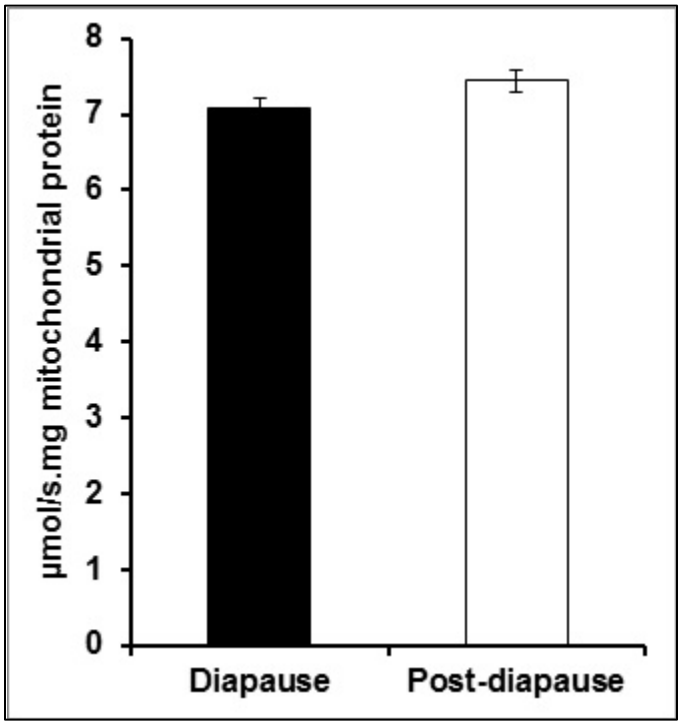

Figure 4.4. Comparison of complex III activity assayed with disrupted mitochondria isolated from diapause and post-diapause embryos in the presence of phosphatase inhibitors. Values are expressed as means ± SEM, N = 5. Complex III activity is not statistically different between diapause and post-diapause embryo mitochondria ($p = 0.07$).

Comparison of Complex IV Activity

Complex IV (COX) assayed with disrupted mitochondria from diapause embryos revealed activity decreased by about 40% as compared to post-diapause embryos (**Fig. 4.5**). COX displayed the greatest depression in activity observed among all respiratory complexes.

Reynolds and Hand (2004) have shown previously that COX activity is correlated to the amount of cytochrome aa_3 protein, and hence it is likely that the lowered COX activity may be a result of reduced COX protein in the diapause mitochondria. Further, the amount/activity of COX differs markedly during diapause from collection year to collection year (Reynolds and Hand 2004), yet this difference is not correlated with any change in whole embryo respiration rate (or if so, only very weakly). As emphasized earlier, apparently excess COX capacity is typical in many tissues, and embryos of *A. franciscana* show an apparently excess COX capacity of 31% (Reynolds and Hand 2004). Thus any potential restriction in respiration attributable to a decrease in COX would be offset in large measure by COX excess capacity.

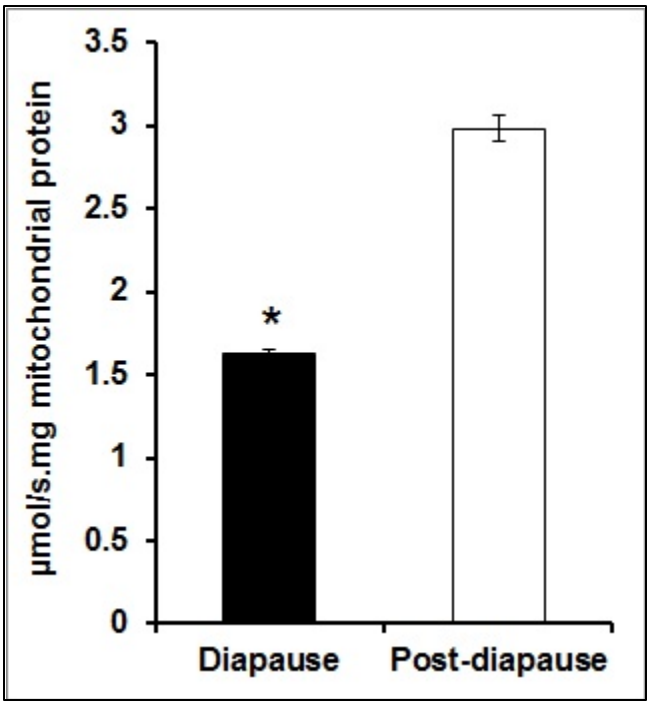

Figure 4.5. Comparison of complex IV activity assayed with disrupted mitochondria isolated from diapause and post-diapause embryos in the presence of phosphatase inhibitors. Values are expressed as means ± SEM, N = 5. Asterisk denotes statistical significance ($p \leq 0.0001$).

Comparison of Complex V Activity

When measured in disrupted mitochondria isolated in the presence of phosphatase inhibitors, complex V activity did not exhibit any statistically-significant difference between diapause and post-diapause states (**Fig. 4.6**). In lysates prepared from diapause and post-diapause embryos, inhibition of the phosphorylation system was detected based on high uncoupled control ratios in undiluted lysates (Patil et al. 2012). As the lysates were diluted, the inhibition of the phosphorylation system was diminished, which is consistent with the presence of a diffusible inhibitor only effective at high lysate concentrations. Of course in the experiment

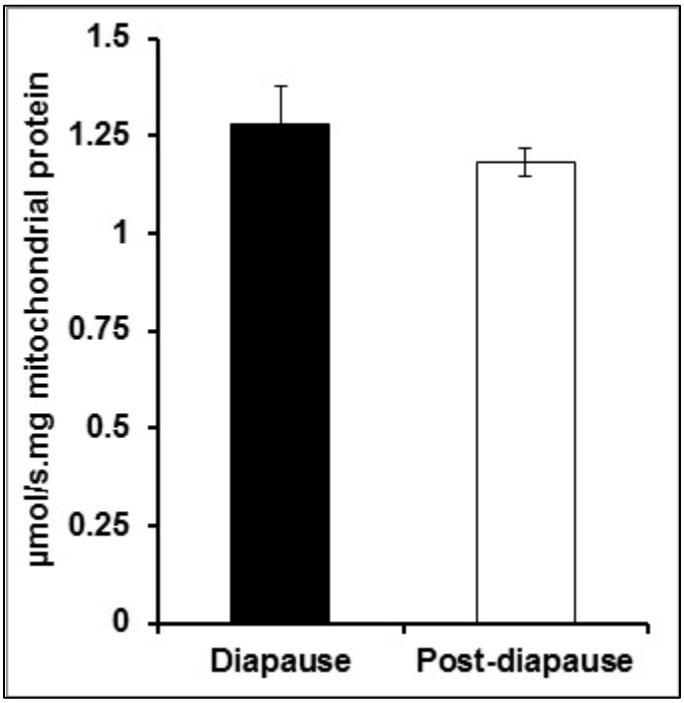

Figure 4.6. Comparison of complex V activity between mitochondria isolated from diapause and post-diapause embryos. Values are expressed as means ± SEM, N = 6. Complex V activity is not statistically different between diapause and post-diapause embryo mitochondria (p = 0.36).

presented here in **Figure 4.6**, any inhibitor would have been removed during the isolation and enzyme extraction procedures employed, and thus the lack of any difference between diapause and post-diapause activity for complex V is not unexpected.

4.4 Discussion

Changes in the functional properties of isolated respiratory complexes measured here, likely contribute little to the dramatic respiratory depression seen in diapausing embryos of *A. franciscana*. It is likely that increased phosphorylation, which could serve to inhibit PDC, contributes to the metabolic depression, but significant PDC inhibition was not captured by the approach used in this study. As previously shown (Patil et al. 2012, Chapter 2) diapause embryos of *A. franciscana* undergo a dramatic downregulation of metabolic activity, as evident from their respiration profile over a period of 5 days post-release from the adult female. The respiratory depression of over 99% can be attributed primarily to the arrest of carbohydrate catabolism and concomitant restriction of carbon flow to mitochondria in diapause embryos (Patil et al. 2012). The exclusive metabolic fuel in *A. franciscana* embryos is carbohydrate (Dutrieu 1960, Emerson 1963, Clegg 1964; Clegg and Conte 1980, Carpenter and Hand 1986a).

Any residual flux from the glycolytic pathway into the mitochondria during diapause could be controlled by pyruvate dehydrogenase. My studies have shown that the phosphorylation of PDC increases substantially when analyzed in SDS extracts of whole embryos as they enter diapause (Chapter 2). PDC can be phosphorylated at three sites on subunit E1α, and phosphorylation at site 1 alone can lead to an inhibition of over 90% (Kolobova et al. 2001, Patel and Korotchkina 2001). However, there are minimal differences in the activity of PDC partially purified from mitochondria isolated from diapause and post-diapause embryos (**Fig. 4.1**). A suite of phosphatase inhibitors was employed throughout the purification of PDC in an attempt to prevent alteration to the phosphorylation status of the enzyme complex; however it is likely that the inhibitors were largely ineffective. It is appropriate to note that in the case of PDC, pyruvate dehydrogenase kinase and pyruvate dehydrogenase phosphatase are both integral components of the complex (Harris et al. 2002); thus it is unclear whether any of the phosphatase

inhibitors employed here reached the matrix location of relevant phosphatase. It is now known that even pyruvate dehydrogenase kinase itself is regulated by tyrosine phosphorylation in physiologically important ways (Hitosugi et al. 2011). Other than the specific kinase and phosphatase for PDC, the majority of enzymes facilitating the reversible phosphorylations of target proteins in the mitochondrial matrix are unknown (Phillips et al. 2011). Nevertheless, dozens of kinase-mediated phosphorylations for the proteins associated with all five respiratory complexes have been identified (Phillips et al. 2011, and references therein).

The respiratory complexes are fueled by NADH and $FADH_2$ generated primarily by PDC and the TCA cycle in the case of the carbohydrate-based metabolism of *A. franciscana* embryos. A decrease in the activity of one or more respiratory complexes could reduce the electron flow through the ETS. As measured in this study, there are only minor impacts on the function of the respiratory complexes during diapause. Complex I is modestly depressed during diapause (18%) as compared to post-diapause embryos. Mitochondrial complex I is the most structurally elaborate of all respiratory complexes, and it catalyzes the transfer of two electrons from NADH to quinone, which is coupled to the translocation of four protons across the inner membrane. It consists of 45 subunits with an approximate total mass of 980 kDa combined mass, while the simpler bacterial enzyme possesses 14 core subunits with an overall mass of 550 kDa (for review see Efremov and Sazanov 2011). Crystal structures of the membrane domain, the hydrophilic domain, and the entire structure have been determined for the bacterial complex (Efremov and Sazanov 2011), and an x-ray analysis of the mitochondrial complex I from yeast has been reported (Hunte et al. 2010). Phosphorylation of selected subunits of Complex I have been documented, but any *in vivo* physiological roles for these modifications are not known (Chen et al. 2004, Palmisano et al. 2007). The reduction in complex I activity reported here is presumably reflected in the diminished respiration observed in lysates prepared from diapause embryos in the

presence of complex I substrates as documented in Chapter 3. The primary reason for the depression of oxidative phosphorylation measured in lysates with pyruvate+malate is likely phosphorylation of PDH (Patil et al. 2012).

Complexes II and III do not display any change in activity in diapause compared to post-diapause embryos. Complexes I and II both transfer electrons to complex III via the ubiquinone pool, and hence complex III would appear as a good candidate for down-stream regulation of electron flow through the ETS. The lack of difference in activities for complexes II and III isolated from diapause and post-diapause embryos are consistent with the work on isolated mitochondria by Reynolds and Hand (2004).

Complex IV or COX was shown to be depressed about 40% during diapause. Reynolds and Hand (2004) have shown a correlation of COX activity with cytochrome aa_3 protein content. COX activity and COX 1 mRNA levels were found to be tightly correlated by Hardewig et al. (1996). Thus changes in COX activity likely reflect differences in the steady-state levels of the enzyme protein. It should be borne in mind that COX has been reported to display 31% apparently excess capacity in *A. franciscana* embryos (Reynolds and Hand 2004). In other words, a decrease of 31% in the amount of functional complex IV would be required before any impact would be seen in ETS capacity. Complex V as depicted in **Figure 4.6** fails to show any difference in activity between mitochondria isolated from diapause and post-diapause embryos.

In summary, modest reductions were measured in the activities of complex I and complex IV isolated from diapause versus post-diapause embryos. Isolated complexes II, III and V do not demonstrate differences in activity. These limited inhibitions observed for complex I and IV are minor contributors to the severe respiratory inhibition observed in diapause embryos.

CHAPTER 5

SUMMARY AND FUTURE DIRECTIONS

Based on the results presented in this dissertation and those of Clegg et al. (1996), there is evidence for strong metabolic downregulation in *Artemia franciscana* embryos during diapause. The restriction of carbohydrate catabolism and effective decrease in the flux of glycolytic carbon is promoted by inhibition of strategic enzymes involved in trehalose catabolism (Patil et al. 2012, Chapter 2). It has been stressed that trehalose is the sole source of fuel in the embryos of *A. franciscana* ((Dutrieu 1960, Muramatsu 1960, Emerson 1963, Clegg 1964, Carpenter and Hand 1986a), and hence downregulation of trehalose catabolism results in severe limitation of metabolic fuel available to the embryo during diapause. Restriction of glycolytic flux will lead to metabolic 'starvation' of the mitochondrion, and in turn will arrest mitochondrial function during diapause.

Additional results, based on studies conducted with embryo lysates (Chapter 3), document during diapause, a depression of oxidative phosphorylation in the case where substrates for respiratory complex I (pyruvate+malate) are used, and secondly, an inhibition of the phosphorylation system. Reduced respiration through complex I is supported by results for pyruvate dehydrogenase, an enzyme which provides NADH to complex I *in vivo* and serves as the entry point for glycolytic carbon into the mitochondrion. Specifically, I have shown with Western blotting that pyruvate dehydrogenase becomes phosphorylated during entrance into diapause (Chapter 2), and as a consequence, one would predict PDH to be strongly inhibited in this state (Kolobova et al. 2001, Patel and Korotchkina 2001). Studies using substrates for respiratory complex II (succinate) combined with pyruvate+malate indicate inhibition of the phosphorylation system (i.e., the $F_1.F_o$-ATP synthase, adenine nucleotide transporter, and

phosphate transporter) (Chapter 3), as evidenced by differences in uncoupled control ratios. For this inhibition to be detected, the increased ETS flux generated by the combination of complex I plus complex II is apparently required. It is noteworthy that the inhibition of the phosphorylation system is relieved as the lysate is serially diluted, which suggests that depression of the phosphorylation system is a result of an inhibitor. The nature of this inhibitor is unknown at present. One example of such an inhibitor might be long-chain acyl CoA esters that are known to inhibit the ANT (e.g., oleoyl-CoA; palmitoyl-CoA, myristoyl-CoA) (Lerner et al. 1972, Chua and Shrago 1977, Soboll et al. 1984). These compounds can inhibit the ANT from either side of the inner mitochondrial membrane (Chua and Shrago 1977) and are modulated in response to various metabolic states (Prentki et al. 1992). Finally, my catalytic activity measurements of respiratory complexes extracted from isolated mitochondria (Chapter 4) reveal a minor lowering of complex I activity during diapause and a drop in activity of complex IV, the latter effect being minimized by COX excess capacity. Taken together, restriction of glycolytic carbon to the mitochondrion appears to the primary mechanism for the *in vivo* metabolic arrest in *A. franciscana* embryos during diapause, which is accentuated by inhibitions within the mitochondrion itself.

The work carried out in this dissertation enables me to speculate on a few broader questions such as "is the mechanism of metabolic downregulation during diapause in *A. franciscana* similar to that under anoxia?" While metabolism is indeed strongly downregulated in diapause, the signals that initiate this process remain unknown for now. Extensive work on *A. franciscana* has been carried out to study anoxic quiescence. Induction of anoxic quiescence leads to a tremendous drop in ATP content (Stocco et al. 1972, Anchordoguy and Hand 1994) in the embryos. More importantly, anoxic incubation causes a drop in the pH_i of the embryos from about 7.9 to as low as 6.3 (Busa et al. 1982). Incubation of developing cysts in elevated CO_2

under normoxia [which acidifies the intracellular pH (pH_i)] induces changes similar to those seen in anoxia, while alkalization of the pH_i with ammonia under anoxia promotes an increase in metabolic activity (Carpenter and Hand 1986a, Hand and Gnaiger 1988). Thus, the major drop in pH_i is believed to play a crucial role in regulating metabolism in anoxia induced quiescence. Hydrated cysts in anoxia induced quiescence depress their metabolism by almost 98% in the first hours (Hand and Gnaiger 1988) and by 99.8% or more over several days (Hand 1995), which is comparable to the > 99% drop in respiration seen in diapausing embryos in this study. While similar mechanisms could control metabolic arrest in diapause cysts, there are however some vital differences that may suggest the contrary. It takes only minutes of anoxia exposure to elicit the majority of metabolic depression in developing cysts, whereas diapause cysts require up to 5 d to reduce their respiration to the lowest levels. The slower rate of downregulation suggests a coordinated downregulation that could involve differential gene expression response in diapause. Enzymes such as trehalase and phosphofructokinase in *A. franciscana* are sensitive to pH changes and are reported to be inhibited during anoxia (Carpenter and Hand 1986a). Based on my findings (Chapter 2), while trehalase appears to be inhibited, the product-to-substrate ratios for PFK do not provide any evidence for inhibition of the enzyme. It has also been reported that diapause embryos, freshly released from ovigerous females, possess an alkaline pH_i and that pH_i depression is not required for maintaining diapause (Drinkwater and Crowe 1987). Taken together, the role of pH_i in diapause hypometabolism appears to be of minor importance. However, it is unclear whether there is any change in pH_i under normoxia during diapause as the metabolic depression phase progresses. It may thus be of interest to determine and evaluate the impact of pH_i in diapause embryos at various time points starting from their release from the adult female to their entry into deep diapause 5 d post-release.

The exact mechanisms during diapause that serve to inhibit the multiple enzymatic sites I identified in Chapter 2 remain unknown. Since trehalose is the sole source of metabolic fuel, inhibition of trehalase would be an efficient step in downregulating glycolytic flux. It is interesting to note that only the initial (hexokinase) and terminal (pyruvate kinase) steps involved in glycolysis are inhibited during diapause. Trehalase is sensitive to pH changes (Hand and Carpenter 1986), however there is little to no evidence of pH depression during diapause. Hexokinase is known to be inhibited by its product; however during diapause the cellular levels of glucose-6-phosphate are significantly lower as compared to metabolically active levels. This observation may rule out the role of glucose-6-phosphate as a regulator of hexokinase during diapause. The cellular ATP:ADP ratio during diapause decreases about 5 fold, but the impact of this decrease on hexokinase activity remains to be evaluated. Inhibition of pyruvate kinase during diapause could potentially be achieved by phosphorylation, which reduces affinity for its substrate phosphoenol pyruvate (Siebenaller 1979) and for its key activator fructose-1,6-bisphosphate. The enzyme is also important in regulating the glycolytic versus oxidative phosphorylation poise of cell metabolism (Christofk et al. 2008; Vander Heiden et al. 2009). Rees and Hand (1991) discuss potential endocrine regulators that may influence PK in estivating snails; however *A. franciscana* embryos exist as undifferentiated gastrula and apparently do not have a developed endocrine system (Clegg and Conte 1980). It is however possible for endocrine modulators to be present in the diapause embryos as a maternal contribution. Finally, the mechanism that may control the phosphorylation of pyruvate dehydrogenase by pyruvate dehydrogenase kinase is another issue unresolved at present. The mechanism by which PDC is regulated by phosphorylation is well studied (Patel and Korotchkina 2001, Kolobova et al. 2001, Sugden and Holness 2006), but the signal that triggers the phosphorylation cascade during diapause in *A. franciscana* is not known. While the studies presented in this dissertation provide

new information about metabolic downregulation and the various sites of inhibition, questions regarding the orchestration of these inhibitions still remain. Studies of the mechanisms involved in enzyme inhibitions during diapause could reveal a signaling cascade employed during diapause and help in explaining the diapause phenomenon at the molecular level.

Previous estimates (Reynolds and Hand 2004) suggest that respiration of intact, aerobic post-diapause embryos is operating close to the state 3 respiration rate (maximum ADP-stimulated rate) measured for isolated mitochondria with succinate plus rotenone. By inference, with a respiratory control ratio (state3/state 4) of approximately 5-6, state 4 (proton leak respiration) would be 15-20% of that observed under maximal phosphorylating conditions, yet respiration of intact embryos is depressed far below this level during diapause (i.e., to less than 1%). Proton leak respiration by definition is the ETS activity required to maintain the proton gradient and compensate for proton leak (Nicholls and Ferguson, 2002). Unless proton leak is reduced during diapause, the question arises as to whether the mitochondrial membrane potential might be compromised during diapause. One would predict that the $F_1.F_o$-ATP synthase could reverse in the face of a severely compromised $\Delta\psi$ and fully deplete cellular ATP. Our measurements of adenylates in bulk diapause embryos collected from the surface of the Great Salt Lake show lower amounts of ATP present in post-diapause embryos (Chapter 2, Table 1). In contrast to ATP depletion anoxia in post-diapause embryos during anoxia, this drop in ATP is less severe. Thus, even though it is decreased during diapause, substantial ATP still exists. Thus, there is a distinct possibility of intervention by the IF_1 inhibitory protein. The IF_1 inhibitor protein has been shown to block the ATP synthase under conditions where $\Delta\Psi$ is compromised (Bason et al. 2011). Exploration into the potential role of IF_1 during diapause may be important in explaining the conservation of adenylates in diapause.

Qiu and MacRae (2010) reported differential gene expression during diapause with specific genes being upregulated with the onset of diapause. Coordinated gene expression would be necessary for production of cell growth regulators and macromolecules such as small stress proteins participating in diapause. Qiu et al. are however unable to pinpoint inductive cues that would initiate the diapause cascade. It would be of interest to identify the specific 'triggers' that lead to commitment of the embryo to the diapause program. Several hormones can serve as regulators of diapause, depending on species and developmental stage (Denlinger 2002). In *Bombyx mori*, embryonic diapause is initiated by diapause hormone, a neuropeptide synthesized by the female (Yamashita 1996). In gypsy moths, embryonic diapause is maintained by elevation of ecdysteroids (Lee and Denlinger 1997). Diapause can also be triggered by inactivation of an endocrine signaling (Denlinger 2012). In the absence of a functional endocrine system (Clegg and Conte 1980) in embryos of *A. franciscana*, the adult female may be capable of contributing such endocrine molecules to the embryos while still in the ovisac. Thus hormonal signals are capable of influencing gene expression, which in turn coordinates the execution of the diapause program, yet little is known about upstream events/signals that lead to hormonal control of diapause.

Embryos of *A. franciscana* exist in the gastrula stage when they enter diapause. Consequently the lack of differentiation of cells would imply that the embryo would rely on external cues/ maternal signals for triggering diapause. In a number of parasitic Hymenoptera, higher Diptera, and some Lepidoptera it is the adult female that decides the diapause fate of her progeny (Denlinger 2012). This arrangement may be particularly useful when the mother has access to environmental cues not readily accessible to her progeny. Most of these cases involve the mother determining the diapause status of her eggs (Denlinger 2002, 2012). The embryos that enter diapause are often in an early stage of development and are not yet equipped with the

sophisticated neural systems required to receive and respond to photoperiodic cues (Denlinger 2012). Very little is known about the mechanisms that regulate such cross-generational effects. Such information could be helpful in explaining how diapause is regulated in *A. franciscana*. An investigation into the role of chemical cues generated by the adult female and passed to the embryo also would be enlightening.

LITERATURE CITED

Akerboom T.P.M., H. Bookelman, P.F. Zuurendonk, R. van der Meer, and J.M. Tager. 1978. Intramitochondrial and extramitochondrial concentrations of adenine nucleotides and inorganic phosphate in isolated hepatocytes from fasted rats. *Eur J Biochem* 84: 413-420.

Anchordoguy T.J., and S.C. Hand. 1994. Acute blockage of the ubiquitin-mediated proteolytic pathway during invertebrate quiescence. *Am J Physiol Regul Integr Comp Physiol* 267: R895-R900.

Bason J.V., M.J. Runswick I.M. Fearnley and J.E. Walker. 2011. Binding of the Inhibitor Protein IF1 to Bovine F1-ATPase. *J Mol Biol* 406: 443-453.

Beauvoit B., Kitai T., and B. Chance. 1994. Contribution of the mitochondrial compartment to the optical properties of the rat liver: A theoretical and practical approach. *Biophysical J* 67: 12501-2510.

Berthelemy-Okazaki N.J. and D. Hedgecock. 1987. Effect of environmental factors on cyst formation in the brine shrimp *Artemia*. In, *Artemia Research and Its Applications*. Vol. 3. Sorgeloos, P., Gengston, D.A., Declier, W. and Jaspers, E., Eds. Universa Press, Wetteren, Belgium. 1967-1983

Bishop T., Ocloo A., and M.D. Brand. 2002. Structure and function of mitochondria in hepatopancreas cells from metabolically depressed snails. *Physiological and Biochemical Zoology* 75: 134-144.

Bricker D. K., E.B. Taylor, J.C. Schell, T. Orsak, A. Boutron, Y. Chen, J.E. Cox, C.M. Cardon, J. G. Van Vranken, N. Dephoure, C. Redin, S. Boudina, S.P. Gygi, M. Brivet, C. S. Thummel and J. Rutter. 2012. A Mitochondrial Pyruvate Carrier Required for Pyruvate Uptake in Yeast, Drosophila, and Humans. *Science* 337: 96-100.

Buchana S., Menze M., Hand S., Pyatt D. and J. Carpenter. 2005. Cryopreservation of Human Hematopoeitic Stem and Progenitor Cells Loaded with Trehalose: Transient Permeabilization via the Adenosine Triphospahte-Dependant P2Z Receptor Channel. *Cell Preserv Technol* 34: 212-222.

Busa W.B. and Crowe J.H. 1983. Intracellular pH regulates transitions between dormancy and development of brine shrimp *(Artemia salina)* embryos. *Science* 221: 366-368.

Busa W.B. and Nuccitelli R., 1984. Metabolic regulation via intracellular pH. *Am J Physiol* 246, R409–R438.

Busa W.B., J.H. Crowe, and G.B. Matson. 1982. Intracellular pH and the metabolic status of dormant and developing *Artemia* embryos. *Arch Biochem Biophys* 216: 711-718.

Carpenter J.F. and S.C. Hand. 1986a. Arrestment of carbohydrate-metabolism during anaerobic dormancy and aerobic acidosis in *Artemia* embryos: determination of pH-sensitive control points. *J Comp Physiol B Biochem Syst Environ Physiol* 156: 451-459.

Carpenter J.F. and S.C. Hand. 1986b. Comparison of ph-dependent allostery and dissociation for phosphofructokinases from *Artemia* embryos and rabbit muscle - nature of the enzymes acylated with diethylpyrocarbonate. *Arch Biochem Biophys* 248: 1-9.

Chance B., Holmes W., Higgins J.J., and C.M. Connelly. 1958. Localization of interaction sites in multi-component transfer systems: Theorems derived from analogues. *Nature* 182: 1190-1193.

Chen R., Fearnley I. M., Peak-Chew S. Y., and J.E. Walker. 2004. The phosphorylation of subunits of complex I from bovine heart mitochondria. *J Biol Chem* 279: 26036–26045.

Christofk H.R., M.G. Vander Heiden, M.H. Harris, A. Ramanathan, R.E. Gerszten, R. Wei, M.D. Fleming, S.L. Schreiber, and L.C. Cantley. 2008. The M2 splice isoform of pyruvate kinase is important for cancer metabolism and tumour growth. *Nature* 452: 230-U274.

Chua, B.H., and Shrago, E. 1977. Reversible inhibition of adenine nucleotide translocation by long chain acyl-CoA esters in bovine heart mitochondria and inverted submitochondrial particles. Comparison with atractylate and bongkrekic acid. *J Biol Chem* 252: 6711-6714.

Clegg J.S. 1964. Control emergence and metabolism by external osmotic pressure and role of free glycerol in developing cysts of *Artemia salina*. *J Exp Biol* 41: 879-892.

Clegg J.S. 2001. Cryptobiosis- A peculiar state of being. *Comp Biochem Phys B- Biochem Mol Biol* 128: 613-624.

Clegg J.S. 2011. Stress-related proteins compared in diapause and in activated, anoxic encysted embryos of the animal extremophile, *Artemia franciscana*. *J Insect Physiol* 57: 660-664.

Clegg J.S. and F.P. Conte. 1980. A review of the cellular and developmental biology of *Artemia*. pp. 11-54 in G. Persoone, P. Sorgeloos, O. Roels and E. Jaspers, eds. The Brine Shrimp *Artemia*. Universa Press, Wetteren, Belgium.

Clegg J.S., L.E. Drinkwater, and P. Sorgeloos. 1996. The metabolic status of diapause embryos of *Artemia franciscana* (SFB). *Physiol Zool* 69: 49-66.

Clegg J.S., S.A. Jackson, P. Liang, and T.H. Macrae. 1995. Nuclear-cytoplasmic translocations of protein p26 during aerobic-anoxic transitions in embryos of *Artemia franciscana*. *Exp Cell Res* 219: 1-7.

Covi J.A. and Hand S.C., 2005. V-ATPase expression during development of *Artemia franciscana* embryos: potential role for proton gradients in anoxia signaling. *J Exp Biol* 208, 2783–2798.

Covi J.A., W.D. Treleaven and S.C. Hand. 2005. V-ATPase inhibition prevents recovery from anoxia in *Artemia franciscana* embryos: quiescence signaling through dissipation of proton gradients. *J Exp Biol* 208: 2799-2808.

Crabtree B. and E.A. Newsholme. 1985. A quantitative approach to metabolic control. *Curr Top Cell Regul* 25: 21-76.

Crowe J.H., Carpenter J.F., and Crowe L.M. 1998. The role of vitrification in anhydrobiosis. *Annu Rev Phys* 60: 73-103.

Crowe J. H. and J. S. Clegg eds. 1973. Anhydrobiosis. Dowden, Hutchinson, and Ross, Inc., Stroudsburg, Pennsylvania. 477 pp.

Crowe J.H., Crowe L.M., Carpenter J.F., and Wistrom C.A. 1987. Stabilization of dry phospholipid bilayers and proteins by sugars. *Biochem J* 242: 1-10.

Crowe J.H., Crowe L.M., Wolkers W.F., Oliver A.E., Ma X., Auh J.-H., Tang M., Zhu S., Norris J., and Tablin F. 2005. Stabilization of Dry Mammalian Cells: Lessons from Nature. *Integr Comp Biol* 45: 810-820.

Denlinger D.L. 2002. Regulation of diapause. *Annu Rev Entomol* 47: 93-122.

Denlinger D. L., Yocum G.D. and Rinehart, J.P. 2011. Hormonal Control of Diapause. pp 430 - 463 in G. Lawrence ed, Insect Endocrinology. Academic Press, San Diego.

Denton R.M. and A.P. Halestrap. 1979. Regulation of pyruvate metabolism in mammalian tissues. *Essays Biochem* 15: 37-77.

Drinkwater L.E. and J.H. Crowe. 1987. Regulation of embryonic diapause in *Artemia*: environmental and physiological signals. *J Exp Zool* 241: 297-307.

Drinkwater L.E. and J.S. Clegg. 1991. Experimental biology of cyst diapause. In: *Artemia* Biology, R.A. Browne, P.Sorgeloos, and C.N.A. Trotman, eds. CRC Press, Boca Raton. 93-117.

Drinkwater L.E. and Crowe J.H. 1991. Hydration State, Metabolism, and Hatching of Mono Lake Artemia Cysts. *Biol Bull* 180: 432 - 439

Dutrieu J. 1960. Observations biochimiques et physiologiques sur le developpement d'*Artemia salina* Leach. *Arch Zool Exp Gen* 99: 1-133.

Eads B. D. and Hand S.C. 2003a. Transcriptional initiation under conditions of anoxia induced quiescence in mitochondria from *Artemia franciscana* embryos. *J Exp Biol* 206: 577-589.

Eads B.D. and Hand S.C. 2003b. Mitochondrial mRNA stability and polyadenylation during anoxia-induced quiescence in the brine shrimp *Artemia franciscana. J Exp Biol* 206: 3681-3692

Efremov R.G. and L.A. Sazanov. 2011. Respiratory complex I: 'steam engine' of the cell? *Curr Opin Struct Biol* 21: 532–540.

Emerson D.N. 1963. The metabolism of hatching embryos of the brine shrimp *Artemia salina*. *Proc South Dakota Acad Sci* 42: 131-135.

Hahn D.A. and Denlinger D.L. 2007. Meeting the energetic demands of insect diapause: Nutrient storage and utilization. *J Insect Physiol* 53: 760 – 773

Hahn D.A. and D.L. Denlinger. 2011. Energetics of insect diapause. *Annu Rev Entomol* 56: 103-121.

Hand S.C. 1998. Quiescence in *Artemia franciscana* embryos: Reversible arrest of metabolism and gene expression at low oxygen levels. *J Exp Biol* 201: 1233-1242.

Hand S.C. and J.F. Carpenter. 1986. pH-induced metabolic transitions in *Artemia* embryos mediated by a novel hysteretic trehalase. *Science* 232: 1535-1537.

Hand S.C. and E. Gnaiger. 1988. Anaerobic dormancy quantified in Artemia embryos - a calorimetric test of the control mechanism. *Science* 239: 1425-1427.

Hand S.C. and I. Hardewig. 1996. Downregulation of cellular metabolism during environmental stress: Mechanisms and implications. *Annu Rev Physiol* 58: 539-563.

Hand S.C., M.A. Menze, A. Borcar, Y. Patil, J.A. Covi, J.A. Reynolds, and M. Toner. 2011. Metabolic restructuring during energy-limited states: Insights from *Artemia franciscana* embryos and other animals. *J Insect Physiol* 57: 584-594.

Hardewig I., T.J. Anchordoguy D.L. Crawford and S.C. Hand. 1996. Profiles of nuclear and mitochondrial encoded mRNAs in developing and quiescent embryos of *Artemia franciscana*. *Mol Cell Biochem* 158: 139-147

Harris R.A., Bowker-Kinley M.M., Huang B., and P. Wu. 2002. Regulation of the activity of the pyruvate dehydrogenase complex. *Adv Enzyme Regul* 42: 249-259.

Heiden M.G.V., L.C. Cantley, and C.B. Thompson. 2009. Understanding the Warburg Effect: The Metabolic Requirements of Cell Proliferation. *Science* 324: 1029-1033.

Heinrich R. and T.A. Rapoport. 1974. Linear steady-state treatment of enzymatic chains - critique of crossover theorem and a general procedure to identify interaction sites with an effector. *Eur J Biochem* 42: 97-105.

Herzig S., E Raemy, S. Montessuit, J Veuthey, N Zamboni, B Westermann, E. R. S. Kunji and J. Martinou. 2012. Identification and Functional Expression of the Mitochondrial Pyruvate Carrier. *Science* 337: 93-96.

Hildyard J.C.W. and A.P. Halestrap. 2003. Identification of the mitochondrial pyruvate carrier in *Saccharomyces cerevisiae*. *Biochem J* 374: 607–611.

Hitosugi T., Fan, J., Chung T-W., Lythgoe K., Wang X., Xie J., Ge Q., Gu T-L., Polakiewicz R.D., Roesel J.L., Chen G.Z., Boggon T.J., Lonial S., Fu, H., Khuri F.R., Sumin Kang S. and J. Chen. 2011. Tyrosine phosphorylation of mitochondrial pyruvate dehydrogenase kinase 1 is important for cancer metabolism. *Mol Cell* 44: 864–877.

Hofmann G. E. and Hand S. C. 1994. Global arrest of translation during invertebrate quiescence. *Proc Natl Acad Sci* USA 91: 8492-8496.

Hochachka P.W. and M. Guppy. 1987. Metabolic Arrest and the Control of Biological Time. Harvard University Press, Cambridge, MA.

Hunte C., Zickermann V., and U. Brandt. 2010. Functional modules and structural basis of conformational coupling in mitochondrial complex I. *Science* 329: 448-451.

Kolobova E., A. Tuganova, I. Boulatnikov, and K.M. Popov. 2001. Regulation of pyruvate dehydrogenase activity through phosphorylation at multiple sites. *Biochem J* 358: 69-77.

Korotchkina, L.G. and Mulchand Patel. 2001. Probing the mechanism of inactivation of human pyruvate dehydrogenase by phosphorylation of three sites. *J Biol Chem* 276: 5731-5738.

Koštál V. 2006. Eco-physiological phases of insect diapause. *J Insect Physiol* 52: 113-127.

Kwast K.E. and S.C. Hand. 1993. Regulatory features of protein-synthesis in isolated-mitochondria from *Artemia* embryos. *Am J Physiol* 265: R1238-R1246.

Kwast K.E. and S.C. Hand. 1996. Depression of mitochondrial protein synthesis during anoxia: Contributions of oxygen sensing, matrix acidification, and redox state. *J Biol Chem* 271: 7313-7319.

Kwast K.E., J.I. Shapiro, B.B. Rees, and S.C. Hand. 1995. Oxidative-phosphorylation and the realkalinization of intracellular pH during recovery from anoxia in *Artemia franciscana* embryos. *Biochim Biophys Acta-Bioenergetics* 1232: 5-12.

Lehninger A.L. 1975. Biochemistry, 2nd ed. Worth Publishers, Inc. New York. p. 537.

Lehninger A.L. 1982. Principles of Biochemistry. Worth Publishers, Inc. New York.

Lerner E., Shug A.L., Elson C., and Shrago E. 1972. Reversible inhibition of adenine nucleotide translocation by long chain fatty acyl coenzyme A esters in liver mitochondria of diabetic and hibernating animals. *J Biol Chem* 247: 1513-1519.

Levin D.B., H.V. Danks, and S.A. Barber. 2003. Variations in mitochondrial DNA and gene transcription in freezing-tolerant larvae of *Eurosta solidaginis* (Diptera: Tephritidae) and *Gynaephora groenlandica* (Lepidoptera: Lymantriidae). *Insect Mol Biol* 12 (3): 281-289.

Lowry O.H. and J.V. Passonneau. 1972. A flexible system of enzymatic analysis. Academic Press, New York.

Lutz P.L. and S.L. Milton. 2004. Negotiating brain anoxia survival in the turtle. *J Exp Biol* 207: 3141-3147.

MacRae T.H. 2010. Gene expression, metabolic regulation and stress tolerance during diapause. CMLS *Cell Mol Life Sci* 67: 2405-2424.

Menze M.A., M.J. Clavenna, and S.C. Hand. 2005. Depression of cell metabolism and proliferation by membrane-permeable and -impermeable modulators: role for AMP-to-ATP ratio. *Am J Physiol-Regul Integr Comp Physiol* 288: R501-R510.

Minkler P.E., J. Kerner, S.T. Ingalls, and C.L. Hoppel. 2008. Novel isolation procedure for short-, medium-, and long-chain acyl-coenzyme A esters from tissue. *Anal Biochem* 376: 275-276.

Muramatsu S. 1960. Studies on the physiology of Artemia embryos: 1. Respiration and its main substrate during the early development of the encysted embryo. *Embryologia* 5: 95-106.

Nambu Z., Tanaka S., Nambu F. and Nakano M. 2008. Influence of temperature and darkness on embryonic diapause termination in dormant *Artemia* cysts that have never been desiccated. *J Exp Zool* 309: 17-24.

Nicholls D.G. and S.J. Ferguson. 2002. Bioenergetics 3. Academic Press, Amsterdam.

Palmisano G., Sardanelli A.M., Signorile A., Papa S., and M.R. Larsen. 2007. The phosphorylation pattern of bovine heart complex I subunits. *Proteomics* 7: 1575–1583.

Patel M.S. and L.G. Korotchkina. 2001. Regulation of mammalian pyruvate dehydrogenase complex by phosphorylation: complexity of multiple phosphorylation sites and kinases. *Exp Mol Med* 33: 191-197.

Patil Y.N., Marden B., Brand M.D. and S.C. Hand. 2012. Metabolic downregulation and inhibition of carbohydrate catabolism during diapause in embryos of *Artemia franciscana*. *Physiol Biochem Zool* (in press).

Peterson G.L. 1977. A simplification of the protein assay method of Lowry et al. which is generally more applicable. *Anal Biochem* 83: 346 - 356.

Pettit F. H., Reed L. J. and Willis A. W. 1982. [65] Pyruvate dehydrogenase complex from bovine kidney and heart. *Meth Enzymol* 89: 376-386.

Phillips D., Aponte A.M., Covian R., and R.S. Balaban. 2011. Intrinsic protein kinase activity in mitochondrial oxidative phosphorylation complexes. *Biochemistry* 50: 2515–2529.

Prentki M., Vischer S., Glennon M.C., Regazzi R., Deeney J.T. and Corkey B.E. 1992. Malonyl-CoA and long chain acyl-CoA esters as metabolic coupling factors in nutrient-induced insulin secretion. *J Biol Chem* 267: 5802-5810.

Qiu Z. and T. MacRae. 2010. A molecular overview of diapause in embryos of the crustacean, *Artemia franciscana*. pp. 165-187 in E. Lubzens, J. Cerda and M. Clark, eds. Dormancy and Resistance in Harsh Environments. Springer Berlin Heidelberg.

Qiu Z., Tsoi S.C.M. and MacRae T.H. 2007. Gene expression in diapause-destined embryos of the crustacean *Artemia franciscana*. *Mech Dev* 124: 856-867.

Rees B.B. and S.C. Hand. 1991. Regulation of glycolysis in the land snail *Oreohelix* during estivation and artificial hypercapnia. *J Comp Physiol B Biochem Syst Environ Physiol* 161: 237-246.

Rees B.B., I.J. Ropson, and S.C. Hand. 1989. Kinetic-properties of hexokinase under near-physiological conditions - relation to metabolic arrest in *Artemia* embryos during anoxia. *J Biol Chem* 264: 15410-15417.

Reynolds J.A. and S.C. Hand. 2004. Differences in isolated mitochondria are insufficient to account for respiratory depression during diapause in *Artemia franciscana* embryos. *Physiol Biochem Zool* 77: 366-377.

Reynolds J.A. and S.C. Hand. 2009. Decoupling development and energy flow during embryonic diapause in the cricket, *Allonemobius socius. J Exp Biol* 212: 2064-2073.

Robbins H.M., G. Van Stappen, P. Sorgeloos, Y.Y. Sung, T.H. MacRae, and P. Bossier. 2010. Diapause termination and development of encysted *Artemia* embryos: roles for nitric oxide and hydrogen peroxide. *J Exp Biol* 213: 1464-1470.

Rolleston F.S. 1972. A theoritical background to the use of measured concentrations of intermediates in study of the control of intermediary metabolism. *Curr Top Cell Regul* 5: 47-75.

Scalettar B.A., J.R. Abney, and C.R. Hackenbrock. 1991. Dynamics, structure, and function are coupled in the mitochondrial matrix. *Proc Natl Acad Sci* USA 88: 8057-8061.

Siebenaller J.F. 1979. Regulation of pyruvate-kinase in *Mytilus edulis* by phosphorylation-dephosphorylation. *Mar Biol Lett* 1: 105-110.

Siess E.A., D.G. Brocks, H.K. Lattke, and O.H. Wieland. 1977. Effect of glucagon on metabolite compartmentation in isolated rat liver cells during gluconeogenesis from lactate. *Biochem J* 166: 225-235.

Soboll S., Seitz H.J., Sies H., Ziegler B., and Scholz R. (1984) Effect of long-chain fatty acyl-CoA on mitochondrial and cytosolic ATP/ADP ratios in the intact liver cell. *Biochem J* 220: 371-376.

Stiggall D. L., Galante Y. M., Hatefi Y., Sidney F. and Lester P. 1979. [34] Preparation and properties of complex V. *Meth Enzymol* 55, 308-315.

Stocco D.M., P.C. Beers, and A.H. Warner. 1972. Effect of anoxia on nucleotide metabolism in encysted embryos of the brine shrimp. *Dev Biol* 27: 479-493.

Storey K.B. and J.M. Storey. 2007. Tribute to P. L. Lutz: putting life on 'pause' - molecular regulation of hypometabolism. *J Exp Biol* 210: 1700-1714.

Stuart J.A. and Brown M.F. 2006. Mitochondrial DNA maintenance and bioenergetics. *Biochim Biophys Acta* 1757: 79 – 89.

Stuart J.A., T.E. Gillis, and J.S. Ballantyne. 1998. Compositional correlates of metabolic depression in the mitochondrial membranes of estivating snails. *Am J Physiol* 275: R1977-R1982

Sugden M. C. and Holness M. J. 2006. Mechanisms underlying regulation of the expression and activities of the mammalian pyruvate dehydrogenase kinases. *Arch Physiol Biochem* 112, 139-149.

Timasheff SN. 2002. Protein hydration, thermodynamic binding, and preferential hydration. *Biochemistry* 41:13473- 13482.

Trounce I. A., Kim Y. L., Jun A. S., Wallace D. C., Giuseppe M. A. and Anne C. 1996. [42]Assessment of mitochondrial oxidative phosphorylation in patient muscle biopsies, lymphoblasts, and transmitochondrial cell lines. *Meth Enzymol* 264: 484-509.

Van Breukelen F., Maier R. and Hand S.C. 2000. Depression of nuclear transcription and extension of mRNA half-life under anoxia in *Artemia franciscana* embryos. *J Exp Biol* 203: 1123 – 1130.

Vander Heiden M.G., L.C. Cantley and C.B. Thompson. 2009. Understanding the Warburg Effect: The Metabolic Requirements of Cell Proliferation. *Science* 22: 1029-1033.

Van Der Linden A., Blust R., Van Laere A. J. and DeCleir W. 1988. Light-induced release of *Artemia* dried embryos from diapause: Analysis of metabolic status. *J Exp Zool* 247: 131-138.

Van Stappen G., Lavens P. and Sorgeloos P. 1998. Effects of hydrogen peroxide treatment in *Artemia* cysts of different geographical origin. *Arch Hydrobiol Spec Issues Advanc Limnol* 52: 281-296.

Webb S.J. 1965. Bound Water in Biological Systems. C C Thomas. Springfield, IL.

Yamashita O. 1996. Diapause hormone of the silkworm, *Bombyx mori*: structure, gene expression and function. *J Insect Physiol.* 42: 669–79.

Yancey PH. 2005 Organic osmolytes as compatable, metabolic and counteracting cryoprotectants in high osmolarity and other stresses. *J Exp Biol* 208:2819-2830.

VITA

Yuvraj Nanasaheb Patil was born and raised in Pune, India. He was heavily influenced by his siblings who were students of chemistry and medicine. Yuvraj reveled in science fiction since a young age and the academic pursuit of science came to pass naturally. Yuvraj studied Pharmacy in Pune where he was pleasantly surprised that he wasn't studying medieval alchemy, soon becoming inspired by the amalgamation of physical, chemical and biological sciences. The relatively new field of biotechnology in medicine greatly fascinated Yuvraj and after getting his B.S. (Pharm.) degree, he strove to earn a position in the National Institute of Pharmaceutical Education and Research (India) to pursue his interest. He was among the four candidates selected to study biotechnology from about a thousand test applicants. Working for his M.S. (Pharm) degree gave Yuvraj the opportunity to better appreciate biology at the cellular level and lay the foundation for his subsequent work in biochemistry. In his research as an M.S. student, Yuvraj studied mitochondrial function and the effect of experimental anti-cancer drugs on mitochondria. After earning his M.S. degree, Yuvraj worked briefly at an NIH sponsored clinical trial in Pune. During this period he got interested in the mitochondrial research carried out in Dr. Steven Hand's lab in Baton Rouge and decided to join LSU. Yuvraj studied changes in the metabolism of brine shrimp during diapause for his PhD dissertation.

Yuvraj plans to pursue a post-doctorate position studying comparative physiology and cellular metabolism and its defects.